Electron and hole relaxation in one-dimensional wires

Master Thesis in Physics

Toke Lynæs Larsen

Niels Bohr Institute
University of Copenhagen

Supervisor: Karsten Flensberg

August 12, 2008

Preface

Thanks to my supervisor Karsten Flensberg for a great deal of patience and to Anders Mathias Lunde for discussion. Also thanks to Kim Georg Lind Pedersen for help with Latex and for comments on a late draft. No thanks to FysikRevy^{TM} (or for that matter any other revue) for stealing my time.

Contents

Chapter 1

Introduction

1.1 What is this all about?

The purpose of this this thesis is to look at the relaxation of electrons and holes in one-dimensional wires and how it may contribute somehow to a measurable effect.

1.2 What is a quantum wire?

Classically speaking a wire is a macroscopic metallic object, usually long and thin, in which an electrical current can run. If we apply a voltage difference V between the ends of the wire, a current I may be measured in it and from this we can calculate the electrical resistance $R = V/I$ of the wire. For sufficiently "nice" (ohmic) wires, the resistance is independent of the voltage we apply to the wire. For a wire with a constant cross-section with area A and a length L we can calculate the resistance from the resistivity ρ (a material constant) as $R = \frac{\rho L}{A}$.

So it seems that the only information we can hope to gain from measuring the resistance (or typically its inverse, the conductance $G = I/V$), is another a number, which basically just depends on the composition of the wire. If we shrink the dimensions of the wire, at some point quantum effects begin to play a role, and the current is no longer as simple as the classical ideas may suggest; we are dealing with a quantum wire. And now suddenly a lot of information about the system can be extracted from the measurement of I against V.

A typical and characteristic features of a quantum wire, is the conductance quantization. Varying some specific system parameter (which could be the voltage applied to a gate or the force applied to a break junction) one reduces the dimensions of a critical part of the quantum wire and the conductance is seen to be reduced in steps following the reduction in modes available for transport through the wire.

1.2.1 The Extreme: the one-dimensional wire

Imagine a quantum wire which resembled a "classical" wire, that is, it has a constant cross-section and a length which is much larger than its transversal dimensions; this is a one-dimensional wire.

Let us look at an example well known from second year physics: the electron-in-a-box [1]. A box in this context is a structure in any number of dimensions where the potential is either zero (inside the box) or infinite (outside the box). We wish to solve the Schrödinger

Equation of a single electron in a 3D rectangular box, and luckily this problem is separable. Using standing wave boundary conditions for the transversal directions (x and y) and periodic boundary conditions for the longitudinal direction (z), the eigenenergies of the system can be written as follows in terms of the three quantum numbers associated with each direction,

$$E_{n_x n_y n_z} = E^{(x)}_{n_x} + E^{(y)}_{n_y} + E^{(z)}_{n_z} \tag{1.1}$$

$$E^{(x)}_{n_x} = \frac{\hbar^2 \pi^2 n_x^2}{2mL_x^2} \quad , n_x = 1, 2, 3, \ldots \tag{1.2}$$

$$E^{(y)}_{n_y} = \frac{\hbar^2 \pi^2 n_y^2}{2mL_y^2} \quad , n_y = 1, 2, 3, \ldots \tag{1.3}$$

$$E^{(z)}_{n_x} = \frac{2\hbar^2 \pi^2 n_x^2}{mL_z^2} \quad , n_z = 0, \pm 1, \pm 2, \ldots . \tag{1.4}$$

We observe, that the eigenenergies associated with a certain direction goes as $1/L^2$, where L is the length of the box in that direction. Thus it requires a much higher energy to excite the electron in a transversal direction than to excite it in the longitudinal direction. For practical purposes the electron may be considered as moving in a 1D channel with only one degree of freedom, the longitudinal momentum k_z, which would form a continuum. Each choice of transversal quantum numbers would then correspond to a different mode of the wire, these being widely separated in energy, and to each mode would be associated a dispersion $E(k_z)$. For the box under consideration the wire modes could be labeled by (n_x, n_y) and the dispersion for that wire mode would then be

$$E_{n_x n_y}(k_z) = \frac{\hbar^2 k_z^2}{2m} + \Big(\frac{\hbar^2 \pi^2 n_x^2}{2mL_x^2} + \frac{\hbar^2 \pi^2 n_y^2}{2mL_y^2} \Big). \tag{1.5}$$

(1,1) would be the lowest laying wire mode and the next lowest wire modes (1,2) and (2,1) (assuming $L_x = L_y \equiv L$) has a dispersion which is shifted upwards by $\frac{3\hbar^2\pi^2}{2mL^2}$ relative to that of (1,1). If we require that only a single mode (the lowest lying) is occupied at zero temperature, we should have

$$\frac{3\hbar^2 \pi^2}{2mL^2} > \frac{\hbar^2 k_F^2}{2m}, \tag{1.6}$$

or roughly $k_F L \lesssim 1$. Here $\hbar k_F$ is the Fermi momentum, the numerically largest momentum, which can be found amongst the occupied states. The smaller $k_F L$ is compared to one, the less likely it is that a wire mode apart from the lowest lying would be involved in any physics of the system, such a system would be called a single-mode wire, as opposed to a multi-mode wire where several modes of the wire would contribute to for instance the current through the wire.

Real 1D wires are somewhat like this primitive box-model; first of all they may not be represented very well by the sharp box-potential, but by something similar with more soft edges, which in the end still supports 1D wire modes. Also, the dispersions of the wire modes would not necessarily just be shifted with respect to each other, the effective band mass could for instance be different between different modes. See Appendix A for a calculation of the single electron eigenstates and -energies in the solid-state system we are concerned about.

1.3 Physical realizations of quantum and 1D wires

Let us look briefly at some of the typical physical realizations of quantum wires and also what issues arises when one wishes to fabricate a true one-dimensional wire and how to overcome these problems.

1.3.1 Quantum Point Contacts

A Quantum Point Contact (QPC) is a narrow constriction between two bulk electrically conducting materials on either side and may show quantum wire behavior. If one slowly opens an electrical contact while monitoring the conductance through it, just before the contact is broken one observes a conductance dropping off in steps, corresponding to the stepwise elimination of conduction channels in the contact. This experiment is not only an example of a QPC but also of a so-called break-junction, so named because it is achieved by physical stress. It is also one of the only quantum wire behavior observable at room temperature; most other quantum wires are achieved in some solid-state structure and requires cryogenic temperatures.

A more interesting QPC is made by constricting a two-dimensional electron gas (2DEG) by electrostatic gating. High quality 2DEGs are supported by the quantum wells in the heterostructures grown by the Molecular-Beam Epitaxy (MBE) method, see the next section for a very short review. By contacting the 2DEG, a current can be made to flow from one side to the other. Metallic gates can be deposited on top of the crystal with a geometry well-defined by lithographic methods and by applying a negative DC voltage to a top-gate, one can locally deplete the 2DEG beneath that gate, thereby controlling the geometry of the 2DEG in turn. Thus by gating one can construct the narrow constriction in the 2DEG and indeed quantum wire behavior is observed, conduction quantization for instance; as the voltage on the gate is lowered, fewer and fewer modes are available for conduction and the conduction falls off in steps of $\frac{2e^2}{h}$.

One of the disadvantages of the QPC is the small separation of the subbands which lead to mode-mixing. Also we cannot use QPC for making finite length 1D wires as random width fluctuations will chop up the wire into discrete quantum dots, which will dominate the conductance [2].

1.3.2 Carbon Nanotubes

A graphene sheet consists of Carbon atoms in a regular hexagonal lattice. If such a sheet could be folded to a cylinder and excess atoms be removed, the outcome would be a carbon nanotube (CNT). CNTs are cylindrical structures with diameters in the nanometer range and lengths many order of magnitudes larger, typically micrometers of even millimeters. As such they greatly resemble the classical wire. By depositing two contacts on top of a CNT one can measure the current through it, and - surprise - the CNT is a prime example of a quantum wire. Luttinger liquid behavior, the trademark of one-dimensionality, have been observed in CNTs [3].

The limitations of CNTs as 1D wires lay in the lack of control the experimentalist has over them, because they are grown. Therefore producing two CNT in parallel, for the purpose of allowing tunneling between the two, is virtually impossible. An alternative option may be to grow a multi-walled CNT (MWNT), one which consists of two or more concentric single-walled

CNTs of different diameters, perhaps this setup may behave as two parallel 1D wires.

1.3.3 Cleaved Edge Overgrowth

As already mentioned, it is possible using MBE to grow crystals, which contain one or more quantum wells, each of which may support a 2DEG. By cleaving such a crystal and growing further on the newly exposed surface, one can confine electrons electrostatically to the edge of the 2D quantum well, thereby creating a 1D electron gas (1DEG) [4]. This method is called Cleaved Edge Overgrowth (CEO) . The fabricated 1DEG has a length defined by the dimensions of the crystal (could be millimeters) and has a very well-defined constant height dictated by the atomically smooth surfaces of the quantum well. Its width is defined by the strength of the electrostatically forces binding the electrons to the edge. Since the height and width of the 1DEG can be very small (depending on the growth conditions), these quantum wires feature large subband separation, possibly resulting in single mode 1D wires. Also one could make several parallel quantum wells in the initial growth and thus creating two (or more) 1DEGs which are parallel along their whole length [5]. This latter option enables tunneling between the wires and opens up a whole new field of wire spectroscopy, more on this later. Unsurprisingly, Luttinger liquid behavior has been observed in these quantum wires [6].

Since this method is what we imagine to be used for fabricating the device we shall discuss in this thesis, the next section will feature a brief review of the CEO method.

1.4 Fabrication and properties of CEO quantum wires

The Cleaved Edge Overgrowth [4] technique can be used for fabricating high quality, parallel 1D wires, and we shall look into its workings here. The principal idea behind CEO is illustrated in Fig. 1.1. The basics of CEO is the Molecular-Beam Epitaxy (MBE) growing method for semi-conductor heterostructures, but instead of growing in just a single direction a cleave is performed and growth is continued on the cleaved surface in another direction.

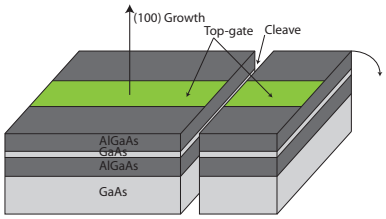

(a) The first growth on the (100) surface and subsequent cleave to expose an (110) surface. In green is the deposited top-gate.

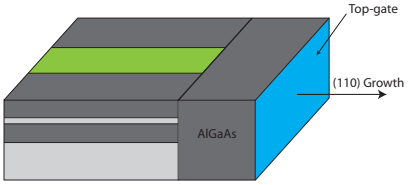

(b) The second growth on the newly exposed (110) surface. A deposited side-gate is blue.

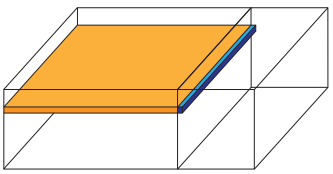

(c) Sketch of electronic systems of the previous figure. Blue is the 1DEG created at the interface and orange is the 2DEG used to contact the 1DEG.

Figure 1.1: Fabrication of single 1D wire by cleaved edge overgrowth. In the first two figures dark gray indicates AlGaAs and light gray indicates GaAs.

1.4.1 Growth by Molecular-Beam Epitaxy

When growing structures using MBE one could use GaAs/AlGaAs or another set of similar materials; we will only consider the GaAs/AlGaAs heterostructures. Starting from a GaAs wafer polished on a (100) surface one can grow a structure upwards with any combination of GaAs and AlGaAs. In the areas with AlGaAs the potential is higher and these areas will act as barriers between the wells where GaAs is used. The growth rate is determined by the flux rate of the atomical vapors, and is fixed by the requirement of good quality growth. But by choosing the growth time of each chemical composition, the experimentalist has control over the thickness of each layer down to the atomical scale.

One can use AlGaAs doped with Si (or another suitable donor atom) to form electric fields in the materials binding electrons to certain regions of the material. Thus one could form a 2-dimensional electron gas (2DEG) in the well.

GaAs readily cleaves on the (110) surface, so if one is to cleave the original grown crystal and continue growth on another surface, it must be the (110) surface. Originally this posed some problems [7], as the growth in that direction required fine-tuning of the growth-parameters, but the trouble have been overcome, and growth on (110) is now possible, although it requires a much higher concentration of dopant compared to (100) growth to achieve the same level of 2DEG density. In order not to contaminate the newly exposed surface, which may degrade the morphology of the yet-to-be-grown crystal, the cleave is performed in the MBE apparatus with the growing conditions for growth on (110) already present, so that growth can be assumed a few seconds after the cleave has been performed.

CEO can also be used for fabricating other structures than 1DEGs, 2DEGs for instance [8]. But if one is to fabricate a 1D wire a typical approach is as follows. On the (100) GaAs wafer is grown a layer of AlGaAs - a couple of μm should do the job. Then the actual well is grown using GaAs. The height of this layer will later define the height of the 1D wire; typical heights are $14-40$ nm in [6], . Finally a second barrier is grown with AlGaAs, probably of comparably size to the other. For addressing the quantum wire a a later stage, the last layer of AlGaAs is doped in such a way, that the quantum well is populated by a 2DEG. Next the sample is cleaved and growth is resumed on the exposed (110) surface. A AlGaAs layer with Si-doping is grown followed by an undoped layer of AlGaAs and finally a thin layer of GaAs as cap. A high quality 1D wire is then formed with a height given by the height of the quantum well, a width determined by the electric field strength from the donor-states in the second growth AlGaAs and a length which may be the whole length of the crystal (millimeters).

From the simultaneous growth on a (110) reference wafer and later magnetoresistance measurements on 2DEG formed on this wafer, the quality of the CEO growth can be estimated. [2] reports finding a density of $n = 3{\cdot}10^{11}$ cm^{-2} and a mobility of $\mu = 1.3{\cdot}10^{6}$ Vs^{-1}, whereas [4] reports very similar values at $n = 4.6 \cdot 10^{11}$ cm^{-2} and a mobility of $\mu = 4.8 \cdot 10^{5}$ Vs^{-1}. In general mobilities of 2DEGs grown on an (110) surface are much less than mobilities for growth on the (100) direction [9].

The 1D wire need not be formed as described by binding the electrons to the side of the well by an electric field from the doped AlGaAs grown on the (110) surface. One could also fabricate intersecting quantum wells [10] and [11], in which the lowest energy eigenstate will be a bound state in the two transversal directions, so that the system contains at least one 1D wire mode.

1.4.2 Controlling geometry

For controlling the geometry of setup, one takes advantage of electrostatic gating. Before cleaving, several top-gates are deposited on top of the first growth, the later cleaving will confine them to this area. By applying a gate voltage to one of these gates and lowering the voltage, several things happens. At some voltage, the 2DEG beneath the gate will pinch off, and transport beneath the gate will only be possible through the 1D wire. As the gate voltage is lowered further, the modes of the wires are depopulated one by one until finally the 1D wire is completely depopulated and no transport is expected to be possible under the gate.

On top of the second growth could also be deposited a metal-stripe to be used as a side-gate. Applying a bias voltage to the side-gate is expected to speak more directly to the 1DEG than to the 2DEG, and so could be used for manipulating the 1DEG density, while not changing the properties of the 2DEG too strongly.

The previously approach was good for fabricating a single 1D wire, but is also by slight modifications usable for producing parallel quantum wires. The first growth on the (100) wafer is simply modified so that instead of just a single quantum well, two quantum wells are grown with a barrier of AlGaAs in between. After cleaving and further growth we will now have two 1D wires which are to a very high precision parallel. Only the upper quantum well is usually made populated by a 2DEG. The top-gate now serves a further purpose; after the wire closest to the top-gate has been pinched off, the lower 1D wire is still populated and so the current, which is observed, has moved through the wire.

1.5 Luttinger liquid theory vs. Fermi liquid theory

In a normal bulk 3D conducting material the interacting electrons are described by the Fermi liquid theory [12]. In essence what this theory says is, that a system of interacting electrons is equivalent to a gas of only very weakly interacting particles, so-called quasiparticles. One of the prime reason for this similarity to a almost non-interacting gas lies in the large phase-space associated with excitations in 3D. It is notably that no matter how strong the interaction between electrons, the correspondence with the weakly interacting gas still holds.

In 1D the phase space available for excitations is much more restricted, which is one of the reason why the Fermi liquid theory fails completely in this case. Instead, interacting 1D electron gasses can be described by the Luttinger liquid theory [13] in which quasiparticles are completely absent. The Luttinger liquid requires linearization of the actual dispersion (or a dispersion which is really linear) and may thus only work well to describe small excitations.

In a Luttinger liquid with spin the excitations can be split into two independent degrees of freedom: the spin and the charge, both reached by a bosonization of the original fermionic system Hamiltonian. The spin-excitations will move with a velocity equal to the Fermi velocity, $v_\sigma = v_F$, while the charge-excitations will move with a velocity $v_c = v_F/g$. g is a coupling parameter characteristic for each Luttinger liquid; it comes out of the bosonization procedure. Experiments [14] have confirmed behavior consistent with this spin-charge separation.

So where a Luttinger liquid seems to be necessary to explain behavior which is observed in 1D wires, it also has the misfortune of requiring a linear dispersion. One of the things we are going to look at (lack of hole relaxation) specifically requires a non-linear band and is therefore inconsistent with the linearization. Instead we may in a sense be using the Fermi liquid theory as we shall use the Boltzmann Equation, which may be derived from the Fermi liquid theory [12].

1.6 Thesis outline

Let us briefly outline what we are going to do in the rest of this thesis.

First of all (Chapter 2) we are going to describe how we imagine a device could be fabricated, which could be used for measuring the relaxation of charge carriers in 1D wires. Following that we will also present a very simple model to explain why this is supposedly the case. Along the way we introduce some notation/notion in the framework of the simple model, which will be employed later on.

In Chapter 3 we will prove, that at zero temperature a single hole in a single-mode 1D wire is not able to relax if both energy and momentum are to be conserved. This result is limited to the class of bands with a positive curvature, but it is not limited by the number of electron-hole pairs created in the process. For the configurations of our device where the current depends on the ability for holes to relax, we expect no current to be measured at all.

Next (Chapter 4) we are going to calculate the current through the device using the semi-classical Boltzmann Equation approach. As we are unable to solve it algebraically, because of the presence of some cumbersome integrals, we solve for the current numerically to first order in the three-particle scattering rate W - that is we allow the excited electron to scatter only once, creating two electron-hole pairs. Finally, we briefly consider what happens to the current, if the range of the interaction is changed.

Chapter 2

Suggested 3-wire setup to measure relaxation and toy model for current

In this chapter we will suggest a method by which the relaxation of charge carriers can be measured. First we will describe how we imagine this device could be fabricated and next we will look into its working and discuss how the current and the relaxation are connected.

2.1 Fabrication and measurements

The device we have in mind is to be fabricated by the already established CEO method as described in the previous chapter.[1] What differs from previous experiments is the geometry chosen. Actually the experiment described by [15] uses a somewhat similar configuration of gates, but only includes a single 1DEG, whereas we need two such, but also .

First of all an ordinary GaAs/AlGaAs heterostructure is to be grown with two parallel quantum wells. The thickness of the wells and the distance between them can be chosen by the growing time with great precision and they in turn determines the height of our 1D wires and the distance between them respectively. Typically achievable values are given in our previous description of CEO. By the doping sequence, only the upper well is occupied by electrons forming a 2DEG, which will later act as the contact to our 1D wires, whereas the lower well is empty.

On the top of the AlGaAs cap layer Tungsten stripes are evaporated. These stripes are to be used as gates to control the geometry. We will need at least three of these top-gates, but evaporating several more stripes will allow the experimentalist to use the same device for several geometries by using different sets of three stripes as gates. Typically they could be $2\mu m$ wide and be spaced with the same distance in between.

After cleave the usual layers are grown on the exposed (110) surface forming two parallel 1D wires of very high quality on the cleaved edge. One could also evaporate a side-gate on top of the second growth, allowing control of the electron density in the wires. This could also be achieved by UV/IR radiation of the wire.

[1] There is no fundamental requirement, that the 1D wire system must be fabricated bye CEO. However, it is currently the only feasible way of doing so.

2.1.1 Defining geometry

To one of the top-gates (G1) is applied a negative voltage so large, that the 2DEG and the upper 1DEG are completely pinched off, and only a single mode is populated in the lower 1DEG. The width of the region where only a lower wire mode is populated is related, though not equal, to the width of the gate. Using a wider gate allows the region where interactions between charge carriers occur to be longer. This could perhaps allow us to switch regime, to go from incoherent regime (long interaction length) to coherent regime (short interaction length).

Having defined the interaction region, we want to be able to contact the wires. This is a bit more tricky. Two other top-gates, G2 and G3 on different sides of G1, are used for this purpose. To each of these are applied a voltage, such that the 2DEG and the upper wire pinches off below. Whether or not it should pinch off all modes except one in the lower wire remains for the experimentalists to determine. In each of the regions between G1 and G2 and between G1 and G3 a contact (C1 and C2 respectively) is made to the 2DEG, a usual choice of material is Indium. These contacts couples directly to the 2DEG and since the 2DEG and the upper wire are in physical contact, we also has good contact with the two sections of the upper wire defined between. The coupling between a 1DEG and a finite length "tap" 2DEG has been studied in [16]. In the semi-infinite regions outside gates G2 and G3, two contacts are also made to the 2DEG (C3 and C4). Since the region is of "infinite" extent, the upper and lower wires are supposedly in equilibrium and so by using these contacts, we can contact the two segments of the lower wire.

In Fig. 2.1 we have made a drawing of the resulting device.

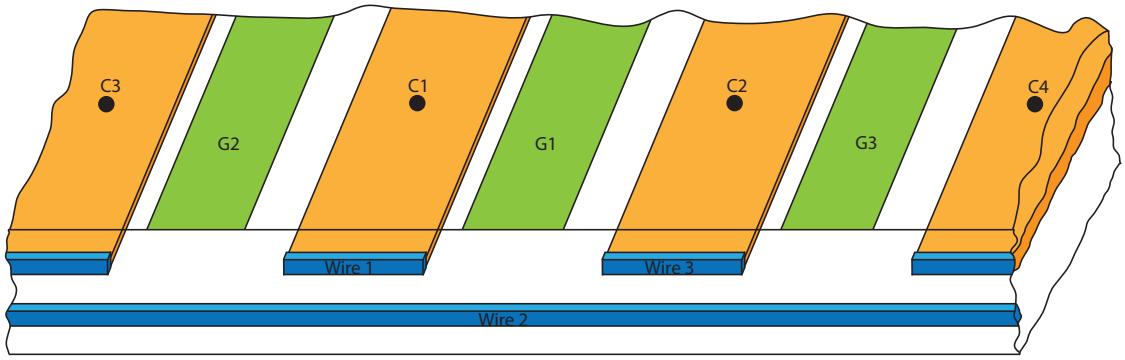

Figure 2.1: Our 3-wire system with geometry-defining top-gates (G1, G2 and G3) and Indium contacts (C1, C2, C3 and C4). 1DEG's are blue and 2DEG's are orange. The Tungsten top-gates are green.

2.1.2 Measurements

When performing the experiment, we use the four contacts made (C1-C4) to control the potential of the two finite segments of the upper wire and of the lower wire.[2]

Also a magnetic field B, perpendicular to the plane of the wires, is present, the purpose of which is to boost tunneling electrons.

[2]So we expect to short-circuit contacts C3 and C4, regarding them as a single contact to the lower wire.

The thing the experimentalist is going to measure, is the current in the right segment of the upper wire. This could be done by usual lock-in methods as is the case for similar experiments.

2.2 Modeling the system, notation and nomenclature

In this section we shall briefly introduce the notation to be used in the rest of this thesis.

When modelling the system, we regard it as consisting of two segments of upper wire and one segment of lower wire. These will be named respectively wire 1, wire 3 and wire 2. The reason for this choice is that an electron which moves from one segment of the upper wire to the other segment must have passed through the lower wire. The area between wire 1 and wire 2 where tunneling between them may occur will be named tunneling junction A, between wire 2 and wire 3 the corresponding area is named tunneling junction B.

Each wire i has a single chemical potential μ_i. By using the contacts to the wires, we can impose a voltage difference between wire 1 and wire 2 (V_A) and on between wire 2 and wire 3 (V_B). These voltage differences translate directly into differences in chemical potentials of the wires. We define the relationship between the chemical potentials and the bias voltages in the following way

$$\mu_3 - \mu_2 \equiv eV_B \tag{2.1}$$
$$\mu_2 - \mu_1 \equiv eV_A, \tag{2.2}$$

so that a positive bias at junction A will try to drive an electrical current from wire 1 to wire 2, and a positive bias at junction B will try to drive one from wire 2 to wire 3. Note that $e > 0$ by definition, so that the charge of the electron is $-e$.

When neccesary we will use the following cartesian coordinate system. Imagine looking into the plane of the wires from the end of the second growth. The x-axis will be to the right along the direction of the wires, the y-axis will be upwards, still in the wire plane, and the z-axis will be out of the wire-plane towards the beholder, parallel to the direction of the second growth.

We write the magnetic field as

$$\mathbf{B} = B\hat{\mathbf{z}}, \tag{2.3}$$

and the associated momentum boost (see Appendix. A) as

$$\hbar q_B(B) = eBd, \tag{2.4}$$

where d is the vertical distance between the center of the upper and lower wire.

2.3 Regimes: coherent and incoherent

We want to look at processes where an electron transfers from wire 1 to wire 3, thereby giving a current in wire 3, which we can measure. The reason for us wanting to look at these types of processes will become clear in the next section. To lowest order in the tunneling, this electron must first tunnel to wire 2, propagate to junction B and tunnel into wire 3.

We basically deal with two regimes:

Coherent regime Everything happens as one process. We only need overall energy conservation. The single tunneling or relaxation event may break energy conservation.

Incoherent regime Regard the individual processes as separate processes. Each single tunneling or relaxation event must conserve energy.

2.4 Toy model for current in incoherent regime

In this section we present a simplified, quantitative model to partially explain the current and the processes going on. Along the way we will introduce some ideas and notions, which will be employed later on.

2.4.1 1D wire tunneling spectroscopy

Each single-mode wire is represented by its dispersion $\varepsilon(k)$. The dispersion could be any function, but we will assume it to be an even function of k with a curvature that is strictly positive everywhere. When we need to be specific, we shall assume it to be the good old quadratic dispersion. Since the different wires are fabricated in the same fashion, we will let each wire be represented by the same dispersion, although the single mode we address could be different physical modes.

Looking at only a pair of wires, if no bias voltage is applied between the wires, they are in equilibrium. In equilibrium each wire is characterized by the same chemical potential μ, which determines the filling of each wire; states far below the chemical potential in energy are filled, whereas states far above are empty. In between these extremes, the filling is determined by the Fermi distribution. At zero temperature the situation is much simpler, here all states with a momentum numerically smaller than the Fermi momentum $\hbar k_F$ are filled and all other states are empty.

Neglecting for a moment tunneling, when we bring the pair of wires out of equilibrium by applying a bias voltage between them what happens is that the dispersions move vertically with respect to each other in such a fashion that the difference between the chemical potentials is the applied voltage (multiplied by the electron charge) while maintaining the total number of electrons in the single wire. What is worth noting is the last claim; that the number of electrons is unchanged by the bias, we would expect a high positive applied bias to increase the number of electrons. However the change induced is fractionally rather small and this approach seems to reproduce the experimental result and may thus be the right way to think about what happens.

Energy conservation dictates that electrons can only move between the wires if the corresponding points on the dispersion are at the same height. Thus a bias voltage that shifts the dispersions vertically will speak more or less directly to energy conservation.

Neglecting for a moment the presence of the magnetic field, tunneling is allowed between states which differ in momentum by an amount inversely proportional to the tunneling junction width. Assuming this width to be large compared with other length scales in the problem, momentum is conserved, and tunneling may thus only occur if the corresponding points on the dispersions are vertically above each other. Turning on the magnetic field will have the effect of boosting tunneling electrons, but will by assumption not change anything else. Maintaining our previous rule of tunneling vertically, we must impose the condition, that the dispersions are also shifted horizontally with respect to each other, by an amount $\hbar q_B$. For positive B,

the dispersions for wire 1 and 3 should always be to the right of the dispersion for wire 2, so that an electron gains momentum by tunneling from the former to the latter. The dispersions for wire 1 and 3 should not be shifted horizontally with respect to each other, as they sit at the same height above wire 2 thus giving electrons the same momentum boost in the two tunneling junctions.[3]

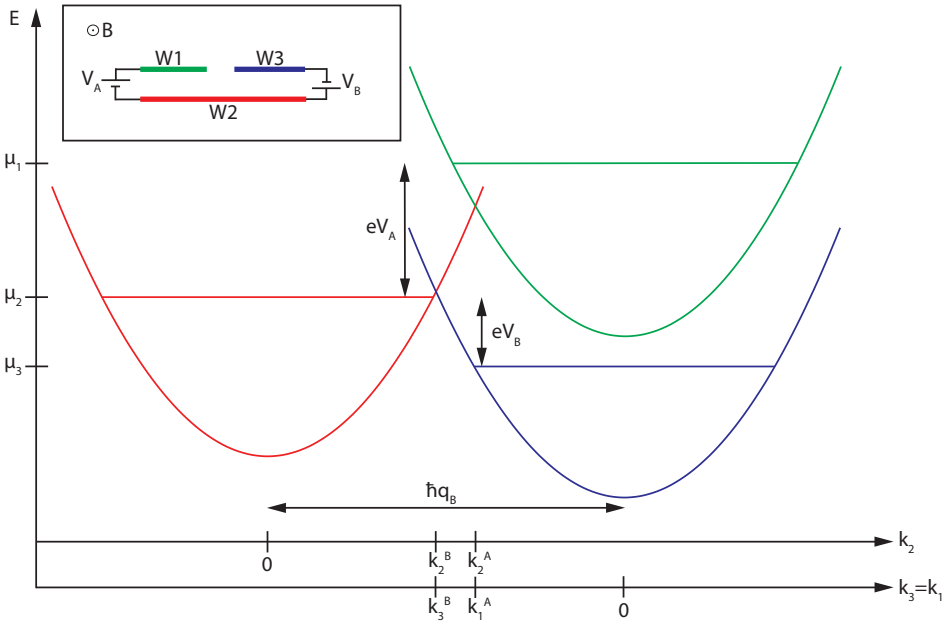

Figure 2.2: The dispersions for our three single-mode wires and how changing the system parameters B, V_A and V_B affects them. INSERT, the physical situation. Note that both voltages are negative in the case displayed. Tunneling is only possible between states at points where dispersions intersect, these have been labeled in terms of their wave-number. Since wave-numbers depends on which wire we are looking at, two wave-number axis have been added; one for the lower wire (2) and one for the upper wires (1 and 3).

To summarize: We have three dispersions and three independent parameters to adjust, two voltages and a magnetic field, which allows us to shift the dispersions vertically and horizontally respectively. If tunneling is to conserve both momentum and energy, it is only allowed between points, where the dispersions intersect. For the class of bands we consider (ones with a strictly positive curvature) two dispersions only intersect each other in precisely one point.[4] This allows us to address the different points along the dispersions separately and thus to perform spectroscopy on a 1D wire.

These results are summarized in Fig. 2.2. In this figure we have also introduced the

[3]We also use that the magnetic field has the same value at the two junctions. If technology would allow for a field gradient so large, that we could independently vary the magnetic field at position no more than a dozen micrometers separated, that would open up new possibilities for spectroscopy, as we could then move the three dispersions completely independent of each other. This may also open up new theoretical pits, as other system parameters may depend on the magnetic field, and they too would then vary across the system.

[4]If the two dispersions are not displaced horizontally with respect to each other, they may also intersect each other in no points at all or in every point. Since we are interested in the intersection of the dispersion of wire 2 with the dispersions of wire 1 and 3, this anomaly may only occur at zero magnetic field, and we shall simply eliminate this possibility from all further calculations. Thus henceforth $B > 0$ when necessary.

following notation for the wave-numbers of the states, where tunneling is allowed: k_2^A and k_1^A are the states where tunneling between wires 1 and 2 are allowed seen from the perspective of wire 2 and 1 respectively, correspondingly k_2^B and k_3^B are the states where tunneling between wires 3 and 2 are allowed as seen from the perspective of wire 2 and 3 respectively.

Now the purpose of this whole exercise becomes apparent. If we for instance want to examine how electrons relax, we could do the following: With one of the upper wires (wire 1) we inject electrons at a position k_2^A far above the Fermi sea in wire 2. With wire 3 we are able to extricate electrons from a position k_2^B in wire 2 of our choice, so we simple scan k_2^B between the Fermi sea and k_2^A while we monitor the current between wire 2 and 3. This current will say something about the distribution of electrons in wire 2 and (hopefully) thereby something about how the electron injected at k_2^A has relaxed.

2.4.2 Possibility of current

So we measure the current I_B in tunneling junction B between wire 2 and 3 and try to extract information about the relaxation in wire 2. However we suspect this relaxation contributes only slightly to the total current, and so we need to look at something which may drown in noise in an actual experiment.

This is why we now impose the requirement, that wire 2 and wire 3 are always kept at the same voltage, that is $V_B = 0$. By imposing this condition we ensure, that the only way for I_B to be non-zero is if wire 1 has somehow disturbed the equilibrium Fermi distribution of wire 2. But the tunneling of electrons between wire 1 and 2 is only possible, if they have a different degree of occupation at the single point where tunneling is possible, and thus the number

$$n_F(\varepsilon_{k_2^A} - \mu_2) - n_F(\varepsilon_{k_1^A} - \mu_1) \tag{2.5}$$

must be non-zero if we are to observe a current. For $T \neq 0$ this is the case everywhere except for the line $V_A = 0$, so what we really mean, is that the current is expected to be proportional to this number. In Fig. 2.3 we have plotted this function at zero temperature as a function of the two remaining free adjustable parameters, V_A and B. Note that we don't expect the current to be non-zero everywhere on the area thus defined, but under no circumstances can a current be measured outside of this area, since in these areas all three wires are in equilibrium at the positions, where tunneling is allowed. For a finite temperature in the Kelvin range no significant change of appearance is expected, only a small smearing of the edges between areas.

Several comments are in order. First of all what we see involves only wires 1 and 2 and is as such an example of the tunneling current between a pair of 1D wires. In this 2-wire case, the current *is* actually non-zero when $n_F(\varepsilon_{k_2^A} - \mu_2) - n_F(\varepsilon_{k_1^A} - \mu_1)$ is non-zero and so if one measures the current and plot the differential conductance $\frac{\partial I_B}{\partial V_A}$, one would observe lines which would correspond to the borders between the areas of Fig. 2.3.

These borders are easily understood with the help of our dispersion curves: If there is to be a tunneling current, the point where tunneling is allowed need to be occupied in one of the wires and unoccupied in the other wire. The border between the areas are then traced out by letting a Fermi point of one of the wires follow the dispersion of the other wire. It then follows that what we observe as the borders are actually just two copies of each of the dispersion turned ninety degrees and scaled according to the connection between $\hbar q_B$ and B and V_A and the chemical potentials. The two left-facing borders are the dispersion of the lower wire (wire 2) and the two right-facing borders are the dispersion of the upper wire (wire 1).

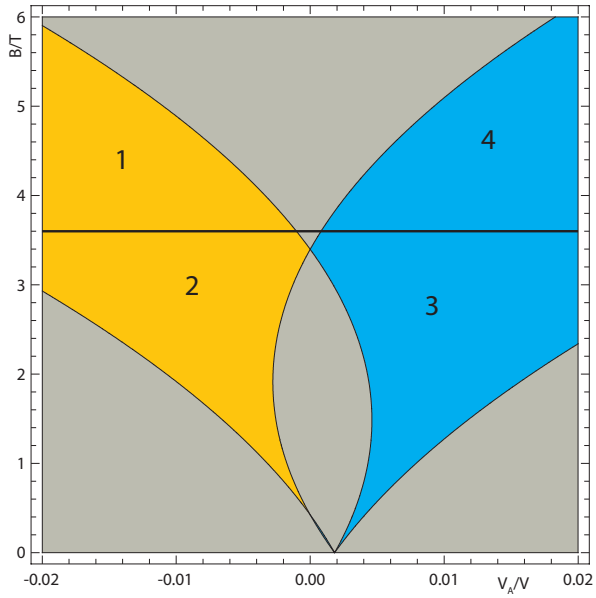

Figure 2.3: A plot of $n_F(\varepsilon_{k_2^A} - \mu_2) - n_F(\varepsilon_{k_1^A} - \mu_1)$ as a function of V_A and B with $V_B = 0$ at $T = 0$. In the yellow areas the value of the function is -1, in the blue areas it is $+1$ and in the grey areas it is 0. The very small area to the right of $V_A = 0$ is blue. We have used a quadratic dispersion with an effective electron mass $m^* = 0.067m_e$, m_e being the free electron mass. We have used reasonable values for the rest of the system parameters: $d = 31nm$, $k_{F1} = 0.7 \cdot 10^8 m^{-1}$, $k_{F2} = 0.9 \cdot 10^8 m^{-1}$, $k_{F3} = 0.8 \cdot 10^8 m^{-1}$.

Looking at the borders we observe two crossing points, a lower situated at zero magnetic field and at a finite voltage V_A' and an upper crossing point situated at zero bias voltage and at a finite magnetic field B'. The upper crossing point is the point where the negative Fermi point of one wire and the positive Fermi point of the other coincide and thus

$$\frac{eB'd}{\hbar} = q_{B'} = k_{F2} + k_{F1}, \tag{2.6}$$

whereas the lower crossing point corresponds to the two dispersions overlapping completely, and therefore

$$eV_A' = \varepsilon_{k_{F2}} - \varepsilon_{k_{F1}}. \tag{2.7}$$

From this we see, that from the two-wire experiment a lot of useful information about the wires could be extracted, namely the dispersions and the Fermi momentums.

2.4.3 Current mechanisms

Returning to Fig. 2.3, we have included a horizontal line at a B-field B'' determined by

$$\frac{eB''d}{\hbar} = q_{B''} = k_{F2} + k_{F3}.^5 \tag{2.8}$$

[5] If wire 1 and wire 3 have the same Fermi momentum, $B' = B''$ and the line will pass through the upper crossing point. We have deliberately chosen k_{F1} and k_{F2} to be slightly different, so as to distinguish between the two magnetic fields. In an actual experiment wire 1 and wire 3 are just segments of the same physical 1D wire and so may have very similar Fermi momentums.

Above this line (for $B > B''$), the wires 2 and 3 are both unoccupied at the point where tunneling between them may occur, whereas below this line (for $B < B''$), both wires are occupied at the tunneling point. This line along with the line $V_A = 0$ partitions the V_A-B-plane into four segments, which have been labeled 1-4 counterclockwise in the figure. In each of the partitions a current may run, but the mechanism for the current is different in each segment. In Fig. 2.4 we have sketched the four different situations and the relaxation in wire 2 which may or may not yield a current.

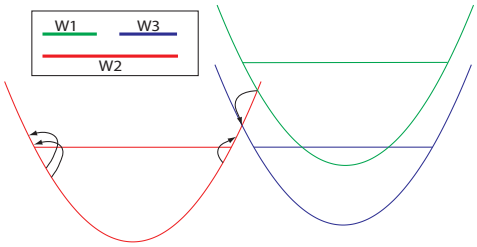

(a) Possible current in area 1. In this situation an electron from wire 1 enters wire 2 at k_2^A. It then relaxes in wire 2 from k_2^A to k_2^B where it can be picked up by wire 3. Since we cannot distinguish electrons, it may also equally well be an electron from the Fermi sea which has been excited to k_2^B, thus the figure is a bit misleading. I_B is negative.

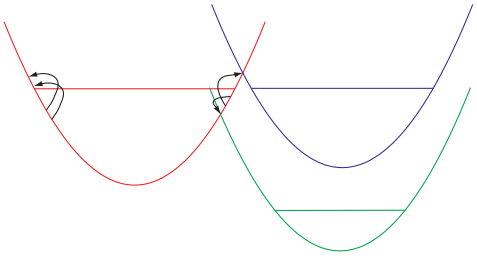

(b) Possible current in area 4. Here an electron at k_2^A has been removed by wire 1. This hole then relaxes towards the Fermi point creating at least one electron-hole pair, of one of which the electron ends up in k_2^B, where it can be picked up by wire 3. I_B is negative.

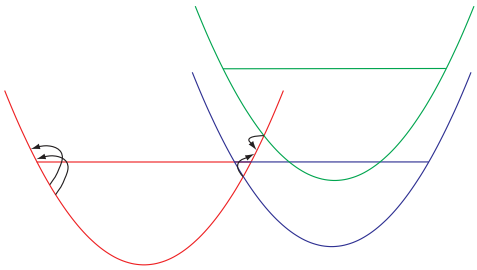

(c) Possible current in area 2. An electron from wire 1 enters wire 2 at k_2^A, where it then relaxes. At least one electron-hole pair is created with a hole situated at k_2^B, so an electron can enter at this position from wire 3. I_B is positive.

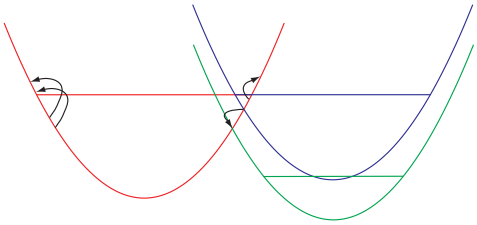

(d) Possible current in area 3. Here an electron is removed from k_2^A in wire 2 by wire 1. The hole at k_2^A relaxes towards the Fermi point either ending up in k_2^B or creating at least one electron-hole pair with a hole situated at k_2^B. Wire 3 then delivers an electron to this position. I_B is positive.

Figure 2.4: The possible mechanisms for a tunneling current in each of the four areas defined in the text and in Fig. 2.3. The electrons being excited up from the Fermi sea in all four cases represent the creation of electron-hole pairs. The Fermi Level has been changed in the right-handed figures for convenience only. INSERT: The color codes (see Fig. 2.2), which are as follows: wire 1 is green, wire 2 is red and wire 3 is blue.

2.5 Conclusion

In this chapter we have looked at a very specific device. First we described a possible way of manufacturing this device and next we looked at a primitive model for the current in through the device, a model which will be expanded on later.

We considered everything to be at zero temperature, but may wonder what (if anything) changes at a finite temperature. The Fermi distribution is no longer a sharp step function but changes smoothly from zero to one over an interval of width (in energy) comparable to k_BT. Replotting Fig. 2.2 at a finite, but small, cryogenic temperature (a couple of millikelvins), wont change its overall appearance, as k_BT is still very small compared to the Fermi energy[6], but will smoothen the edges. As for the four areas we introduced, they will now overlap, or formulated in another way, several of the processes depicted in Fig. 2.4 may contribute to the current at the same time.

[6]The smallest Fermi energi is approximately $33K$ for the choice of parameters in Fig. 2.3

Chapter 3

Impossibility of hole relaxation at zero temperature

We consider a single-mode 1D wire at zero temperature. In the ground state of the wire all electron states with energy below the Fermi energy ε_F (corresponding to states with momentum between $\pm\hbar k_F$) are occupied and all states with energy above are empty. The simplest way to excite this system is one of two things: either an electron can be put into the wire above the Fermi energy or an electron from below the Fermi energy can be removed from the wire (creation of a hole). In either case, momentum and energy conserving electron scattering could allow the excitation, be it an electron or a hole, to relax, that is to move closer to the Fermi energy, see Fig. 3.1 for examples of this, while creating one or more electron-hole pairs.

The class of bands we shall consider are those, which are an even function of k, $\varepsilon(k) = \varepsilon(-k)$, and have a positive, non-zero curvature everywhere, $\frac{\partial^2\varepsilon}{\partial k^2} > 0$.[1] We shall see, that in these bands, two-electron scattering - even at a finite temperature - cannot change the distribution function. Furthermore at zero temperature, a single hole cannot relax no matter how many other electrons are involved in the scattering.

We note that the class of bands considered include the good old quadratic band, $\varepsilon(k) = \frac{\hbar^2 k^2}{2m}$, since its curvature is just a positive constant ($\hbar^2/m$).

3.1 Two-particle scattering

We start by looking at two-particle processes.[2] If the two-electron scattering conserves energy and momentum, it is governed by

$$\varepsilon(k_1) + \varepsilon(k_2) = \varepsilon(k_1') + \varepsilon(k_2') \tag{3.1}$$

$$k_1 + k_2 = k_1' + k_2', \tag{3.2}$$

corresponding to a situation where electrons with momenta k_1 and k_2 scatter off each other and end up with momenta k_1' and k_2' respectively.[3] Defining the energy and momentum changes

[1] Thus we also require, that the second derivative exists everywhere. We will also assume that this second order derivative is nicely enough behaved, that it can again be integrated once and twice to yield the original functions. The choice of zero point of the dispersion is such that $\varepsilon(0) = 0$.

[2] Note, that since temperature does not enter at all in this section, it also applies to the case of finite temperature.

[3] If the spins of the electrons are equal, the electrons are indistinguishable, and all we really know is that after scattering one of them has momentum k_1' and the other has momentum k_2'. However for convenience we

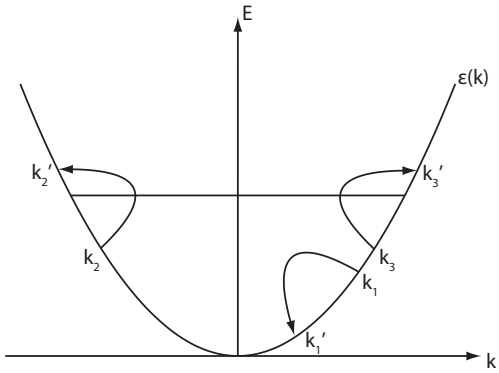

(a) Relaxation of a hole from k_1' to k_1 in which an electron moves the opposite way.

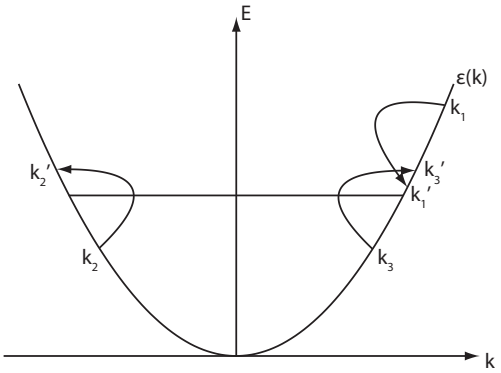

(b) Relaxation of an electron from k_1 to k_1'.

Figure 3.1: Examples of how an electron or a hole may relax by three-electron scattering in a quadratic band. In both cases two electrons are excited from below the Fermi energy (at k_2 and k_3) to above it (k_2' and k_3'), thus creating two electron-hole pairs.

for each electron as

$$\Delta E_i \equiv \varepsilon(k_i') - \varepsilon(k_i), \quad \Delta q_i \equiv k_i' - k_i, \qquad i = 1, 2, \tag{3.3}$$

eq's (3.1) and (3.2) now assumes the form $0 = \Delta q_1 + \Delta q_2$ and $0 = \Delta E_1 + \Delta E_2$ and so we note that ΔE_2 must be opposite in sign to ΔE_1 and likewise for the Δq's, and we may as well choose $\Delta E_1 \leq 0$, $\Delta q_1 \leq 0$ and $\Delta E_2 \geq 0$, $\Delta q_2 \geq 0$.[4] If $\Delta q_1 = \Delta q_2 = 0$ nothing happens at all (no change to the distribution function), so let us assume that they are non-zero, meaning that we can introduce the "average slope" α for each electron

$$\alpha_i \equiv \frac{\Delta E_i}{\Delta q_i} \geq 0. \tag{3.4}$$

If we define a generalized slope as a function of initial momentum k and momentum change $\Delta q \neq 0$ as

$$\alpha(k, \Delta q) \equiv \frac{\varepsilon(k + \Delta q) - \varepsilon(k)}{\Delta q}, \tag{3.5}$$

we get by differentiation

$$\frac{\partial \alpha(k, \Delta q)}{\partial k} = \frac{\frac{\partial \varepsilon}{\partial k}(k + \Delta q) - \frac{\partial \varepsilon}{\partial k}(k)}{\Delta q} > 0. \tag{3.6}$$

In the last step we use that the band is assumed to have a positive curvature everywhere, $\frac{\partial^2 \varepsilon}{\partial k^2} > 0$, which by integration yields $\frac{\partial \varepsilon}{\partial k}(k) > \frac{\partial \varepsilon}{\partial k}(q) \Leftrightarrow k > q$. We conclude that $\alpha(k, \Delta q)$ is a strictly growing function of k, i.e. that $\alpha(k, \Delta q) < \alpha(q, \Delta q) \Leftrightarrow k < q$. By combining everything

can think of them as described here, it doesn't really matter in this context.

[4] The sign of the Δq's can be changed by letting all $k \to -k$, which will not change the validity of a solution to eq's (3.1) and (3.2), since the band is even.

derived this far

$$\begin{aligned} 0 &= \Delta E_1 + \Delta E_2 = \alpha_1 \Delta q_1 + \alpha_2 \Delta q_2 = \Delta q_2(\alpha_2 - \alpha_1) && (3.7)\\ \Leftrightarrow 0 &= \alpha_2 - \alpha_1 = \frac{\varepsilon(k_2') - \varepsilon(k_2)}{\Delta q_2} - \frac{\varepsilon(k_1') - \varepsilon(k_1)}{\Delta q_1} \\ &= \frac{\varepsilon(k_2 + \Delta q_2) - \varepsilon(k_2)}{\Delta q_2} - \frac{\varepsilon(k_1') - \varepsilon(k_1' - \Delta q_1)}{\Delta q_1} \\ &= \frac{\varepsilon(k_2 + \Delta q_2) - \varepsilon(k_2)}{\Delta q_2} - \frac{\varepsilon(k_1') - \varepsilon(k_1' + \Delta q_2)}{-\Delta q_2} \\ &= \alpha(k_2, \Delta q_2) - \alpha(k_1', \Delta q_2) && (3.8)\\ \Leftrightarrow \alpha(k_2, \Delta q_2) &= \alpha(k_1', \Delta q_2) && (3.9)\\ \Leftrightarrow k_2 &= k_1' \Leftrightarrow k_2' = k_1. && (3.10) \end{aligned}$$

Thus the only processes allowed are those, where the two electrons exchange their momenta (or where nothing happens at all). We therefore conclude that an excited electron or hole cannot relax by a mechanism involving just a single other electron! An excited electron could however get its spin flipped by being exchanged with an electron with opposite spin, and similarly for holes, probably providing some sort of measurable effect somehow.

One could ask if the opposite is also true; is two-particle scattering possible in a band where the curvature is zero in just one finite interval?[5] The answer must be yes, provided that the two electrons scatter within this region of the band! Since the curvature is zero in a finite interval, by integration twice, the dispersion is linear in this interval. And for a linear dispersion (no matter how small), two-particle scattering is possible, since momentum and energy conservation amounts to the same thing.

3.2 Three-particle scattering

Since two-particle scattering is forbidden for the type of bands considered, we turn to the next order processes: three-particle scattering. The extra degrees of freedom introduced by the third electron guaranties, that in general three-particle scattering at a finite temperature is allowed.

However, it turns out, that at zero temperature, the relaxation of holes is impossible by three-particle processed. In other words, the equations

$$\begin{aligned} k_1 + k_2 + k_3 &= k_1' + k_2' + k_3' && (3.11)\\ \varepsilon(k_1) + \varepsilon(k_2) + \varepsilon(k_3) &= \varepsilon(k_1') + \varepsilon(k_2') + \varepsilon(k_3') && (3.12) \end{aligned}$$

have no solutions fulfilling $|k_2|, |k_3| < k_F$, $|k_2'|, |k_3'| > k_F$ and $k_F < |k_1'| < |k_1|$.[6] An easy explanation is as follows: the electron relaxing does so at a point, where the slope of the dispersion is "small" and so yields a relative low energy per momentum. The electrons being excited must do so at places, where the slope of the dispersion is numerically larger and so

[5] This is the second smallest relaxation of the requirement that the curvature be positive, non-zero everywhere. The smallest relaxation is that the curvature could be zero in a series of discrete points, but this probably still does not allow for two-particle scattering.

[6] We will label the relaxing electron 1 and the two electrons being excited 2 and 3. The label i will sometimes be used to refer to any one electrons and at other times to refer only to any one of the electrons being excited. Also we let k_i and k_i' denote the momentum of electron i before and after the scattering respectively.

spends relatively much energy per momentum. Thus if the momentum taken up by the excited electrons are to match the momentum given up by the relaxing electron, the excited electrons will have to absorb more energy than is given up by the first energy, which clearly departs with the concept of energy conservation.

But let us now proceed to prove this claim more rigourously. For ease of calculation we immediately recast the equations in dimensionless form; measuring wave-vectors in units of k_F and energies in units of ε_F. Using the same symbols for the new dimensionless variables, the equations (3.11) and (3.12) are unchanged, and the conditions under which they should have no solutions are $|k_2|, |k_3| < 1$, $|k_2'|, |k_3'| > 1$ and $1 < |k_1'| < |k_1|$. The dispersion now fulfills $\varepsilon(-1) = \varepsilon(1) = 1$, $\varepsilon(0) = 0$ and $\frac{\partial^2 \varepsilon(k)}{\partial k^2} > 0$.

As in the previous section we introduce the energy and momentum change for each electron as

$$\Delta E_i \equiv \varepsilon(k_i') - \varepsilon(k_i), \quad \Delta q_i \equiv k_i' - k_i, \qquad i = 1, 2, 3, \tag{3.13}$$

and note that if one of the Δq's was zero, that electron would just be a spectator and we would not be dealing with three-particle scattering. Thus all Δq's are non-zero and we can again introduce the average slope for each electron

$$\alpha_i \equiv \frac{\Delta E_i}{\Delta q_i}. \tag{3.14}$$

Furthermore we must have $\Delta E_1 \leq 0$ and $\Delta E_2, \Delta E_3 \geq 0$ by definition.

In order to deal effectively with the unknown sign of the k's, we treat the two branches of the dispersion separately and deal with right-movers (R) with $k > 0$ and left-movers (L) with $k < 0$. An electron which is excited out from below the Fermi energy, can do so in four different ways, α (R→R), β (R→L), γ (L→L) and δ (L→R), see Fig. 3.2. One would also expect the electron relaxing to be able to do so in four different ways, but because - as previously noted - the defining equations are symmetric under the mirror operation $k \to -k$, it is sufficient to look at just half of the cases: a (R→ R) and b (L→ R), see Fig. 3.2 as well.

3.2.1 Derivation of inequalities

Defining two functions of k as

$$f(k) = \varepsilon(k) - k \tag{3.15}$$
$$g(k) = \varepsilon(k) + k, \tag{3.16}$$

we immediately observe that $f(-1) = g(1) = 2$ and $f(0) = f(1) = g(-1) = g(0) = 0$. By differentiation twice, $\frac{\partial^2 f(k)}{\partial k^2} = \frac{\partial^2 g(k)}{\partial k^2} = \frac{\partial^2 \varepsilon(k)}{\partial k^2} > 0$, and so the derivative of f and g must be monotonously growing: $\frac{\partial f(k)}{\partial k} < \frac{\partial f(k+\delta k)}{\partial k} \Leftrightarrow \delta k > 0$ and likewise for g. This implies that each function can have at most one extremum, and looking at the functional values in -1, 0 and 1, this extremum must exist and be a minimum, located between 0 and 1 for f and between -1 and 0 for g. Away from this minimum each function must grow.

From these observations immediately follow the following inequalities for each of the 6 types of electron processes defined above:

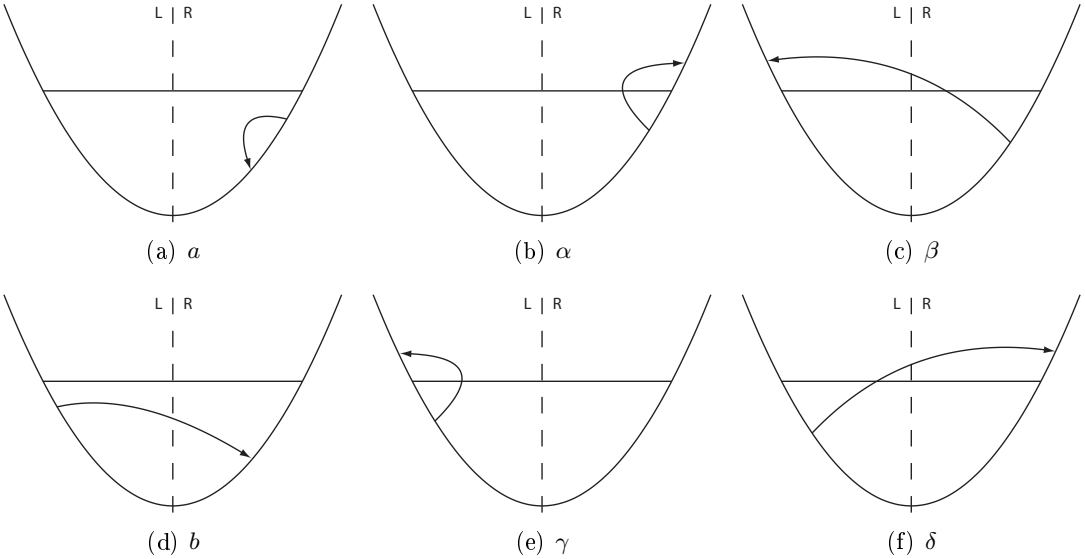

(a) a (b) α (c) β

(d) b (e) γ (f) δ

Figure 3.2: Definition of the four different ways an electron can be excited up from below the Fermi energy and of the two different (relevant) ways an electron inside the Fermi sea can relax.

$$
\begin{aligned}
\alpha: \quad & 0 < k_i < 1 < k_i' && \Rightarrow \Delta E_i - \Delta q_i = f(k_i') - f(k_i) > f(1) - f(k_i) \\
& && > f(1) - f(1) = 0 && (3.17)\\
\beta: \quad & k_i' < -1 < 0 < k_i < 1 && \Rightarrow \Delta E_i - \Delta q_i = f(k_i') - f(k_i) > f(-1) - f(1) = 2 && (3.18)\\
\gamma: \quad & k_i' < -1 < k_i < 0 && \Rightarrow \Delta E_i + \Delta q_i = g(k_i') - g(k_i) > g(-1) - g(-1) = 0 && (3.19)\\
\delta: \quad & -1 < k_i < 0 < 1 < k_i' && \Rightarrow \Delta E_i + \Delta q_i = g(k_i') - g(k_i) > g(1) - g(0) = 2 && (3.20)\\
a: \quad & 0 < k_1' < k_1 < 1 && \Rightarrow -2 < \Delta E_1 + \Delta q_1 < 0 && (3.21)\\
b: \quad & -1 < k_1 < 0 < k_1' < 1 && \Rightarrow \Delta E_1 + \Delta q_1 > 0 \wedge \Delta E_1 - \Delta q_1 < 0. && (3.22)
\end{aligned}
$$

We also introduce a generalized slope function, depending on two momenta

$$\alpha(k,k') \equiv \frac{\varepsilon(k') - \varepsilon(k)}{k' - k}, \tag{3.23}$$

which by differentiation with respect to the second index gives

$$
\begin{aligned}
\frac{\partial \alpha(k,k')}{\partial k'} &= \frac{\frac{\partial \varepsilon}{\partial k}(k')}{k'-k} - \frac{\varepsilon(k') - \varepsilon(k)}{(k'-k)^2} = \frac{1}{(k'-k)^2}\Big((k'-k)\frac{\partial \varepsilon}{\partial k}(k') - (\varepsilon(k') - \varepsilon(k))\Big) \\
&= \frac{1}{(k'-k)^2}\Big((k'-k)\frac{\partial \varepsilon}{\partial k}(k') - \int_k^{k'} \mathrm{d}k'' \frac{\partial \varepsilon}{\partial k}(k'')\Big) > 0. \qquad (3.24)
\end{aligned}
$$

The last step is realized by considering separately the two cases and evaluating the integrand up or down. For $k' > k$,

$$\int_k^{k'} \mathrm{d}k'' \frac{\partial \varepsilon}{\partial k}(k'') < \frac{\partial \varepsilon}{\partial k}(k') \int_k^{k'} \mathrm{d}k'' = \frac{\partial \varepsilon}{\partial k}(k')(k'-k), \tag{3.25}$$

while for $k' < k$

$$\int_k^{k'} \mathrm{d}k'' \frac{\partial \varepsilon}{\partial k}(k'') = -\int_{k'}^{k} \mathrm{d}k'' \frac{\partial \varepsilon}{\partial k}(k'') < -\frac{\partial \varepsilon}{\partial k}(k') \int_{k'}^{k} \mathrm{d}k'' = \frac{\partial \varepsilon}{\partial k}(k')(k'-k). \tag{3.26}$$

Because k and k' enter $\alpha(k,k')$ in a symmetrical manner, the derivative with respect to k must be positive as well. Thus $\alpha(k,k')$ must be a growing function of both momenta. With the help of this function, we immediately get the following relationship between the slopes of the intra-branch processes (α, γ and a)

$$a: \qquad \alpha_i > 0 \tag{3.27}$$

$$\alpha: \quad \alpha_i = \tfrac{\varepsilon(k_i')-\varepsilon(k_i)}{k_i'-k_i} = \alpha(k_i', k_i) > \alpha(k_1, k_i) > \alpha(k_1, k_1') = \alpha_1 \tag{3.28}$$

$$\gamma: \qquad \alpha_i < -\alpha_1. \tag{3.29}$$

To reach the first inequality we used that $k_i' > k_1$, because k_i' is the only of the four momenta to be above k_F, and that the electron being excited must start above where the relaxing electron ends up ($k_1' < k_i$) which follows from energy conservation. The second inequality follows by similar reasoning.

3.2.2 Proving impossibility of solutions

We now have the tools ready to prove the lack of solutions to the original problem. The three initial momenta are all interchangeable and all that matters are the number of left or right movers, giving us the four initial states RRR, RRL, RLL and LLL. The final momenta are not interchangeable as one of them should be positioned below the Fermi energy and we should thus distinguish between this electron, which can be either L or R and the remaining 2 electrons above the Fermi sea which can be either RR, RL or LL. This gives a total of $4 \times 2 \times 3 = 24$ situation to consider. Because of overall mirror symmetry, we need only look at half of these (12) so to be explicit, let us say that the final momentum below the Fermi surface is always an R.

We proceed to apply our tools to each of the individual cases. In general, apart from in the trivial cases, we assume the existence of a solution and proceed to prove that this leads to a contradiction. Because of the indistinguishability of electrons, we are free to choose which final momenta belongs to which initial momenta, if this helps us solve the problem.[7]

(1) RRR → RRR

We choose to regard this process at that of one a electron (1) and two α electrons (2 and 3), $\alpha_1 < \alpha_2, \alpha_3$ and $\Delta q_1, \Delta q_2 > 0$ and so we must have

$$0 = \Delta E_1 + \Delta E_2 + \Delta E_3 = \alpha_1 \Delta q_1 + \alpha_2 \Delta q_2 + \alpha_3 \Delta q_3 > \alpha_1(\Delta q_1 + \Delta q_2 + \Delta q_3) = 0. \tag{3.30}$$

(2) RRL → RRR

This case is easy. Since all electrons move towards higher momenta, momentum conservation is going to be hard to fulfill, and so the process is trivially forbidden.

[7] We are also free to do it, if it doesn't help us, but that would just be plain silly!

(3) RLL → RRR

This case is similar to the previous one.

(4) LLL → RRR

This case is similar to the two previous ones.

(5) RRR → RRL

This case consists of one a electron (1), an α electron (2) and a β electron (3), so $\alpha_2 > \alpha_1 > 0$, $\Delta q_2 > 0$, $\Delta E_3 > 0$ and $\Delta q_3 < 0$, yielding

$$\begin{aligned} 0 &= \Delta E_1 + \Delta E_2 + \Delta E_3 \\ &> \Delta E_1 + \Delta E_2 = \alpha_1 \Delta q_1 + \alpha_2 \Delta q_2 \\ &> \alpha_1(\Delta q_1 + \Delta q_2) = \alpha_1(-\Delta q_3) \\ &> 0. \end{aligned} \tag{3.31}$$

(6) RRL → RRL

We have one a electron (1), an α (2) and a γ (3), so $-\alpha_3, \alpha_2 > \alpha_1 > 0$ and $-\Delta q_3, \Delta q_2 > 0$, resulting in

$$\begin{aligned} 0 &= \Delta E_1 + \Delta E_2 + \Delta E_3 = \alpha_1 \Delta q_1 + \alpha_2 \Delta q_2 + \alpha_3 \Delta q_3 \\ &> \alpha_1(\Delta q_1 + \Delta q_2) + \alpha_3 \Delta q_3 = \Delta q_3(\alpha_3 - \alpha_1) \\ &> 0. \end{aligned} \tag{3.32}$$

(7) RLL → RRL

Here we have one a (1), a γ (2) and a δ (3), so we have $\Delta E_1 + \Delta q_1 > -2$, $\Delta E_2 + \Delta q_2 > 0$ and $\Delta E_3 + \Delta q_3 > 2$ and

$$\begin{aligned} 0 &= \Delta E_1 + \Delta E_2 + \Delta E_3 \\ &> -2 - \Delta q_1 - \Delta q_2 + 2 - \Delta q_3 = 0. \end{aligned} \tag{3.33}$$

(8) LLL → RRL

This process is composed of one b electron (1), a γ electron (2) and a δ electron (3). Using the inequalities $\Delta E_1 + \Delta q_1 > 0$, $\Delta E_2 + \Delta q_2 > 0$ and $\Delta E_3 + \Delta q_3 > 2$,

$$\begin{aligned} 0 &= \Delta E_1 + \Delta E_2 + \Delta E_3 \\ &> -\Delta q_1 - \Delta q_2 + 2 - \Delta q_3 = 2 \\ &> 0. \end{aligned} \tag{3.34}$$

(9) RRR → RLL

In this process all electrons jump towards lower momenta, so it can easily be excluded.

(10) RRL → RLL

This case is similar to the previous one.

(11) RLL → RLL

Excluded by same reason as the two previous ones.

(12) LLL → RLL

Here we have one b electron (1), and two γ electrons (2 and 3). Now $\Delta E_1 + \Delta q_1 > 0$, $\Delta E_2 + \Delta q_2 > 0$ and $\Delta E_3 + \Delta q_3 > 0$, so that

$$0 \quad = \quad \Delta E_1 + \Delta E_2 + \Delta E_3 > -\Delta q_1 - \Delta q_2 - \Delta q_3 = 0. \tag{3.35}$$

Since all of the 12 cases yielded either a contradiction (all of the form $0 > 0$) or could be excluded by (lack of) momentum conservation, we have now shown, that at zero temperature a single hole cannot relax by three-particle scattering.

3.3 N-particle scattering

In this section we will generalize the results of the previous section and show, that at zero temperature a single hole cannot relax by N-electron scattering ($N > 3$). Taken together with the two previous sections we then know, that at zero temperature a single hole cannot relax at all by scattering off other electrons in energy and momentum conserving processes.

Before the scattering there are N_R R electrons and N_L L electrons and after the scattering they have shifted to N'_R R electrons and N'_L L electrons, with $N_R + N_L = N'_L + N'_R = N$. Because of the overall mirror symmetry we require without loss of generalization that the final momentum below the Fermi momentum is always an R, so that $N'_R \geq 1$. In the scattering the first electron performs either an a-process or a b-process and of the remaining electrons n_α performs an α-process, n_β performs a β-process, n_γ performs a γ-process and n_δ performs a δ-process, and so $1 + n_\alpha + n_\beta + n_\gamma + n_\delta = N$. The set of electrons performing an α-process is denoted S_α and likewise for a, b, β, γ and δ.

The procedure with which we shall disprove the existence of solutions is the same as in the three-particle case; we assume the existence of a solution and using the inequalities derived previously along with energy and momentum conservation we lead this assumption to a contradiction. Again we are also free to imagine the initial and final momenta to be connected in any way we like, as to make the calculation easier. It turns out that we only need to consider four cases.

3.3.1 $N'_R = N_R$ and $N'_L = N_L$

We choose $n_a = 1$, $n_\alpha = N_R - 1$, $n_\beta = 0$, $n_\gamma = N_L$ and $N_\delta = 0$. We have the inequalities $\alpha_1 > 0$, $\forall i \in S_\alpha : \alpha_i > \alpha_1 \wedge \Delta q_i > 0$ and $\forall i \in S_\gamma : -\alpha_i > \alpha_1 \wedge -\Delta q_i > 0$, which results in

$$\begin{aligned} 0 &= \Delta E_1 + \sum_{i\in S_\alpha} \Delta E_i + \sum_{i\in S_\gamma} \Delta E_i = \alpha_1 \Delta q_1 + \sum_{i\in S_\alpha} \alpha_i \Delta q_i + \sum_{i\in S_\gamma} \alpha_i \Delta q_i \\ &> \alpha_1 \sum_{i\in S_a \cup S_\alpha} \Delta q_i + \sum_{i\in S_\gamma} \alpha_i \Delta q_i = \sum_{i\in S_\gamma} (\alpha_i - \alpha_1) \Delta q_i \\ &> 0. \end{aligned} \tag{3.36}$$

If $n_\alpha = 0$ the first inequality becomes an equality but the second inequality still holds and if instead $n_\gamma = 0$ it is the other way around. Since both cannot be zero at the same time (that would be a one electron process), this case is forbidden.

3.3.2 $N'_R = N_R - M$ and $N'_L = N_L + M$ with $M \geq 1$

We choose $n_a = 1$, $n_\alpha = N'_R - 1$, $n_\beta = M$, $n_\gamma = N_L$ and $N_\delta = 0$. If $n_\alpha = 0$ all electrons jump towards lower momenta and the process is trivially forbidden, so we let $n_\alpha \neq 0$. Using the inequalities $\alpha_1 > 0$, $\forall i \in S_\alpha : \alpha_i > \alpha_1$ and, $\forall i \in S_\beta \cup S_\gamma : \Delta q_i < 0 \wedge \Delta E_i > 0$, we get

$$\begin{aligned} 0 &= \Delta E_1 + \sum_{i\in S_\alpha} \Delta E_i + \sum_{i\in S_\beta \cup S_\gamma} \Delta E_i = \alpha_1 \Delta q_1 + \sum_{i\in S_\alpha} \alpha_i \Delta q_i + \sum_{i\in S_\beta \cup S_\gamma} \Delta E_i \\ &> \alpha_1 (\Delta q_1 + \sum_{i\in S_\alpha} \Delta q_i) + \sum_{i\in S_\beta \cup S_\gamma} \Delta E_i = \alpha_1 (- \sum_{i\in S_\beta \cup S_\gamma} \Delta q_i) + \sum_{i\in S_\beta \cup S_\gamma} \Delta E_i \\ &> \sum_{i\in S_\beta \cup S_\gamma} \Delta E_i \\ &> 0. \end{aligned} \tag{3.37}$$

3.3.3 $N'_R = N_R + M$ and $N'_L = N_L - M$ with $N_R = 0$

We choose $n_b = 1$, $n_\alpha = 0$, $n_\beta = 0$, $n_\gamma = N'_L$ and $N_\delta = M - 1$. With the help of the inequalities $\Delta E_1 + \Delta q_1 > 0$, $\forall i \in S_\gamma : \Delta E_i + \Delta q_i > 0$ and $\forall i \in S_\delta : \Delta E_i + \Delta q_i > 2$, we see that

$$\begin{aligned} 0 &= \Delta E_1 + \sum_{i\in S_\gamma} \Delta E_i + \sum_{i\in S_\delta} \Delta E_i \\ &> -\Delta q_1 + \sum_{i\in S_\gamma} (-\Delta q_i) + \sum_{i\in S_\delta} (2 - \Delta q_i) = 2n_\delta \\ &\geq 0. \end{aligned} \tag{3.38}$$

3.3.4 $N'_R = N_R + M$ and $N'_L = N_L - M$ with $N_R \geq 1$

We choose $n_a = 1$, $n_\alpha = N_R - 1$, $n_\beta = 0$, $n_\gamma = N'_L$ and $N_\delta = M \geq 1$. We have the following inequalities $\Delta E_1 + \Delta q_1 > -2$, $\forall i \in S_\alpha : \Delta E_i > 0 \wedge \Delta q_i > 0$, $\forall i \in S_\gamma : \Delta E_i + \Delta q_i > 0$ and

$\forall i \in S_\delta : \Delta E_i + \Delta q_i > 2$, which yield

$$\begin{aligned} 0 &= \sum_{i \in S_a \cup S_\alpha \cup S_\gamma \cup S_\delta} \Delta E_i \\ &> -2 - \Delta q_1 + \sum_{i \in S_\gamma} (-\Delta q_i) + \sum_{i \in S_\delta} (2 - \Delta q_i) = 2(n_\delta - 1) + \sum_{i \in S_\alpha} \Delta q_i \\ &> 2(n_\delta - 1) \\ &\geq 0. \end{aligned} \tag{3.39}$$

3.4 Concluding remarks

This chapter was a rather technical exercise. However the conclusion should not be lost in mathematical detail: it is energetically forbidden for a single hole to relax by scattering on a zero-temperature Fermi sea. As the hole must relax at a position where the average slope of dispersion is numerically smaller than at the position of the electron-hole pairs it create, there will be surplus momentum if energy is conserved (or a shortage of energy if momentum is conserved). The same conclusions (that holes cannot relax and electrons cannot relax by creating only a single electron-hole pair) are reached by [17] in what appears to be a graphical manner.

Chapter 4

Current in the incoherent regime using the Boltzmann Equation

In this chapter we will attempt to actually calculate the tunneling current through our system in the incoherent regime. Our approach will use the Boltzmann equation [18], which is a semi-classical transport equation. Semi-classical in this context means, that we work on a sufficiently large length and momentum scale that the electrons can be treated as classically well-defined particles, each having both a momentum and a position.[1] This enables us to introduce an electron distribution function, which is a probability distribution function describing the probability of finding electrons with a certain momentum at a certain position. The Boltzmann equation couples the "drift" evolution of the distribution function, that is the evolution due to the classical motion of the electrons, to the evolution due to collision between electrons or, as we shall use it, tunneling between wires, which effectively corresponds to coupled source and drain terms.

4.1 Setting up and solving

We model our system (see Fig. 4.1) as consisting of three one-dimensional, single-mode wires with leads. Each wire is described by an electron distribution function $g_i(k\sigma, x)$, $i = 1, 2, 3$ and is also assigned a chemical potential μ_i. Voltages are applied between the leads as shown, such that $\mu_3 - \mu_2 = eV_B$ and $\mu_2 - \mu_1 = eV_A$. We use that the tunneling barriers represent the majority of the electrical resistance in the circuit and therefore almost all of the voltage drops occur across the barriers and a single chemical potential can be assigned to each wire. Tunneling junctions exists between wire 1 and 2 (junction A) and between wire 2 and 3 (junction B). Furthermore a magnetic field B is applied perpendicular to (actually out of) the plane of the paper.

Each of the distribution functions is governed by a Boltzmann equation,

$$v_k \frac{\partial g_i(k\sigma, x)}{\partial x} = \Big(\frac{\partial g_i(k\sigma, x)}{\partial t}\Big)_{tunn.} + \Big(\frac{\partial g_i(k\sigma, x)}{\partial t}\Big)_{coll.} \quad , i = 1, 2, 3. \tag{4.1}$$

The first term on the right-hand side describes tunneling between the wires and will couple the equations to each other, while the second term describes intra-wire collisions, which only

[1] Quantum mechanically we know, that electrons cannot have well-defined values of momentum and position at the same instant of time.

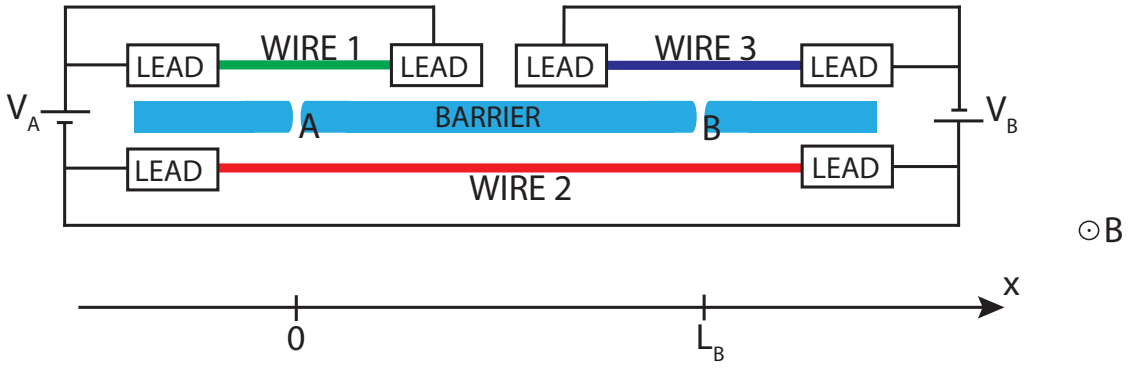

Figure 4.1: The system as we model it for calculating the current in the incoherent regime via the Boltzmann equation. Looking at a single of the three 1D wires both ends connects to a lead, both of which are kept at the same voltage. Between the leads of different wires bias DC voltages are applied as indicated. In between the upper wires and the lower wire is a barrier which has just two small openings, allowing electrons to transfer between wire 1 and wire 2 at tunneling junction A at $x = 0$ and between wire 2 and wire 3 at junction B at $x = L_B$.

involves the electrons of the wire in consideration. As it turns out, the collision terms are considerably more cumbersome to deal with than the tunneling terms, and so we will end up solving for the distribution functions (and ultimately for the tunneling current, which is what is measured) pertubatively in the collisions. Imagine that the collision terms can be written as

$$\left(\frac{\partial g_i(k\sigma, x)}{\partial t}\right)_{coll.} = \lambda A[g_i(k\sigma, x)], \tag{4.2}$$

where A is a dimensionless functional and λ is the coupling parameter. We then imagine writing the solution to Eq. (4.1), which will of course depend on λ, as a Taylor series in λ,

$$g_i(k\sigma, x) = g_i^{(0)}(k\sigma, x) + g_i^{(1)}(k\sigma, x) + g_i^{(2)}(k\sigma, x) + g_i^{(3)}(k\sigma, x) + \ldots, \tag{4.3}$$

where the upper index indicates to what order in λ that term is.

4.1.1 Tunneling terms

We model the tunneling between a pair of neighboring wires by the Hamiltonian

$$H_T = t \int_0^W \mathrm{d}x \Psi_{u\sigma}^\dagger(x) \Psi_{l\sigma}(x) \mathrm{e}^{-iq_B x} + H.c. \tag{4.4}$$

Here $\Psi_{i\sigma}(x)$ is the field operator that annihilates an electron in wire i of spin σ at position x, and $\Psi_{i\sigma}^\dagger(x)$ is the field operator that creates one. The indices u and l refer to the lower or upper wire. The term $\mathrm{e}^{-iq_B x}$ will eventually be responsible for the momentum boost gained by electrons when tunneling. t is the tunneling amplitude, which is assumed to be constant in the window from $x = 0$ to $x = W$ where tunneling is enabled by this Hamiltonian. This Hamiltonian also implies that when tunneling, an electron conserves its spin as well as its position along the wires.

Introducing the Fourier transform of the field operators

$$\Psi(x) = \frac{1}{\sqrt{L}} \sum_k c_k \mathrm{e}^{ikx} \qquad \Psi^\dagger(x) = \frac{1}{\sqrt{L}} \sum_k c_k^\dagger \mathrm{e}^{-ikx}, \tag{4.5}$$

[2] we can write H_T as

$$H_T = \frac{t}{L} \sum_{k_1 k_2} c^\dagger_{uk_1\sigma} c_{lk_2\sigma} f(k_2 - k_1 - q_B) + H.c., \tag{4.6}$$

where the function f, that determines how electron momentum can be changed upon tunneling, is

$$f(k) \equiv \int_0^W \mathrm{d}x \mathrm{e}^{ikx} = \frac{\mathrm{e}^{ikW} - 1}{ik}. \tag{4.7}$$

[3] Ideally we would like the function $|f(k)|$ to be nonzero only for $k = 0$, so that tunneling would conserve momentum, that is $k_2 = k_1 + q_B$. By rewriting the amplitude as $|f(k)| = 2|\sin(kW/2)/k|$, we observe a central peak centered at zero with side peaks of amplitudes which goes as $1/k^2$. The FWHM of the central peak, and thus also how much momentum conservation is violated, is of order $\Delta k = 2\pi/W$, so we need a large junction width to have momentum conservation. On the other hand, as we shall soon see, we also want the junctions to be relatively narrow, so that we can treat them as point-like in our Boltzmann equations.

We now want to determine the tunneling rate for transferring one electron from the state $k_u\sigma$ in the upper wire to the state $k_l\sigma$ in the lower wire. Starting in an initial state $|i\rangle$, an eigenstate of the number operators, and ending in a final state $|f\rangle$, the rate is dictated by the Fermi Golden Rule,

$$\Gamma_{f\leftarrow i} = \frac{2\pi}{\hbar} |\langle f|H_T|i\rangle|^2 \delta(E_f - E_i), \tag{4.8}$$

where the final state differs from the initial state by the moving of one electron from upper to lower wire,

$$|f\rangle = c^\dagger_{lk_l\sigma} c_{uk_u\sigma} |i\rangle. \tag{4.9}$$

By using H_T in the form Eq. (4.6), we quickly arrive at

$$\langle f|H_T|i\rangle = \frac{t^*}{L} f^*(k_l - k_u - q_B) \langle i|c^\dagger_{uk_u\sigma} c_{uk_u\sigma}|i\rangle \langle i|c_{lk_l\sigma} c^\dagger_{lk_l\sigma}|i\rangle \tag{4.10}$$

$$\Gamma_{f\leftarrow i} = \frac{2\pi}{\hbar} \frac{|t|^2}{L^2} |f(k_l - k_u - q_B)|^2 \langle i|c^\dagger_{uk_u\sigma} c_{uk_u\sigma}|i\rangle \langle i|c_{lk_l\sigma} c^\dagger_{lk_l\sigma}|i\rangle \delta(E_f - E_i). \tag{4.11}$$

This was the rate of tunneling for a specific initial state $|i\rangle$, to get to the more general rate we multiply by P_i, the probability for starting in this particular state, and sum over all initial states. Since we want the semi-classical distribution function to appear, we have to introduce some position dependence by hand. We arrive at

$$\Gamma_{lk_l\sigma\leftarrow uk_u\sigma} = \sum_i P_i \Gamma_{f\leftarrow i} \tag{4.12}$$

$$\Gamma_{lk_l\sigma\leftarrow uk_u\sigma}(x) = \begin{cases} \frac{2\pi}{\hbar} \frac{|t|^2}{L^2} |f(k_l - k_u - q_B)|^2 \cdot \\ \cdot g_u(k_u\sigma, x)\big(1 - g_l(k_l\sigma, x)\big)\delta(E_f - E_i) & 0 < x < W \\ 0 & \text{else} \end{cases} \tag{4.13}$$

[2] The wire is of length L and k is quantized on this length so that $k_n = n2\pi/L$. Since the length L will play no role, we use the same L for both wires.

[3] For $k = 0$ the integral gives trivially W and the right hand side converges to W for $k \to 0$.

Contained in this expression is the requirement, that electrons does not change their position when tunneling. The population of the upper wire state $k_u\sigma$ can change for two reasons due to tunneling alone; either electrons may enter the state by tunneling from the lower wire or they may leave the state by tunneling to the lower wire,

$$\begin{aligned}\Big(\frac{\partial g_u(k_u\sigma,x)}{\partial t}\Big)_{tunn.} &= \sum_{k_l}\Big(\Gamma_{uk_u\sigma\leftarrow lk_l\sigma}(x)-\Gamma_{lk_l\sigma\leftarrow uk_u\sigma}(x)\Big)\\ &= \begin{cases}\frac{2\pi}{\hbar}\frac{|t|^2}{L^2}\sum_{k_l}\big(g_l(k_l\sigma,x)-g_u(k_u\sigma,x)\big)\cdot & 0<x<W\\ \cdot|f(k_l-k_u-q_B)|^2\delta(E_f-E_i) & \\ 0 & \text{else}\end{cases}\end{aligned} \quad . (4.14)$$

A convenient partial cancelation of terms occurred. To continue we take the width to be such that $|f(k_l-k_u-q_B)|\to W\delta_{k_l,k_u+q_B}$. The energy conservation can be written

$$E_i-E_f=\varepsilon(k_l)-\varepsilon(k_u)+\big(\mu_l-\mu_u+\varepsilon(k_{Fu})-\varepsilon(k_{Fl})\big), \tag{4.15}$$

where we have introduced the chemical potential and Fermi wavenumber of each wires, their appearance are not really important at this stage, what matters is, that together the two delta-functions - representing energy and momentum conservation - allow only for a single value of k_u, which we shall denote k_u^*. This is the only momentum (in the upper wire) for which tunneling is possible. The sum over k_l is solved by first converting to an integral over k_l and then converting to an integral over energy. When the dust settles, what remains is (for $0<x<W$)

$$\begin{aligned}\Big(\frac{\partial g_u(k_u\sigma,x)}{\partial t}\Big)_{tunn.} &= \frac{2\pi}{\hbar}\frac{|t|^2}{L^2}W^2\sum_{k_l}\big(g_l(k_l\sigma,x)-g_u(k_u\sigma,x)\big)\delta_{k_l,k_u+q_B}\delta(E_f-E_i) \qquad (4.16)\\ &= \frac{2\pi}{\hbar}\frac{|t|^2}{L^2}W^2\big(g_l(k_u^*+q_B\sigma,x)-g_u(k_u^*\sigma,x)\big)\frac{L}{2\pi}\Big(\frac{\partial\varepsilon(k_l)}{\partial k_l}\Big)^{-1}\Big|_{k_l=k_u^*+q_B}\delta_{k_u,k_u^*}.\end{aligned}$$

Apart from a lot of constants, this rate contains a difference in occupation in the two wires at the points where tunneling is possible and the density of states of the other wire at the relevant momentum. In the following we will collect everything apart from the distribution function in a tunneling rate Γ, and we will assume that this rate is a constant. This is done purely out of convenience, as it would not be too hard to include the just found dependence on momenta.

4.1.2 Tunneling terms for 3-wire system

We now return to the full 3-wire situation in which we have one lower wire and two segments of upper wire. Along with the requirement of energy conservation in the single tunneling event, since we are in the incoherent regime, this allows tunneling at a specific junction only if the electron possesses a certain momentum. If the tunneling should be possible at junction A the electron must possess a momentum $\hbar k_1^A$ in wire 1 or a momentum $\hbar k_2^A$ in wire 2 and be at the position $x=0$, and likewise for tunneling junction B, which is situated at $x=L_B$.

We thus write the tunneling terms as

$$\Big(\frac{\partial g_1(k\sigma,x)}{\partial t}\Big)_{tunn.} = \Gamma_A\big(g_2(k+q_B\sigma,x)-g_1(k\sigma,x)\big)f(k-k_1^A,Q_A)f(x,W_A) \quad (4.17)$$

$$\begin{aligned}\Big(\frac{\partial g_2(k\sigma,x)}{\partial t}\Big)_{tunn.} &= \Gamma_A\big(g_1(k-q_B\sigma,x)-g_2(k\sigma,x)\big)f(k-k_2^A,Q_A)f(x,W_A)\\ &+ \Gamma_B\big(g_3(k-q_B\sigma,x)-g_2(k\sigma,x)\big)f(k-k_2^B,Q_B)\cdot\\ &\cdot f(x-L_B,W_B) \quad (4.18)\end{aligned}$$

$$\begin{aligned}\Big(\frac{\partial g_3(k\sigma,x)}{\partial t}\Big)_{tunn.} &= \Gamma_B\big(g_2(k+q_B\sigma,x)-g_3(k\sigma,x)\big)f(k-k_3^B,Q_B)\cdot\\ &\cdot f(x-L_B,W_B). \quad (4.19)\end{aligned}$$

The function f,

$$f(y,\Delta)\equiv\Theta(y+\Delta/2)-\Theta(y-\Delta/2), \quad (4.20)$$

where Θ is the step function, plays the role of defining the tunneling junctions. Essentially because of the approximations we will make along the way, we may as well have used a delta-function, but that turned out to be a bit difficult to work with; therefore this peculiar choice. What is means, as seen from wire 1, is the following: a tunneling window is open around position $x=0$ of width W_A, where electrons may tunnel to wire 2 if their wavenumber lies in the window centered at k_1^A with width Q_A. For all electrons in the window, the tunneling rate is equal and given by Γ_A, assuming no occupancy of the receiving state.

The leads are supposedly perfect, absorbing all incoming states and filling the outgoing states according to a Fermi distribution. We write the boundary condition in a single wire as

$$g_i(k\sigma,x)=n_F(\varepsilon_k-\mu_i) \quad \text{for}\begin{cases} x\to\infty & ,k<0\\ x\to-\infty & ,k>0\end{cases}. \quad (4.21)$$

For the single wire, if one sits to the right of all tunneling junctions, the left-moving electrons are Fermi distributed and likewise for right-moving electrons to the left of all tunneling junctions. For the upper wires this is a coarse approximation, as the lead sits only in one end of the wire. A more realistic boundary condition would require the electrons to reflect perfectly at the wire end not containing the lead.

We are at this point interested in solving for the distribution function to zeroth order in the collisions, that is to determine $g_i^{(0)}$. These are easily seen to be the solution to the equations

$$v_k\frac{\partial g_i^{(0)}(k\sigma,x)}{\partial x}=\Big(\frac{\partial g_i(k\sigma,x)}{\partial t}\Big)^{(0)}_{tunn.} \quad ,i=1,2,3, \quad (4.22)$$

since no collisions may be involved. For $k>0$, integrating from $-\infty$, we find that,

$$v_k\big(g_i^{(0)}(k\sigma,x)-n_F(\varepsilon_k-\mu_i)\big)=\int_{-\infty}^{x}\mathrm{d}x' v_k\frac{\partial g_i^{(0)}(k\sigma,x')}{\partial x'}=\int_{-\infty}^{x}\mathrm{d}x'\Big(\frac{\partial g_i(k\sigma,x')}{\partial t}\Big)^{(0)}_{tunn.}. \quad (4.23)$$

A very simplifying assumption at this point, is that the junction widths W_A and W_B are sufficiently small, that we may treat the distribution functions as being constants along the width of the junctions in both position and momentum space. Recognizing that the tunneling terms to zeroth order in the collisions are just the expressions Eq.s (4.17) with the zeroth order distribution functions $g_i^{(0)}$ inserted. This allows everything except the junction-defining

function $f(x)$ to be pulled outside the integral and thus we arrive at the following for wire 1 (still only valid for $k > 0$)

$$v_k\big(g_1^{(0)}(k\sigma,x)-n_F(\varepsilon_k-\mu_1)\big) = \Gamma_A\big(g_2^{(0)}(k_2^A\sigma,0)-g_1^{(0)}(k_1^A\sigma,0)\big)f(k-k_1^A,Q_A)F(x,W_A), \quad (4.24)$$

where F is the integral of f,

$$F(x-L,\Delta) \equiv \int_{-\infty}^{x} \mathrm{d}x' f(x'-L,\Delta) = \begin{cases} 0 & ,x \le L-\frac{\Delta}{2} \\ x-L+\frac{\Delta}{2} & ,L-\frac{\Delta}{2} \le x \le L+\frac{\Delta}{2} \\ \Delta & ,L+\frac{\Delta}{2} \le x \end{cases} .$$

For $k < 0$ we integrate Eq.s (4.22) from $+\infty$ and arrive for wire 1 at

$$\begin{aligned} v_k\big(g_1^{(0)}(k\sigma,x) - n_F(\varepsilon_k-\mu_1)\big) &= -\Gamma_A\big(g_2^{(0)}(k_2^A\sigma,0) - g_1^{(0)}(k_1^A\sigma,0)\big)\cdot \\ &\quad \cdot f(k-k_1^A,Q_A)F(-x,W_A), \end{aligned} \quad (4.25)$$

because

$$\int_{\infty}^{x} \mathrm{d}x' f(x'-L,\Delta) = F(x-L,\Delta) - \Delta = -F(L-x,\Delta). \quad (4.26)$$

Using that $sgn(v_k) = sgn(k)$[4], Eq. (4.24) and Eq. (4.25) can be recombined to a single equation. By simple rearrangements, the resulting expressions concerning all three wires valid for all $k \neq 0$ are

$$\begin{aligned} g_1^{(0)}(k\sigma,x) &= n_F(\varepsilon_k-\mu_1) + \frac{\Gamma_A}{|v_k|}\big(g_2^{(0)}(k_2^A\sigma,0) - g_1^{(0)}(k_1^A\sigma,0)\big)f(k-k_1^A,Q_A) \\ &\quad \big(F(x,W_A)\Theta(k) + F(-x,W_A)\Theta(-k)\big) \end{aligned} \quad (4.27)$$

$$\begin{aligned} g_2^{(0)}(k\sigma,x) &= n_F(\varepsilon_k-\mu_2) + \frac{\Gamma_A}{|v_k|}\big(g_1^{(0)}(k_1^A\sigma,0) - g_2^{(0)}(k_2^A\sigma,0)\big)f(k-k_2^A,Q_A) \\ &\quad \big(F(x,W_A)\Theta(k) + F(-x,W_A)\Theta(-k)\big) \\ &\quad + \frac{\Gamma_B}{|v_k|}\big(g_3^{(0)}(k_3^B\sigma,L_B) - g_2^{(0)}(k_2^B\sigma,L_B)\big)f(k-k_2^B,Q_B) \\ &\quad \big(F(x-L_B,W_B)\Theta(k) + F(L_B-x,W_B)\Theta(-k)\big) \end{aligned} \quad (4.28)$$

$$\begin{aligned} g_3^{(0)}(k\sigma,x) &= n_F(\varepsilon_k-\mu_3) + \frac{\Gamma_B}{|v_k|}\big(g_2^{(0)}(k_2^B\sigma,L_B) - g_3^{(0)}(k_3^B\sigma,L_B)\big)f(k-k_3^B,Q_B) \\ &\quad \big(F(x-L_B,W_B)\Theta(k) + F(L_B-x,W_B)\Theta(-k)\big) \end{aligned} \quad (4.29)$$

In order to proceed we need justify another assumption: that the tunneling windows overlap in neither momentum nor position space. That they do not overlap in position space is straightforward, that follows from the physical realization of the system, the wires 1 and 3 simply does not extend across each other and so tunneling to wire 2 must occur at different positions along wire 2. That the windows do not overlap in momentum space is actually not a necessity. There may be choices of the bias voltages and magnetic field, where $k_2^A = k_2^B$ and where as a consequence a current could run even in the absence of collisions. However, we will simply impose on our system, the requirement, that this is not the case. Were it the case, the dominating contribution to the overall current would be the noninteracting one, which is beyond this approach.

[4] This follows from the positive curvature of the dispersion.

By evaluating at the right positions and solving, we find, that the distribution functions to zeroth order in the collisions are

$$\begin{aligned} g_1^{(0)}(k\sigma,x) &= n_F(\varepsilon_k-\mu_1)+\frac{\Gamma_A}{|v_k|}f(k-k_1^A,Q_A)\big(F(x,W_A)\Theta(k)+F(-x,W_A)\Theta(-k)\big)\cdot \\ &\quad\cdot\frac{n_F(\varepsilon_{k_2^A}-\mu_2)-n_F(\varepsilon_{k_1^A}-\mu_1)}{1+\frac{1}{2}\Gamma_A W_A(|v_{k_2^A}|^{-1}+|v_{k_1^A}|^{-1})} \end{aligned} \tag{4.30}$$

$$\begin{aligned} g_2^{(0)}(k\sigma,x) &= n_F(\varepsilon_k-\mu_2) \\ &\quad+\frac{\Gamma_B}{|v_k|}f(k-k_2^B,Q_B)\big(F(x-L_B,W_B)\Theta(k)+F(L_B-x,W_B)\Theta(-k)\big)\cdot \\ &\quad\cdot\frac{n_F(\varepsilon_{k_3^B}-\mu_3)-n_F(\varepsilon_{k_2^B}-\mu_2)}{1+\frac{1}{2}\Gamma_B W_B(|v_{k_2^B}|^{-1}+|v_{k_3^B}|^{-1})} \\ &\quad+\frac{\Gamma_A}{|v_k|}f(k-k_2^A,Q_A)\big(F(x,W_A)\Theta(k)+F(-x,W_A)\Theta(-k)\big)\cdot \\ &\quad\cdot\frac{n_F(\varepsilon_{k_1^A}-\mu_1)-n_F(\varepsilon_{k_2^A}-\mu_2)}{1+\frac{1}{2}\Gamma_A W_A(|v_{k_2^A}|^{-1}+|v_{k_1^A}|^{-1})} \end{aligned} \tag{4.31}$$

$$\begin{aligned} g_3^{(0)}(k\sigma,x) &= n_F(\varepsilon_k-\mu_3)+\frac{\Gamma_B}{|v_k|}f(k-k_3^B,Q_B)\big(F(x-L_B,W_B)\Theta(k) \\ &\quad+F(L_B-x,W_B)\Theta(-k)\big)\frac{n_F(\varepsilon_{k_2^B}-\mu_2)-n_F(\varepsilon_{k_3^B}-\mu_1)}{1+\frac{1}{2}\Gamma_B W_B(|v_{k_2^B}|^{-1}+|v_{k_3^B}|^{-1})}. \end{aligned} \tag{4.32}$$

One may wonder whether these functions represents valid distribution functions, do their values lay between 0 and 1? The short answer is luckily yes. At k-values where electrons cannot tunnel, the property is trivially true, since all g's then are just Fermi distributions. Since the functions are well-behaved (sort of) with respect to x, what happens at the positions of the tunneling junctions is not relevant, since that would be single points compared to the whole length of the wire between the junctions.[5] Finally the most interesting things may happen for k-values in the tunneling windows but away from the tunneling junctions. Looking at only one of the distribution functions, since the argument is trivially extended to include the others, we rewrite,

$$\begin{aligned} g_1^{(0)}(k_1^A\sigma,x) &= n_F(\varepsilon_{k_1^A}-\mu_1)+\frac{\widetilde{\Gamma}_A W_A}{2|v_{k_1^A}|}\big(n_F(\varepsilon_{k_2^A}-\mu_2)-n_F(\varepsilon_{k_1^A}-\mu_1)\big) \\ &= n_F(\varepsilon_{k_1^A}-\mu_1)\Big(1-\frac{\widetilde{\Gamma}_A W_A}{2|v_{k_1^A}|}\Big)+n_F(\varepsilon_{k_2^A}-\mu_2)\Big(\frac{\widetilde{\Gamma}_A W_A}{2|v_{k_1^A}|}\Big) \\ &= n_F(\varepsilon_{k_1^A}-\mu_1)\Big(\frac{1+\frac{\Gamma_A W_A}{2|v_{k_2^A}|}}{1+\frac{1}{2}\Gamma_A W_A(|v_{k_2^A}|^{-1}+|v_{k_1^A}|^{-1})}\Big)+n_F(\varepsilon_{k_2^A}-\mu_2)\Big(\frac{\widetilde{\Gamma}_A W_A}{2|v_{k_1^A}|}\Big). \end{aligned}$$

The second RHS expression is upward bound by $\left(1-\frac{\widetilde{\Gamma}_A W_A}{2|v_{k_1^A}|}\right)+\left(\frac{\widetilde{\Gamma}_A W_A}{2|v_{k_1^A}|}\right)=1$ and the third RHS expression is always positive, and so $0<g_1^{(0)}(k_1^A\sigma,x)<1$ as hoped for.

[5] But don't worry, the g's also fulfill the condition $0\le g\le 1$ at these points.

4.1.3 Current

In the experiment we don't measure the distribution functions, but rather a current. The tunneling current from wire 2 to wire 3 is arrived at using Eq. (4.19),

$$\begin{aligned} I_B &= (-e)\sum_\sigma \int_{-\infty}^{\infty} \mathrm{d}x \int_{-\infty}^{\infty} \frac{\mathrm{d}k}{2\pi} \Big(\frac{\partial g_3(k\sigma, x)}{\partial t} \Big)_{tunn.} \\ &= (-e)\Gamma_B \frac{Q_B W_B}{2\pi} \sum_\sigma \big(g_2(k_2^B \sigma, L_B) - g_3(k_3^B \sigma, L_B) \big). \end{aligned} \tag{4.33}$$

To zeroth order in the collisions, this current is

$$\begin{aligned} I_B^{(0)} &= (-e)\Gamma_B \frac{Q_B W_B}{2\pi} \sum_\sigma \big(g_2^{(0)}(k_2^B \sigma, L_B) - g_3^{(0)}(k_3^B \sigma, L_B) \big) \\ &= (-e)\Gamma_B \frac{Q_B W_B}{2\pi} 2 \frac{n_F(\varepsilon_{k_2^B} - \mu_2) - n_F(\varepsilon_{k_3^B} - \mu_3)}{1 + \frac{1}{2}\Gamma_B W_B (|v_{k_2^B}|^{-1} + |v_{k_3^B}|^{-1})}, \end{aligned} \tag{4.34}$$

an expression we more or less would have expected, it involves the difference in occupations of the one state in each wire, where tunneling is allowed, and then a lot of other stuff. Looking at the denominator we observe, that the smaller the velocities of the tunneling electrons are the smaller apparently is the current. This is easily explained; if the electrons from the source wire are slow to move, they take time to arrive in the tunneling windows, likewise in the drain, here the slow-moving electrons will remain longer in the tunneling window and thus blocking further tunneling electrons. The remainder of the numerator is just proportionalities, the current is of course proportional to both the charge of the charge carriers, the tunneling rate and the width of the tunneling junction in both position and momentum space. Finally there is a factor 2 due to spin.

We have till this point solved everything to infinite order (ie. self-consistently) in the tunneling and seen that it is possible. The results are, however, rather ugly to look at, because of the denominators. But the infinite-order results are nothing but a normalization of the first order results. Defining new tunneling rates $\widetilde{\Gamma}_A$ and $\widetilde{\Gamma}_B$,

$$\widetilde{\Gamma}_A \equiv \frac{\Gamma_A}{1 + \frac{1}{2}\Gamma_A W_A (|v_{k_2^A}|^{-1} + |v_{k_1^A}|^{-1})} \qquad \widetilde{\Gamma}_B \equiv \frac{\Gamma_B}{1 + \frac{1}{2}\Gamma_B W_B (|v_{k_2^B}|^{-1} + |v_{k_3^B}|^{-1})}, \tag{4.35}$$

all results hitherto obtained (Eq.s (4.30), (4.31), (4.32) and (4.34)) can be written without the ugly denominator by replacing the Γ in the numerator by $\widetilde{\Gamma}$.

4.1.4 Collision terms

We are now ready to implement the interesting part of the Boltzmann equation Eq. (4.1), the intra-wire collisions. We consider a single, single-mode wire.[6] Only multiple electron-electron scattering are taken into account, that is no impurity scattering. The simplest possibility is

[6] Since we in this section deal only with a single wire at a time, we will omit the wire index for the time being.

two-electron scattering, the rate for which is

$$\Gamma_{k'_a\sigma_a,k'_b\sigma_b\leftarrow k_a\sigma_a,k_b\sigma_b} = \sum_i P_i\Gamma_{f\leftarrow i} \tag{4.36}$$

$$\Gamma_{f\leftarrow i} = \frac{2\pi}{\hbar}|\langle f|V|i\rangle|^2\delta(E_f - E_i) \tag{4.37}$$

$$|f\rangle = c^\dagger_{k'_a\sigma_a}c^\dagger_{k'_b\sigma_b}c_{k_b\sigma_b}c_{k_a\sigma_a}|i\rangle \tag{4.38}$$

$$V = \frac{1}{2L}\sum_{k_1k_2q}\sum_{\sigma_1\sigma_2} c^\dagger_{k_1+q\sigma_1}c^\dagger_{k_2-q\sigma_2}U_q c_{k_2\sigma_2}c_{k_1\sigma_1} \tag{4.39}$$

$$E_f - E_i = \varepsilon_{k'_a} + \varepsilon_{k'_b} - \varepsilon_{k_a} - \varepsilon_{k_b}. \tag{4.40}$$

Since V conserves momentum and because of overall translational symmetry of the wire in consideration, the initial and final state must have the same momentum, which again implies that $k'_a + k'_b = k_a + k_b$. Thus the rate contains both energy and momentum conservation,

$$\Gamma_{k'_a\sigma_a,k'_b\sigma_b\leftarrow k_a\sigma_a,k_b\sigma_b} \propto \delta_{k_a+k_b,k'_a+k'_b}\delta(\varepsilon_{k'_a} + \varepsilon_{k'_b} - \varepsilon_{k_a} - \varepsilon_{k_b}). \tag{4.41}$$

For the class of bands we consider, the only possible solutions are $k_a = k'_a \wedge k_b = k'_b$ and $k_a = k'_b \wedge k_b = k'_a$ cf. section (). Thus two-electron scattering can at most lead to a spin-flip. If the leads supply a non spin-polarized current, this possibility of spin-flip can lead to no contribution to the current, due to a pure symmetry argument. If however we imagine supplying a spin-polarized current and also measuring a spin-polarized current, two-electron scattering may lead to a change in current.

The next level of complexity is the three-electron scattering. This in general will give a contribution to the current, since there are non-trivial solutions to the three-body energy and momentum conserving scattering. Calculating the rate $\Gamma_{f\leftarrow i}$ is the subject of the next subsection. From this rate is easily derived the corresponding Boltzmann term.

4.1.5 Calculating the three particle scattering rate

The system starts out in some fock-state $|i\rangle$ and ends up in another fock-state $|f\rangle$, which is separated from $|i\rangle$ by the reshuffling of precisely three electrons. Thus we can write

$$|f\rangle = c^\dagger_{a'}c^\dagger_{b'}c^\dagger_{c'}c_c c_b c_a|i\rangle. \tag{4.42}$$

We require, that the same wavenumber does not appear in both the group of unprimed wavenumbers and the group of primed wavenumbers (but may appear more than once in the same group) to ensure, that we are dealing with genuine three-particle processes. What goes into the scattering rate is the expression

$$\langle f|T|i\rangle = \langle i|c^\dagger_a c^\dagger_b c^\dagger_c c_{c'}c_{b'}c_{a'}T|i\rangle = \langle i|c^\dagger_a c^\dagger_b c^\dagger_c c_{c'}c_{b'}c_{a'}(V + VG_0V + VG_0VG_0V + \ldots)|i\rangle, \tag{4.43}$$

where

$$T = V + VG_0T = V + VG_0V + VG_0VG_0V + \ldots \tag{4.44}$$

$$G_0 = \frac{1}{E_i - H_0 + \mathrm{i}\eta} \tag{4.45}$$

$$H_0 = \sum_{k\sigma}\varepsilon_k c^\dagger_{k\sigma}c_{k\sigma} = \sum_{k\sigma}\varepsilon_k n_{k\sigma} \tag{4.46}$$

$$V = \frac{1}{2L}\sum_{k_1k_2q}\sum_{\sigma_1\sigma_2} c^\dagger_{k_1+q\sigma_1}c^\dagger_{k_2-q\sigma_2}U_q c_{k_2\sigma_2}c_{k_1\sigma_1}. \tag{4.47}$$

Here T is the so-called T-matrix, G_0 the free propagator, H_0 the non-interacting Hamiltonian containing the single particle dispersion ε, and V is the interaction in second quantization, in which appears V_q, which is the Fourier transform of the (first quantization) interaction.[7]. We are now going to calculate $\langle f|T|i\rangle$. Since whatever operates on the initial state ket $|i\rangle$ must in the end bring us back to the same state for this to yield something non-zero, the term to first order in V is zero, since a single V can at most remove electrons from two of the unprimed states, and the remaining three c's with primed indices cannot help us (since we required all primed states to be different from the unprimed states). The next term, that to second order in V, is generally non-zero, and will thus be the focus of our main concern,

$$\langle i|c_a^\dagger c_b^\dagger c_c^\dagger c_{c'} c_{b'} c_{a'} V G_0 V|i\rangle = \frac{1}{4L^2}\sum_{k_1k_2q}\sum_{\sigma_1\sigma_2}\sum_{k_1'k_2'q'}\sum_{\sigma_1'\sigma_2'}\frac{U_qU_{q'}}{\varepsilon_{k_2'}+\varepsilon_{k_1'}-\varepsilon_{k_2'-q'}-\varepsilon_{k_1'+q'}+\mathrm{i}\eta}\cdot$$
$$\cdot\langle i|c_a^\dagger c_b^\dagger c_c^\dagger c_{c'} c_{b'} c_{a'} c_{k_1+q\sigma_1}^\dagger c_{k_2-q\sigma_2}^\dagger c_{k_2\sigma_2} c_{k_1\sigma_1} c_{k_1'+q'\sigma_1'}^\dagger c_{k_2'-q'\sigma_2'}^\dagger c_{k_2'\sigma_2'} c_{k_1'\sigma_1'}|i\rangle. \quad (4.48)$$

We need to look at all the possible pairings of operators, each pair consisting of a raising operator and a lowering operator. There can be no pairing between the 3 c's and the three $c^\dagger$'s, since their arguments are never equal. Thus each of these 6 ladder operators must be paired with an operator coming from one of the V's. Pairing internally in a V is also not possible, because if one pair of operators in a V were to have the same argument, the other pair is forced also to have equal arguments, this V would then perform absolutely no function (other than multiplying with U_q evaluated at some q) and with only the other V left, the result would be zero; as of the reason of throwing away the term linear in V. Conclusion: there must be a pairing between a c from one V and a $c^\dagger$ from the other V, which can be done in $4+4=8$ ways.[8]

Let us take a closer look at two of these eight terms. Consider the term originating in the pairing of the first $c^\dagger$ from the first V with the last c from the second V,

$$\frac{1}{4L^2}\sum_{k_1k_2q}\sum_{\sigma_1\sigma_2}\sum_{k_1'k_2'q'}\sum_{\sigma_1'\sigma_2'}U_qU_{q'}\frac{1}{\varepsilon_{k_2'}+\varepsilon_{k_1'}-\varepsilon_{k_2'-q'}-\varepsilon_{k_1'+q'}+\mathrm{i}\eta}\cdot$$
$$\cdot\langle i|c_a^\dagger c_b^\dagger c_c^\dagger c_{c'} c_{b'} c_{a'}\overbrace{c_{k_1+q\sigma_1}^\dagger c_{k_2-q\sigma_2}^\dagger c_{k_2\sigma_2} c_{k_1\sigma_1} c_{k_1'+q'\sigma_1'}^\dagger c_{k_2'-q'\sigma_2'}^\dagger c_{k_2'\sigma_2'} c_{k_1'\sigma_1'}}|i\rangle, \quad (4.49)$$

and the term from the pairing of the second $c^\dagger$ from the first V with the last C from the

[7] For simplicity we have at this point imposed a spin-independent dispersion.

[8] Two c's to select from in first V and two $c^\dagger$'s to select from in second V, $2\times 2=4$ permutations. Add also permutations where a $c^\dagger$ from first V and a c from second V are selected.

second V,

$$\begin{aligned}
&\frac{1}{4L^2}\sum_{k_1k_2q}\sum_{\sigma_1\sigma_2}\sum_{k_1'k_2'q'}\sum_{\sigma_1'\sigma_2'}U_qU_{q'}\frac{1}{\varepsilon_{k_2'}+\varepsilon_{k_1'}-\varepsilon_{k_2'-q'}-\varepsilon_{k_1'+q'}+\mathrm{i}\eta}\cdot\\
&\cdot\langle i|c_a^\dagger c_b^\dagger c_c^\dagger c_{c'}c_{b'}c_{a'}c_{k_1+q\sigma_1}^\dagger\overbrace{c_{k_2-q\sigma_2}^\dagger c_{k_2\sigma_2}c_{k_1\sigma_1}c_{k_1'+q'\sigma_1'}^\dagger c_{k_2'-q'\sigma_2'}^\dagger c_{k_2'\sigma_2'}c_{k_1'\sigma_1'}}|i\rangle\\
=\;&\frac{1}{4L^2}\sum_{k_1k_2q}\sum_{\sigma_1\sigma_2}\sum_{k_1'k_2'q'}\sum_{\sigma_1'\sigma_2'}U_qU_{q'}\frac{1}{\varepsilon_{k_2'}+\varepsilon_{k_1'}-\varepsilon_{k_2'-q'}-\varepsilon_{k_1'+q'}+\mathrm{i}\eta}\cdot\\
&\cdot\langle i|c_a^\dagger c_b^\dagger c_c^\dagger c_{c'}c_{b'}c_{a'}\overbrace{c_{k_2-q\sigma_2}^\dagger c_{k_1+q\sigma_1}^\dagger c_{k_1\sigma_1}c_{k_2\sigma_2}c_{k_1'+q'\sigma_1'}^\dagger c_{k_2'-q'\sigma_2'}^\dagger c_{k_2'\sigma_2'}c_{k_1'\sigma_1'}}|i\rangle\\
=\;&\frac{1}{4L^2}\sum_{k_1k_2q}\sum_{\sigma_1\sigma_2}\sum_{k_1'k_2'q'}\sum_{\sigma_1'\sigma_2'}U_{-q}U_{q'}\frac{1}{\varepsilon_{k_2'}+\varepsilon_{k_1'}-\varepsilon_{k_2'-q'}-\varepsilon_{k_1'+q'}+\mathrm{i}\eta}\cdot\\
&\cdot\langle i|c_a^\dagger c_b^\dagger c_c^\dagger c_{c'}c_{b'}c_{a'}\overbrace{c_{k_1+q\sigma_1}^\dagger c_{k_2-q\sigma_2}^\dagger c_{k_2\sigma_2}c_{k_1\sigma_1}c_{k_1'+q'\sigma_1'}^\dagger c_{k_2'-q'\sigma_2'}^\dagger c_{k_2'\sigma_2'}c_{k_1'\sigma_1'}}|i\rangle. \qquad (4.50)
\end{aligned}$$

We did some rewriting; in the first step a pair of raising operators were anti-commuted as was a pair of lowering operators, and in the second step we made some substitutions: $k_1 \to k_2$, $k_2 \to k_1$ and $q \to -q$. What we observe is, that the two terms by rearrangement are almost similar in appearance, the only difference being U_{-q} where the other has U_q. Introducing the symmetrized potential $\widetilde{U}$,

$$\widetilde{U}_q \equiv U_q + U_{-q}, \qquad (4.51)$$

we can now write the sum of the two terms as

$$\begin{aligned}
&\frac{1}{4L^2}\sum_{k_1k_2q}\sum_{\sigma_1\sigma_2}\sum_{k_1'k_2'q'}\sum_{\sigma_1'\sigma_2'}\widetilde{U}_qU_{q'}\frac{1}{\varepsilon_{k_2'}+\varepsilon_{k_1'}-\varepsilon_{k_2'-q'}-\varepsilon_{k_1'+q'}+\mathrm{i}\eta}\cdot\\
&\cdot\langle i|c_a^\dagger c_b^\dagger c_c^\dagger c_{c'}c_{b'}c_{a'}\overbrace{c_{k_1+q\sigma_1}^\dagger c_{k_2-q\sigma_2}^\dagger c_{k_2\sigma_2}c_{k_1\sigma_1}c_{k_1'+q'\sigma_1'}^\dagger c_{k_2'-q'\sigma_2'}^\dagger c_{k_2'\sigma_2'}c_{k_1'\sigma_1'}}|i\rangle. \qquad (4.52)
\end{aligned}$$

The other 3 pairs of terms is treated in a similar fashion, and we can now write[9]

$$\begin{aligned}
\langle f|T|i\rangle \;=\;&\frac{1}{4L^2}\sum_{k_1k_2q}\sum_{\sigma_1\sigma_2}\sum_{k_1'k_2'q'}\sum_{\sigma_1'\sigma_2'}\widetilde{U}_q\widetilde{U}_{q'}\frac{1}{\varepsilon_{k_2'}+\varepsilon_{k_1'}-\varepsilon_{k_2'-q'}-\varepsilon_{k_1'+q'}+\mathrm{i}\eta}\cdot\\
&\cdot\Big(\langle i|c_a^\dagger c_b^\dagger c_c^\dagger c_{c'}c_{b'}c_{a'}c_{k_1+q\sigma_1}^\dagger c_{k_2-q\sigma_2}^\dagger c_{k_2\sigma_2}\overbrace{c_{k_1\sigma_1}c_{k_1'+q'\sigma_1'}^\dagger}c_{k_2'-q'\sigma_2'}^\dagger c_{k_2'\sigma_2'}c_{k_1'\sigma_1'}|i\rangle \qquad (4.53)\\
&+\langle i|c_a^\dagger c_b^\dagger c_c^\dagger c_{c'}c_{b'}c_{a'}\overbrace{c_{k_1+q\sigma_1}^\dagger c_{k_2-q\sigma_2}^\dagger c_{k_2\sigma_2}c_{k_1\sigma_1}c_{k_1'+q'\sigma_1'}^\dagger c_{k_2'-q'\sigma_2'}^\dagger c_{k_2'\sigma_2'}c_{k_1'\sigma_1'}}|i\rangle\Big).
\end{aligned}$$

Next we pull out the contractions. Calculating them is easy enough, $\langle i|c_{k\sigma}^\dagger c_{k'\sigma'}|i\rangle = \delta_{\sigma\sigma'}\delta_{kk'}\langle i|n_{k\sigma}|i\rangle$. Since, as noted before, no contractions are possible[10] between the remaining ladder operators of VG_0V and so we may anticommute them at will, without

[9] It is easy to see, that the energy denominator is invariant under the substitution $k_1' \to k_2'$, $k_2' \to k_1'$ and $q' \to -q'$ and so remains unchanged altogether.

[10] OK, they are possible, they just give zero.

changing the outcome. Thus

$$\begin{aligned}\langle f|T|i\rangle &= \frac{1}{4L^2}\sum_{k_2q\sigma_2}\sum_{k_1'k_2'q'}\sum_{\sigma_1'\sigma_2'}\widetilde{U}_q\widetilde{U}_{q'}\frac{1}{\varepsilon_{k_2'}+\varepsilon_{k_1'}-\varepsilon_{k_2'-q'}-\varepsilon_{k_1'+q'}+\mathrm{i}\eta}\cdot \\ &\cdot\Big(\langle i|c_a^\dagger c_b^\dagger c_c^\dagger c_{c'}c_{b'}c_{a'}c_{k_1'+q'+q\sigma_1'}^\dagger c_{k_2-q\sigma_2}^\dagger c_{k_2\sigma_2}c_{k_2'-q'\sigma_2'}^\dagger c_{k_2'\sigma_2'}c_{k_1'\sigma_1'}|i\rangle\langle i|(1-n_{k_1'+q'\sigma_1'})|i\rangle \\ &+\langle i|c_a^\dagger c_b^\dagger c_c^\dagger c_{c'}c_{b'}c_{a'}c_{k_2-q\sigma_2}^\dagger c_{k_2\sigma_2}c_{k_1'-q\sigma_1'}^\dagger c_{k_1'+q'\sigma_1'}^\dagger c_{k_2'-q'\sigma_2'}^\dagger c_{k_2'\sigma_2'}|i\rangle\langle i|n_{k_1'\sigma_1'}|i\rangle\Big) \\ &= \frac{1}{4L^2}\sum_{k_2q\sigma_2}\sum_{k_1'k_2'q'}\sum_{\sigma_1'\sigma_2'}\widetilde{U}_q\widetilde{U}_{q'}\langle i|c_a^\dagger c_b^\dagger c_c^\dagger c_{c'}c_{b'}c_{a'}c_{k_1'+q'+q\sigma_1'}^\dagger c_{k_2-q\sigma_2}^\dagger c_{k_2'-q'\sigma_2'}^\dagger c_{k_2'\sigma_2'}c_{k_2\sigma_2}c_{k_1'\sigma_1'}|i\rangle \\ &\Big(\frac{\langle i|(1-n_{k_1'+q'\sigma_1'})|i\rangle}{\varepsilon_{k_2'}+\varepsilon_{k_1'}-\varepsilon_{k_2'-q'}-\varepsilon_{k_1'+q'}+\mathrm{i}\eta}-\frac{\langle i|n_{k_1'+q\sigma_1'}|i\rangle}{\varepsilon_{k_2'}+\varepsilon_{k_1'+q}-\varepsilon_{k_2'-q'}-\varepsilon_{k_1'+q+q'}+\mathrm{i}\eta}\Big).\end{aligned} \tag{4.54}$$

In the last step we made the substitution $k_1'-q\to k_1'$ in the second term in order to collect all the ladder operators in one chunk. Now we are almost done, what remains is just six contractions. Instead of permuting the contractions, we shall permute the leftmost six operators and then just contract in the order the operators appear.[11] The possible ways the two pairs of three operators each can be ordered are

$$\sum_{\alpha\beta\gamma\in P(abc)}\mathrm{sgn}(\alpha\beta\gamma)\sum_{\alpha'\beta'\gamma'\in P(a'b'c')}\mathrm{sgn}(\alpha'\beta'\gamma')c_\alpha^\dagger c_\beta^\dagger c_\gamma^\dagger c_{\gamma'}c_{\beta'}c_{\alpha'}. \tag{4.55}$$

The matrix element of interest is reduced to

$$\begin{aligned}\langle f|T|i\rangle &= \frac{1}{4L^2}\sum_{\alpha\beta\gamma\in P(abc)}\sum_{\alpha'\beta'\gamma'\in P(a'b'c')}\sum_{k_2q\sigma_2}\sum_{k_1'k_2'q'}\sum_{\sigma_1'\sigma_2'}\mathrm{sgn}(\alpha\beta\gamma)\mathrm{sgn}(\alpha'\beta'\gamma')\widetilde{U}_q\widetilde{U}_{q'}\cdot \\ &\cdot\langle i|\overbrace{c_\alpha^\dagger\overbrace{c_\beta^\dagger\overbrace{c_\gamma^\dagger c_{\gamma'}}c_{\beta'}}c_{\alpha'}\overbrace{c_{k_1'+q'+q\sigma_1'}^\dagger\overbrace{c_{k_2-q\sigma_2}^\dagger\overbrace{c_{k_2'-q'\sigma_2'}^\dagger c_{k_2'\sigma_2'}}c_{k_2\sigma_2}}c_{k_1'\sigma_1'}}}|i\rangle\cdot \\ &\cdot\Big(\frac{\langle i|(1-n_{k_1'+q'\sigma_1'})|i\rangle}{\varepsilon_{k_2'}+\varepsilon_{k_1'}-\varepsilon_{k_2'-q'}-\varepsilon_{k_1'+q'}+\mathrm{i}\eta}-\frac{\langle i|n_{k_1'+q\sigma_1'}|i\rangle}{\varepsilon_{k_2'}+\varepsilon_{k_1'+q}-\varepsilon_{k_2'-q'}-\varepsilon_{k_1'+q+q'}+\mathrm{i}\eta}\Big) \\ &= \frac{1}{4L^2}\sum_{\alpha\beta\gamma\in P(abc)}\sum_{\alpha'\beta'\gamma'\in P(a'b'c')}\mathrm{sgn}(\alpha\beta\gamma)\mathrm{sgn}(\alpha'\beta'\gamma')\widetilde{U}_{k_\beta-k_\beta'}\widetilde{U}_{k_\gamma-k_\gamma'}\cdot \\ &\cdot\langle i|n_\alpha n_\beta n_\gamma(1-n_{\alpha'})(1-n_{\beta'})(1-n_{\gamma'})|i\rangle\delta_{\sigma_\alpha\sigma_\alpha'}\delta_{\sigma_\beta\sigma_\beta'}\delta_{\sigma_\gamma\sigma_\gamma'}\delta_{k_\alpha+k_\beta+k_\gamma,k_\alpha'+k_\beta'+k_\gamma'}\cdot \\ &\cdot\Big(\frac{\langle i|(1-n_{k_\gamma+k_\alpha-k_\gamma'\sigma_\alpha})|i\rangle}{\varepsilon_{k_\gamma}+\varepsilon_{k_\alpha}-\varepsilon_{k_\gamma'}-\varepsilon_{k_\alpha+k_\gamma-k_\gamma'}+\mathrm{i}\eta}-\frac{\langle i|n_{k_\alpha+k_\beta-k_\beta'\sigma_1'}|i\rangle}{\varepsilon_{k_\gamma}+\varepsilon_{k_\alpha'+k_\gamma'-k_\gamma}-\varepsilon_{k_\gamma'}-\varepsilon_{k_\alpha'}+\mathrm{i}\eta}\Big).\end{aligned} \tag{4.56}$$

All of a sudden, but not unexpected at all, appears both momentum and spin conservation. Remembering Fermi's Golden Rule (similar to Eq. (4.37)), we will want to use $\langle f|T|i\rangle$ in connection with energy conservation, which takes on the form

$$E_i=E_f\Leftrightarrow\varepsilon_{k_\alpha}+\varepsilon_{k_\beta}+\varepsilon_{k_\gamma}=\varepsilon_{k_\alpha'}+\varepsilon_{k_\beta'}+\varepsilon_{k_\gamma'}. \tag{4.57}$$

[11] The two procedures are precisely the same, but the way they are performed look different.

Applying this to the second energy denominator (and also applying momentum conservation at will) we find

$$\begin{aligned}\langle f|T|i\rangle &= \frac{1}{4L^2}\sum_{\alpha\beta\gamma\in P(abc)}\sum_{\alpha'\beta'\gamma'\in P(a'b'c')}\mathrm{sgn}(\alpha\beta\gamma)\mathrm{sgn}(\alpha'\beta'\gamma')\widetilde{U}_{k_\beta-k'_\beta}\widetilde{U}_{k_\gamma-k'_\gamma}\cdot \\ &\cdot\langle i|n_\alpha n_\beta n_\gamma(1-n_{\alpha'})(1-n_{\beta'})(1-n_{\gamma'})|i\rangle\delta_{\sigma_\alpha\sigma'_\alpha}\delta_{\sigma_\beta\sigma'_\beta}\delta_{\sigma_\gamma\sigma'_\gamma}\delta_{k_\alpha+k_\beta+k_\gamma,k'_\alpha+k'_\beta+k'_\gamma}\cdot \\ &\cdot\Big(\frac{\langle i|(1-n_{k_\gamma+k_\alpha-k'_\gamma\sigma_\alpha})|i\rangle}{\varepsilon_{k_\gamma}+\varepsilon_{k_\alpha}-\varepsilon_{k'_\gamma}-\varepsilon_{k_\alpha+k_\gamma-k'_\gamma}+\mathrm{i}\eta}+\frac{\langle i|n_{k_\alpha+k_\beta-k'_\beta\sigma'_1}|i\rangle}{\varepsilon_{k_\alpha}+\varepsilon_{k_\beta}-\varepsilon_{k'_\beta}-\varepsilon_{k'_\alpha+k'_\gamma-k_\gamma}-\mathrm{i}\eta}\Big).\end{aligned} \tag{4.58}$$

Finally we substitute $\gamma\leftrightarrow\beta$ and $\gamma'\leftrightarrow\beta'$ in the second term. Each substitution will change the sign of the sgn-function, but those two signs conveniently cancel each other. The two energy denominators will become almost equal, the only difference will be a $+\mathrm{i}\eta$ in the one, where the other has a $-\mathrm{i}\eta$. The imaginary part of the denominator was originally introduced in order to deal with eventual singularities, so let us examine, when - and if at all - such occurs. For simplicity we look at a quadratic band.

$$0 = \varepsilon_{k_\alpha}+\varepsilon_{k_\beta}-\varepsilon_{k'_\beta}-\varepsilon_{k'_\alpha+k'_\gamma-k_\gamma} \tag{4.59}$$

$$\Leftrightarrow 0 = k_\alpha^2+k_\gamma^2-k_\gamma'^2-(k_\alpha+k_\gamma-k'_\gamma)^2=2(k_\alpha-k'_\gamma)(k'_\gamma-k_\gamma), \tag{4.60}$$

but the only way for this to be true, would be for one of the final momenta to equal an initial momentum, which we have strictly forbidden, since that would correspond to two-particle scattering. So no singularities occur and we can throw away the $\mathrm{i}\eta$ without concern. The argument probably extends to the general class of bands we usually consider.

Returning to our calculations, there will be a partial cancelation of terms. Also a lot of the other junk that appears under the summations is really independent of those and can be pulled outside. Our penultimate result is

$$\begin{aligned}\langle f|T|i\rangle &= \frac{1}{4L^2}\langle i|n_a n_b n_c(1-n_{a'})(1-n_{b'})(1-n_{c'})|i\rangle\delta_{k_a+k_b+k_c,k'_a+k'_b+k'_c} \\ &\sum_{\alpha\beta\gamma\in P(abc)}\sum_{\alpha'\beta'\gamma'\in P(a'b'c')}\frac{\mathrm{sgn}(\alpha\beta\gamma)\mathrm{sgn}(\alpha'\beta'\gamma')\widetilde{U}_{k_\beta-k'_\beta}\widetilde{U}_{k_\gamma-k'_\gamma}\delta_{\sigma_\alpha\sigma'_\alpha}\delta_{\sigma_\beta\sigma'_\beta}\delta_{\sigma_\gamma\sigma'_\gamma}}{\varepsilon_{k_\alpha}+\varepsilon_{k_\gamma}-\varepsilon_{k'_\gamma}-\varepsilon_{k_\alpha+k_\gamma-k'_\gamma}},\end{aligned} \tag{4.61}$$

which contains $6\times 6=36$ terms. Introducing the following quantity

$$\begin{aligned}\mathbb{V}(aa',bb',cc')\equiv\delta_{\sigma_a\sigma'_a}\delta_{\sigma_b\sigma'_b}\delta_{\sigma_c\sigma'_c} &\Big(\frac{\widetilde{U}_{k_b-k'_b}\widetilde{U}_{k_c-k'_c}}{\varepsilon_{k_a}+\varepsilon_{k_b}-\varepsilon_{k'_b}-\varepsilon_{k_a+k_b-k'_b}}+\frac{\widetilde{U}_{k_b-k'_b}\widetilde{U}_{k_c-k'_c}}{\varepsilon_{k_a}+\varepsilon_{k_c}-\varepsilon_{k'_c}-\varepsilon_{k_a+k_c-k'_c}} \\ &+\frac{\widetilde{U}_{k_c-k'_c}\widetilde{U}_{k_a-k'_a}}{\varepsilon_{k_b}+\varepsilon_{k_c}-\varepsilon_{k'_c}-\varepsilon_{k_b+k_c-k'_c}}+\frac{\widetilde{U}_{k_c-k'_c}\widetilde{U}_{k_a-k'_a}}{\varepsilon_{k_b}+\varepsilon_{k_a}-\varepsilon_{k'_a}-\varepsilon_{k_b+k_a-k'_a}} \\ &+\frac{\widetilde{U}_{k_a-k'_a}\widetilde{U}_{k_b-k'_b}}{\varepsilon_{k_c}+\varepsilon_{k_a}-\varepsilon_{k'_a}-\varepsilon_{k_c+k_a-k'_a}}+\frac{\widetilde{U}_{k_a-k'_a}\widetilde{U}_{k_b-k'_b}}{\varepsilon_{k_c}+\varepsilon_{k_b}-\varepsilon_{k'_b}-\varepsilon_{k_c+k_b-k'_b}}\Big),\end{aligned} \tag{4.62}$$

we can write the 36 terms in a more compact fashion as

$$\begin{aligned}\langle f|T|i\rangle=\frac{1}{4L^2}\langle i|n_a n_b n_c(1-n_{a'})(1-n_{b'})(1-n_{c'})|i\rangle\delta_{k_a+k_b+k_c,k'_a+k'_b+k'_c}\big(&\mathbb{V}(aa',bb',cc') \\ +\mathbb{V}(ab',bc',ca')+\mathbb{V}(ac',ba',cb')-\mathbb{V}(aa',bc',cb')-\mathbb{V}(ac',bb',ca')-\mathbb{V}(ab',ba',cc')\big).&\end{aligned} \tag{4.63}$$

Our derivation of this expression valid for three particle interactions follows more or less [19] even borrowing a large part of the notation from this paper, but there is one notable difference in approach. Where [19] ignores the possibility of the intermediate state being already occupied we have included this possibility. So where we only assume the correlation Eq. (4.42) between the initial and final states, the paper assumes the initial state to consist of a vacuum with only the tree states a, b and c occupied and likewise for the final state being the states a', b' and c' occupied and nothing else. Since there is an intermediate step in the three particle scattering which involves a seventh state, whether or not this seventh state is occupied or not may play a role for the outcome, which we have taken into consideration in our approach. It is worth noting, however, that our result agrees with that of the paper, and so it is apparently of no importance whether or not one assumes the intermediate state to be empty.

Now must of our trouble is over. The scattering rate from the initial state to the final state is

$$\Gamma_{f\leftarrow i} = \frac{2\pi}{\hbar}\big|\langle f|T|i\rangle\big|^2\delta(E_i - E_f), \tag{4.64}$$

from which follows the scattering rate $\Gamma_{a'b'c'\leftarrow abc}$ as before. Assuming that the collisions are local, the position dependence of the scattering rate, is implemented by hand by putting the same position everywhere.

$$\begin{aligned}
\Gamma_{a'b'c'\leftarrow abc} &= \sum_i P_i\Gamma_{f\leftarrow i} && (4.65)\\
\Gamma_{a'b'c'\leftarrow abc}(x) &= \frac{2\pi}{\hbar}\frac{1}{16L^4}g(k_a\sigma_a,x)g(k_b\sigma_b,x)g(k_c\sigma_c,x)(1-g(k'_a\sigma'_a,x))(1-g(k'_b\sigma'_b,x))\cdot\\
&\quad\cdot(1-g(k'_c\sigma'_c,x))\delta_{k_a+k_b+k_c,k'_a+k'_b+k'_c}\delta(\varepsilon_{k_a}+\varepsilon_{k_b}+\varepsilon_{k_c}-\varepsilon_{k'_a}-\varepsilon_{k'_b}-\varepsilon_{k'_c})\cdot\\
&\quad\cdot\Big|\mathbb{V}(aa',bb',cc')+\mathbb{V}(ab',bc',ca')+\mathbb{V}(ac',ba',cb')\\
&\quad-\mathbb{V}(aa',bc',cb')-\mathbb{V}(ac',bb',ca')-\mathbb{V}(ab',ba',cc')\Big|^2\\
&\equiv W_{a'b'c'\leftarrow abc}g(k_a\sigma_a,x)g(k_b\sigma_b,x)g(k_c\sigma_c,x))\cdot\\
&\quad\cdot(1-g(k'_a\sigma'_a,x))(1-g(k'_b\sigma'_b,x))(1-g(k'_c\sigma'_c,x)), && (4.66)
\end{aligned}$$

and finally the collision term for use in the Boltzmann equation is arrived at

$$\begin{aligned}
\Big(\frac{\partial g(k_a\sigma_a x)}{\partial t}\Big)_{coll.} &= \sum_{bc}\sum_{a'b'c'}\big(\Gamma_{abc\leftarrow a'b'c'}(x)-\Gamma_{a'b'c'\leftarrow abc}(x)\big)\\
&= \sum_{bc}\sum_{a'b'c'}W_{a'b'c'\leftarrow abc}\big(g(k'_a\sigma'_a,x)g(k'_b\sigma'_b,x)g(k'_c\sigma'_c,x))(1-g(k_a\sigma_a,x))\cdot\\
&\quad\cdot(1-g(k_b\sigma_b,x))(1-g(k_c\sigma_c,x))-g(k_a\sigma_a,x)g(k_b\sigma_b,x)g(k_c\sigma_c,x))\cdot\\
&\quad\cdot(1-g(k'_a\sigma'_a,x))(1-g(k'_b\sigma'_b,x))(1-g(k'_c\sigma'_c,x))\big). && (4.67)
\end{aligned}$$

We have employed that the rate W has some built in symmetry, $W_{a'b'c'\leftarrow abc} = W_{abc\leftarrow a'b'c'}$, which follows from its definition and the definition of $\mathbb{V}$.

4.1.6 Solving to lowest order in W

We are now ready to calculate the current to first order in the collisions, which as it has turned out, is also to first order in W. Equating the first order terms of both sides of Eq. (4.1), we

get

$$v_k \frac{\partial g_i^{(1)}(k\sigma,x)}{\partial x} = \Big(\frac{\partial g_i(k\sigma,x}{\partial t}\Big)^{(1)}_{tunn.} + \Big(\frac{\partial g_i(k\sigma,x}{\partial t}\Big)^{(1)}_{coll.} \quad , i = 1,2,3. \tag{4.68}$$

Since the tunneling terms Eq. (4.17) does not contain any W explicitly, $\Big(\frac{\partial g_i(k\sigma,x}{\partial t}\Big)^{(1)}_{tunn.}$ must be linear in W through the distribution functions; so we simply replace every appearance of g_i in Eq. (4.17) by $g_i^{(1)}$ to arrive at $\Big(\frac{\partial g_i(k\sigma,x}{\partial t}\Big)^{(1)}_{tunn.}$. Since W appears explicitly in Eq. (4.67), $\Big(\frac{\partial g_i(k\sigma,x}{\partial t}\Big)^{(1)}_{coll.}$ is found by inserting $g_i^{(0)}$ in that expression.

The boundary condition for the $g_i^{(1)}$'s (as for that matter for any $g_i^{(j)}$ with $j > 0$) is

$$g_i^{(1)}(k\sigma,x) = 0 \quad \text{for} \begin{cases} x \to \infty & , k < 0 \\ x \to -\infty & , k > 0 \end{cases} . \tag{4.69}$$

The procedure is pretty much the same as before. We integrate every single Boltzmann equation; for $k > 0$ it is from $-\infty$ to x and for $k < 0$ it is from $+\infty$ to x. The left hand sides of Eq.'s (4.68) all trivially yield $v_k g_i^{(1)}(k\sigma,x)$. The tunneling terms are treated as previously by assuming, that the distribution function varies only on a scale larger than that set by $f(x,W)$; thus we again encounter the integral F of f. For $k > 0$ we arrive at

$$\begin{aligned} v_k g_1^{(1)}(k\sigma,x) &= \Gamma_A\big(g_2^{(1)}(k_2^A\sigma,0) - g_1^{(1)}(k_1^A\sigma,0)\big) f(k-k_1^A,Q_A) F(x,W_A) \\ &\quad + \int_{-\infty}^{x} \mathrm{d}x' \Big(\frac{\partial g_1(k\sigma,x')}{\partial t}\Big)^{(1)}_{coll.} \end{aligned} \tag{4.70}$$

$$\begin{aligned} v_k g_2^{(1)}(k\sigma,x) &= \Gamma_A\big(g_1^{(1)}(k_1^A\sigma,0) - g_2^{(1)}(k_2^A\sigma,0)\big) f(k-k_2^A,Q_A) F(x,W_A) \\ &\quad + \Gamma_B\big(g_3^{(1)}(k_3^B\sigma,L_B) - g_2^{(1)}(k_2^B\sigma,L_B)\big) f(k-k_2^B,Q_B) F(x-L_B,W_B) \\ &\quad + \int_{-\infty}^{x} \mathrm{d}x' \Big(\frac{\partial g_2(k\sigma,x')}{\partial t}\Big)^{(1)}_{coll.} \end{aligned} \tag{4.71}$$

$$\begin{aligned} v_k g_3^{(1)}(k\sigma,x) &= \Gamma_B\big(g_2^{(1)}(k_2^B\sigma,L_B) - g_3^{(1)}(k_3^B\sigma,L_B)\big) f(k-k_3^B,Q_B) F(x-L_B,W_B) \\ &\quad + \int_{-\infty}^{x} \mathrm{d}x' \Big(\frac{\partial g_3(k\sigma,x')}{\partial t}\Big)^{(1)}_{coll.}. \end{aligned} \tag{4.72}$$

For $k < 0$ the results are very similar, $F(x,W)$ is replaced by $-F(-x,W)$ and the lower limit on the remaining integral is changed to $+\infty$. To continue, we impose the physical requirement that $V_B = 0$. As earlier discussed this could be a good idea on the grounds, that we measure the current between wire 2 and 3. If a current is observed it must then be due to something disturbing the equilibrium distribution of wire 2, since there is no voltage difference between wire 2 and 3. And this something is precisely the electrons from wire 1.

The Fermi distribution is invariant under the kind of collisions we consider. This follows from inserting the Fermi distribution in the RHS of the expression Eq. (4.67) and applying the H-theorem[12], which states that with energy conservation ($\varepsilon_1 + \varepsilon_2 + \varepsilon_3 = \varepsilon_{1'} + \varepsilon_{2'} + \varepsilon_{3'}$),

$$\begin{aligned} &n_F(\varepsilon_1)n_F(\varepsilon_2)n_F(\varepsilon_3)(1-n_F(\varepsilon_{1'}))(1-n_F(\varepsilon_{2'}))(1-n_F(\varepsilon_{3'})) \\ &-(1-n_F(\varepsilon_1))(1-n_F(\varepsilon_2))(1-n_F(\varepsilon_3))n_F(\varepsilon_{1'})n_F(\varepsilon_{2'})n_F(\varepsilon_{3'}) = 0, \end{aligned} \tag{4.73}$$

[12] No, it's not a capital h, it is in fact a capital η.

a property unique to the Fermi distribution. A simple proof of the H-theorem can be found in Appendix B.

The requirement of no voltage difference leads to $n_F(\varepsilon_{k_3^B} - \mu_3) = n_F(\varepsilon_{k_2^B} - \mu_2)$, which results in

$$g_3^{(0)}(k\sigma, x) = n_F(\varepsilon_k - \mu_3). \tag{4.74}$$

Therefore $\left(\frac{\partial g_3(k\sigma,x')}{\partial t}\right)^{(1)}_{coll.} = 0$, and Eq. (4.72) and its cousin valid for $k < 0$ could together be solved for $g_3^{(1)}(k\sigma, x)$. We will however only solve it for the point, where we will need it,

$$\begin{aligned} g_3^{(1)}(k_3^B\sigma, L_B) &= \Gamma_B\big(g_2^{(1)}(k_2^B\sigma, L_B) - g_3^{(1)}(k_3^B\sigma, L_B)\big)\frac{W_B}{2|v_{k_3^B}|} && (4.75)\\ \Leftrightarrow g_3^{(1)}(k_3^B\sigma, L_B) &= \frac{g_2^{(1)}(k_2^B\sigma, L_B)}{1 + \frac{2|v_{k_3^B}|}{\Gamma_B W_B}}. && (4.76) \end{aligned}$$

The zeroth order current is zero, $I_B^{(0)} = 0$, because of the lack of voltage difference. The total current up to first order in W is given by the first order term

$$\begin{aligned} I_B^{(1)} &= (-e)\Gamma_B\frac{Q_B W_B}{2\pi}\sum_\sigma\big(g_2^{(1)}(k_2^B\sigma, L_B) - g_3^{(1)}(k_3^B\sigma, L_B)\big)\\ &= (-e)\frac{Q_B|v_{k_3^B}|}{\pi}\Big(1 + \frac{2|v_{k_3^B}|}{\Gamma_B W_B}\Big)^{-1}\sum_\sigma g_2^{(1)}(k_2^B\sigma, L_B). && (4.77) \end{aligned}$$

Thus we only need know $g_2^{(1)}$ at a single point. Evaluating Eq. (4.71) at this point, the first term drops out as the tunneling windows do not overlap, and by using Eq. (4.76) we can solve for $g_2^{(1)}(k_2^B\sigma, L_B)$. Thus for $k_2^B > 0$,

$$g_2^{(1)}(k_2^B\sigma, L_B) = \Big(|v_{k_2^B}| + |v_{k_3^B}|\big(1 + \frac{2|v_{k_3^B}|}{\Gamma_B W_B}\big)^{-1}\Big)^{-1}\int_{-\infty}^{L_B}\mathrm{d}x'\Big(\frac{\partial g_2(k_2^B\sigma, x')}{\partial t}\Big)^{(1)}_{coll.}. \tag{4.78}$$

We finally arrive at an expression for the current, valid for $k_2^B > 0$,

$$I_B^{(1)} = (-e)\frac{Q_B W_B}{2\pi}\frac{\widetilde{\Gamma}_B}{|v_{k_2^B}|}\sum_\sigma\int_{-\infty}^{L_B}\mathrm{d}x'\Big(\frac{\partial g_2(k_2^B\sigma, x')}{\partial t}\Big)^{(1)}_{coll.}. \tag{4.79}$$

For the other case, $k_2^B < 0$, simply change the sign of the RHS and change the lower limit of the integral to $+\infty$. The collision rate we need in both cases is

$$\begin{aligned} \Big(\frac{\partial g_2(k_2^B\sigma, x')}{\partial t}\Big)^{(1)}_{coll.} &= \sum_{k_1\sigma_1}\sum_{k_2\sigma_2}\sum_{k_1'\sigma_1'}\sum_{k_2'\sigma_2'}\sum_{k_3'\sigma_3'} W_{k_1\sigma_1 k_2^B\sigma k_3\sigma_3 \leftarrow k_1'\sigma_1' k_2'\sigma_2' k_3'\sigma_3'}\Big(g_2^{(0)}(k_1'\sigma_1', x')\cdot\\ &\cdot g_2^{(0)}(k_2'\sigma_2', x')g_2^{(0)}(k_3'\sigma_3', x')(1 - g_2^{(0)}(k_1\sigma_1, x'))(1 - g_2^{(0)}(k_2^B\sigma, x'))\\ &(1 - g_2^{(0)}(k_3\sigma_3, x')) - g_2^{(0)}(k_1\sigma_1, x')g_2^{(0)}(k_2^B\sigma, x')g_2^{(0)}(k_3\sigma_3, x')\cdot\\ &\cdot(1 - g_2^{(0)}(k_1'\sigma_1', x'))(1 - g_2^{(0)}(k_2'\sigma_2', x'))(1 - g_2^{(0)}(k_3'\sigma_3', x'))\Big). \end{aligned} \tag{4.80}$$

Recalling Eq. (4.31) and $V_B = 0$, we have

$$g_2^{(0)}(k\sigma, x) = n_F(\varepsilon_k - \mu_2) + \frac{\widetilde{\Gamma}_A}{|v_{k_2^A}|} f(k - k_2^A, Q_A)\big(F(x, W_A)\Theta(k_2^A) + F(-x, W_A)\Theta(-k_2^A)\big) \cdot \\ \cdot\big(n_F(\varepsilon_{k_1^A} - \mu_1) - n_F(\varepsilon_{k_2^A} - \mu_2)\big). \quad (4.81)$$

As it appears $g_2^{(0)}$ is just a Fermi distribution except in the vicinity of the point $k = k_2^A$, where it could have another value due to tunneling to or from wire 1. Thus, due to the H-theorem and the fact that W contains energy conservation, at least one of the sums of Eq. (4.80) must hit near k_2^A for the collision rate (and thereby the current) to be non-zero. If one of the primed sums hits k_2^A, none of the unprimed sums can, as that would amount to two-particle processes. So we deal with two kind of processes, an unprimed sum hitting k_2^A and a primed sum hitting k_2^A. There is nothing fundamental wrong in two (two or three) of the unprimed (primed) sums hitting k_2^A, this would correspond to processes where two (or three) electrons jump from wire 1 into wire 2 (or the other way) and then interact with each other (and perhaps an electron from the Fermi sea of wire 2), involving at least one electron starting or ending with $k = k_2^B$.[13]

We will at this point focus only on what we believe to be the dominating processes, the ones where only a single excitation from wire 1 is involved. Thus we get two terms; one in which an unprimed sum hits k_2^A and one in which a primed sum hits k_2^A. For the k's that do not hit k_2^A, the corresponding $g_2^{(0)}$ are replaced by the Fermi distribution (or the first term of Eq. (4.81) if you like). Actually this seems to be invalid, because the sum of that k should no longer include k_2^A, but as that is just a single point, and the summand is well behaved as a function of that k, we do not change the outcome by including a single point in the sum.[14] For the single k sums that hits k_2^A, we get a distribution function $g_2^{(0)}(k_2^A\sigma, x$ which can be written as a sum of two parts, see Eq. (4.81): A Fermi distribution plus some deviation. Multiplying out with the other Fermi distributions, only the second term survives, as the first term is killed by the H-theorem. Note that the second term survives in the same form in both $g_2^{(0)}(k_2^A\sigma, x)$ and $1 - g_2^{(0)}(k_2^A\sigma, x)$, since the one minus a Fermi distribution is required for the H-theorem to work.

Assuming that F changes so abruptly, that we can treat it as a step function, all x-dependence should be easily integrated out of the current. For $k_2^A \cdot k_2^B < 0$, however, the integral diverges. This divergence is an artefact of the model: Apparently there is a finite, constant probability per length of the wire for electrons to scatter into or away from $k = k_2^B$. Now imagine the following situation, an electron jumps from wire 1 to 2 at the A junction and becomes left moving as $k_2^A < 0$, at some point to the left of the junction it scatters into $k_2^B > 0$ and moves to the right until it can tunnel into wire 3 at the B junction. Since the scattering may happen in an semi-infinite region, and no further scattering is taken into account as we only look at the current to first order in the scattering, this process will lead to an infinite contribution to the current. The way to deal with this divergence is of course to replace the L_B that appears when the integral converges for $k_2^A \cdot k_2^B > 0$ by an effective interaction length L_i and claim that the results always holds. We shall then further neglect that L_i may vary with circumstances.

[13] It may seem impossible, due to the Pauli Principle, for three electrons to jump from wire 1 to the same k-value in wire 1. But remember that the scale of the k-values are determined by their use in the Boltzmann equation and each may represent several "true" k-states.

[14] If this bothers you, simply change the sums to integrals, then it is obvious that a single point does not change the integral, if there are no delta functions in the integrand.

Changing the k sum that hits k_2^A into an integral, $\sum_k \to \int \mathrm{d}k \frac{L}{2\pi}$, before performing it, we get the current,

$$I_B^{(0)} = (-e)\frac{Q_B W_B}{2\pi}\frac{\widetilde{\Gamma}_B}{|v_{k_2^B}|}\frac{Q_A W_A}{2\pi}\frac{\widetilde{\Gamma}_A}{|v_{k_2^A}|} LL_i\big(n_F(\varepsilon_{k_1^A}-\mu_1)-n_F(\varepsilon_{k_2^A}-\mu_2)\big)\times Z, \quad (4.82)$$

where Z is the part containing all the sums,

$$\begin{aligned}
Z &\equiv Z_1 - Z_2 + Z_3 - Z_4 && (4.83)\\
Z_1 &= (1-n_F(\varepsilon_{k_2^B}-\mu_2))3\sum_{\sigma}\sum_{k_1\sigma_1}\sum_{k_2\sigma_2}\sum_{k_1'\sigma_1'}\sum_{k_2'\sigma_2'}\sum_{\sigma_3'} W_{k_1\sigma_1 k_2^B\sigma k_2\sigma_2\leftarrow k_1'\sigma_1' k_2'\sigma_2' k_2^A\sigma_3'}\\
&\quad \times n_F(\varepsilon_{k_1'}-\mu_2)n_F(\varepsilon_{k_2'}-\mu_2)(1-n_F(\varepsilon_{k_1}-\mu_2))(1-n_F(\varepsilon_{k_2}-\mu_2)) && (4.84)\\
Z_2 &= n_F(\varepsilon_{k_2^B}-\mu_2)2\sum_{\sigma}\sum_{k_1\sigma_1}\sum_{\sigma_2}\sum_{k_1'\sigma_1'}\sum_{k_2'\sigma_2'}\sum_{k_3'\sigma_3'} W_{k_1\sigma_1 k_2^B\sigma k_2^A\sigma_2\leftarrow k_1'\sigma_1' k_2'\sigma_2' k_3'\sigma_3'}\\
&\quad \times n_F(\varepsilon_{k_1}-\mu_2)(1-n_F(\varepsilon_{k_1'}-\mu_2))(1-n_F(\varepsilon_{k_2'}-\mu_2))(1-n_F(\varepsilon_{k_3'}-\mu_2) && (4.85)\\
Z_3 &= n_F(\varepsilon_{k_2^B}-\mu_2)3\sum_{\sigma}\sum_{k_1\sigma_1}\sum_{k_2\sigma_2}\sum_{k_1'\sigma_1'}\sum_{k_2'\sigma_2'}\sum_{\sigma_3'} W_{k_1\sigma_1 k_2^B\sigma k_2\sigma_2\leftarrow k_1'\sigma_1' k_2'\sigma_2' k_2^A\sigma_3'}\\
&\quad \times n_F(\varepsilon_{k_1}-\mu_2)n_F(\varepsilon_{k_2}-\mu_2)(1-n_F(\varepsilon_{k_1'}-\mu_2))(1-n_F(\varepsilon_{k_2'}-\mu_2)) && (4.86)\\
Z_4 &= (1-n_F(\varepsilon_{k_2^B}-\mu_2))2\sum_{\sigma}\sum_{k_1\sigma_1}\sum_{\sigma_2}\sum_{k_1'\sigma_1'}\sum_{k_2'\sigma_2'}\sum_{k_3'\sigma_3'} W_{k_1\sigma_1 k_2^B\sigma k_2^A\sigma_2\leftarrow k_1'\sigma_1' k_2'\sigma_2' k_3'\sigma_3'}\\
&\quad \times n_F(\varepsilon_{k_1'}-\mu_2)n_F(\varepsilon_{k_2'}-\mu_2)n_F(\varepsilon_{k_3'}-\mu_2)(1-n_F(\varepsilon_{k_1}-\mu_2)). && (4.87)
\end{aligned}$$

That does it; this is the tunneling current in junction B to first order in the three-particle scattering rate W.

We notice that the four terms appearing here precisely corresponds the four processes discussed in Fig. 2.4 and we have therefore labeled them accordingly.

4.2 Numerical calculation of current

What remains for us to do is the not-so-simple task of now performing the sums of Eq.s (4.84)-(4.87). We have in all cases four k-sums and 6 σ-sums. Since the scattering rate W which appears in all four expressions contains both energy and momentum conservation, we are able to eliminate two of the k-sums using these delta-functions.

One of the delta-functions is a Dirac delta-function and we thus convert one of the sums to an integral $\sum_k \to \int \mathrm{d}k \frac{L}{2\pi}$ before eliminating it. The two remaining sums are also converted to integrals in the same fashion, and we thus make a convenient observation: The L-dependence of the current cancel out. From converting three sums to integrals we get L^3 and there is an explicit L in Eq. (4.82), but the scattering rate W contains L^{-4} (Eq. (4.66)) and so there is a complete cancelation of terms. This means that we can take the continuity limit $L \to \infty$ and the results will still be well behaved.

That leaves just two remaining k-integrals, which in general cannot be solved algebraically. In order to proceed we restrict ourselves to the zero-temperature case and then attempt to solve the remaining integrals numerically. Our goal will be to be able to calculate the current at any point in Fig. 2.3.

4.2.1 No current by kinematic arguments

Looking at the current to only first order in W corresponds to allowing only a single scattering to occur. Taking the second order term into account would correspond to terms where two consecutive three-particle scatterings had occurred. As it turns out, not everywhere in the areas previously defined (area 1 and area 2), is the relaxation possible.

In area 2 the relaxing electron can give up no more than a specific amount of energy, as it cannot relax below the Fermi sea. But if the electron which must be excited lies further down from the Fermi sea than this amount, the process is not possible. Quantitatively we must have

$$\varepsilon_{k_2^A} - \varepsilon_{k_{F2}} \geq \varepsilon_{k_{F2}} - \varepsilon_{k_2^B}. \tag{4.88}$$

In the parts of area 2 where this is not fulfilled, we expect the current to be small, as the single excited electron can never relax sufficiently for a hole to appear at k_2^B. The argument is valid also to higher order in N-particle scattering rates as long as only one excited electron is involved.

The argument could perhaps be further refined by using some of the inequalities derived in Chapter 3, but that would require the limitations to a specific number of particles in the scattering, so what we have stated is the most general.

There is no easily discovered analog to this in area 1.

4.2.2 Electron relaxation part I: Z1

We use the delta-functions to eliminate k_1 and k_2 as this leaves only the integrals running over finite domains, hoping that these are easier to deal with numerically. Using symmetry arguments we can also eliminate several redundant calculations, optimizing the numerical integration. First of all, since we have overall spin-symmetry, we fix one of the spins and multiply the result by two. Since k_1 and k_2 appear completely symmetric (as the should), the elimination of them can be performed two ways. We simply choose one of these and multiply by (again) a factor of two. Finally the integration variables k_1' and k_2' also appear symmetrically so instead of integrating over the complete square $-k_{F2} \leq k_1' \leq k_{F2} \wedge -k_{F2} \leq k_2' \leq k_{F2}$, we integrate only over the triangle $-k_{F2} \leq k_1' \leq k_{F2} \wedge -k_{F2} \leq k_2' \leq k_1'$ and multiply by a factor two.

4.2.3 Electron relaxation part II: Z2

First we assumed that it would be smart to use the delta-functions to eliminate two equivalent momenta k_2' and k_2', as this would allow for some further reduction using similar symmetry arguments as earlier. However it turned out, that performing either of the remaining two integrals (over k_1 and k_1') would yield a divergence. This divergence may be integrable if treated analytical, but treating it numerically it was not integrable.

So instead we choose to eliminate an initial and a final momenta (k_1 and k_1'), a procedure which yielded no intermediate singularities.[15] So we need to integrate numerically over the two remaining momenta k_2' and k_3', which must be positioned outside the Fermi sea. Looking at the scattering situation in Fig. 2.4(c), k_2^A, k_1', k_2' and k_3' are situated above the Fermi sea and k_1 and k_2^B below it. When we deal with actual numbers, we chosse a set of Fermi momenta such that $k_{F2} \geq k_{F1}$, which implies that $k_2^A > 0$ everywhere in area 2. Thus two of

[15] Which indicates that the previous divergence should be integrable.

the primed momenta must be at $k > k_{F2}$ and the remaining at $k < -k_{F2}$. Since all unprimed momenta are equivalent, we choose the negative one to be k_1' and multiply by a factor of three and choose to integrate (again) over the triangle $k_{F2} < k_2' < k_3' < k_{F2}$ and multiply by two. Fixing one of the spins at an arbitrary value gives a final factor of two.

The integrand of the first integral to be numerically solved for only yielded something non-zero in a very small area outside the Fermi sea. Thus simply making the integration go over the whole k-axis apart from the Fermi sea resulted in garbled results, mostly zero. For a much better result we had to single out the small domain, where the integrand was non-zero and integrate over only this. Doing so was rather technical as the borders of that domain depended on most of the other parameters of the system.

4.2.4 Hole relaxation: Z3 and Z4

We know already (see Chapter 3), that there is no way a single hole can relax at zero temperature. This means that the processes shown in Figs. 2.4(b) and 2.4(d) are not possible, and no current is going to run if it depends on hole-relaxation. Thus without performing any further calculations we immediately know, that no current is going to run in area 3 and 4. This results extends to N-particle scattering processes as long as only a single hole at a time is involved.

4.2.5 The tunneling current

An finally we arrive at our goal: The tunneling current to first order in the three-particle scattering rate in the incoherent regime as a function of V_A and B with $V_B = 0$ at zero temperature. The current resulting from the numerical calculation in area 1 and area 2 is displayed in Fig. 4.2. In areas 3 and 4 the same tunneling current is, as mentioned, zero, and so we felt no reason to plot it here.

We had to make particular choices of system parameters for the calculations, these are as follows

$$\begin{aligned} m^* &= 0.067 \cdot m_e \\ d &= 31nm \\ k_{F1} &= 0.7 \cdot 10^8 1/m \\ k_{F2} &= 0.9 \cdot 10^8 1/m \\ k_{F3} &= 0.8 \cdot 10^8 1/m, \end{aligned}$$

which are, respectively, the effective electron mass, the distance from center to center of the two wires and the Fermi wavevectors of the three wires. It is precisely the same choice we made for the calculations behind Fig. 2.3. For the interaction we made the following choice

$$V(q) = \frac{4\pi e_0^2}{q^2 + q_t^2}, \tag{4.89}$$

with $q_t = 0.2k_{F2}$. The origin of this potential is the finite-range Coulomb Potential (the Yukawa Potential),

$$\frac{e_0^2}{r} \mathrm{e}^{-q_t r}, \tag{4.90}$$

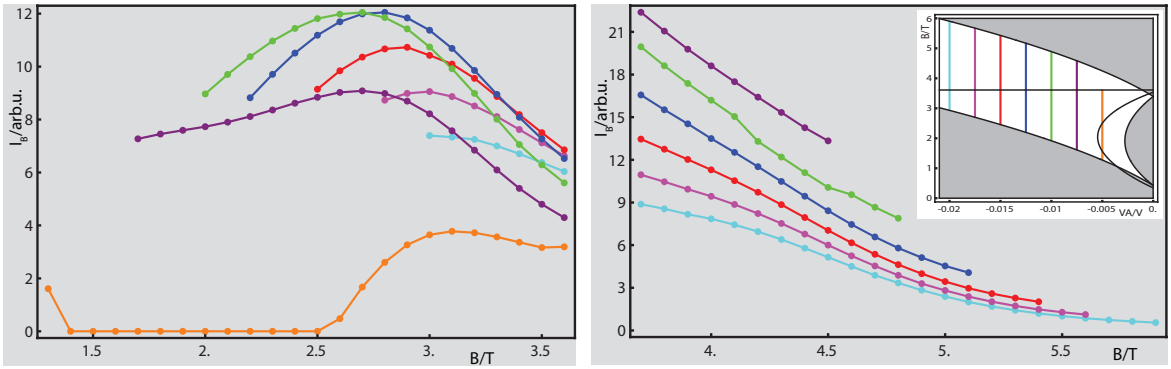

(a) Tunneling current in area 2.

(b) Tunneling current in area 1.

Figure 4.2: The tunneling current to first order in the three-particle scattering rate W in the incoherent regime at zero temperature. Displayed are traces at constant values of V_A, respectively -0.02V, -0.0175V, -0.015V, -0.0125V, -0.01V, -0.0075V and -0.005V (the latter only in area 2). The scaling factors of the two vertical scales are the same, so the size of the current can be compared between the two regions. Note that a change of sign in current is expected as one crosses from one region into the other; thus only the magnitude of current is plotted. INSERT: the locations of the cross-sections in the areas 1 and 2, as defined in Fig. 2.3. The second right-facing parabola is defined by the equality sign of Eq. (4.88).

which when Fourier Transformed to momentum space yields Eq. (4.89). The range of the real-space potential is $1/q_t$, which for the present choice of q_t is $\approx 56nm$.

In the insert of Fig. 4.2 we have also included the parabola given by the equality sign of Eq. (4.88). In area 2 (that is below the horizontal line) the current must be zero to the right of this parabola, as relaxation in this area would require a departure from energy conservation. Only one of our traces actually includes points in this region, but we observe the expected behavior as the current along this trace goes towards zero and is zero where we expects it to be.

In general the current in area 2 seems to display much more interesting structures than the current in area 1. In the latter area the current grows monotonically towards lower B-fields and diminishes monotonically towards lower voltages, all in all a rather boring behavior. In contrast the current traces in area 2 shows a local maxima, whose position moves with the value of V_A for the trace.

4.3 How the current depends on the interaction

We also briefly tried to examine what changing the interaction does to the current. Maintaining every other parameter, we changed only the range of the interaction (contained in q_t) and calculated the current along a constant V_A trace through areas 1 and 2. The results are shown in Fig. 4.3.

Because of the nature of the interaction, Eq. (4.89), the current grows monotonically with q_t at every single point.

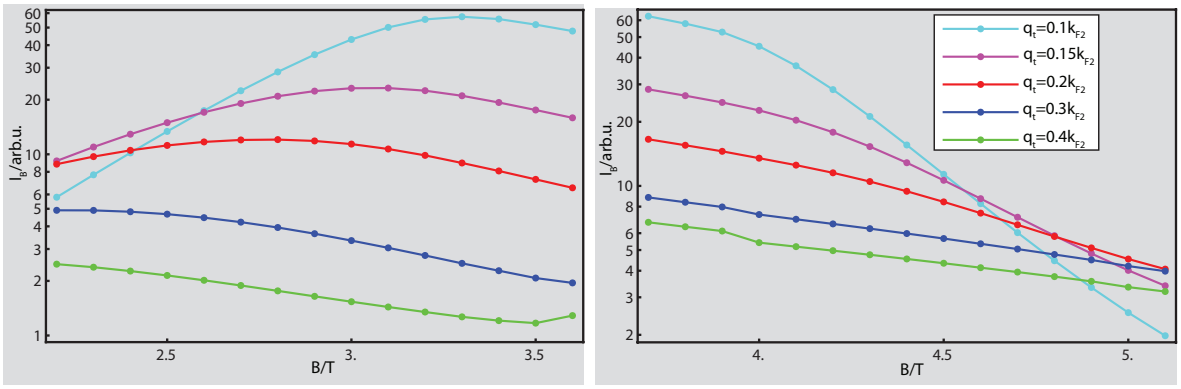

(a) Tunneling current in area 2.

(b) Tunneling current in area 1.

Figure 4.3: Traces of tunneling current along $V_A = -0.0125V$ with varying values for the range of the interaction. The curves labeled $q_t = 0.2k_{F2}$ is identical to the blue curves of Fig. 4.2. The figures have been scaled by q_t, so magnitude of current cannot be compared between different curves. The vertical scales are logarithmic because the data encompasses a large range of values.

4.4 Further development

When we solved for the current we included only terms to first order in three-particle scattering. Hoping to improve the results could be done in to possible ways. Either we could also include the first order term in the four-particle scattering rate or we could go to second order in the three-particle scattering.

Going to first order in three-particle scattering resulted in a two-dimensional integral, which we could solve for numerically. If we go to second order in the three-particle scattering we get a five-dimensional integral: Two integrations for each three-particle scattering and a further integration for the momentum of the intermediate state. Whereas we could solve a 2D integral numerically, though it did take considerable amounts of time, we can never hope for solving a 5D integral in a similar manner. Another approach is clearly needed. We could hope for making approximations which would enable us to solve for the current exactly. The easiest such approximation to make, is linearizing the band between the end-points of the relaxing electron and assuming the scattering rate W to be constant. This however requires us to know the endpoint of the relaxation, so only in the case where both k_2^A and k_2^B lies far above the Fermi sea and we can clearly regard k_2^B as the endpoint of relaxation of the electron at k_2^A, is this approach meaningful. And this requirement is only fulfilled for large magnetic fields (the upper left corner of the insert of Fig. 4.2(b)), where the current is just featureless, which is why we have not included the results of this calculation, however they did correspond reasonably well to the results of the numerical integration in the region.

So far we have only considered calculating the current at zero temperature, and so we now ask ourselves, if we can deal with a finite temperature as well. The expression for the current in Eq. (4.82) is still valid, but there is no longer the clear association of the processes depicted in Fig. 2.4 and described by Eq.s (4.84)-(4.87) with the areas defined in Fig. 2.3. So within a couple of k_BT's (converted to corresponding values in either B-field or voltages) of the borders, one has to include more than a single of the current terms, perhaps at certain points in the BV_A-diagram all four terms. Each of the current terms (the two latter no longer

being necessarily zero) is reduced to a 2D integral precisely as in the zero-temperature case.[16] But contrasted to before, where the limits of the integrals where well-defined by the domains, where solutions where possible, this is no longer the case, as everything is smoothed out by the Fermi distribution. In principle every integral should now run over the entire k-axis, but we may argue that it is sufficient to expand the integration domains of the zero-temperature case with a couple of $k_B T$'s converted to momenta. This former approach, while simpler, probably only yields gibberish, because the domains where the integrand is non-zero is very small, and so we must stick to the latter approach.

[16] Well only the same way for the two terms which actually played a role at zero temperature. But the two hole-relaxation terms can be treated similar.

Chapter 5

Conclusion/summary

We have in this thesis looked at the connection between electron-electron interaction in one-dimensional wires and the current in a specific solid-state device consisting of three one-dimensional wires.

The particular reason for using one-dimensional wires is, that tunneling between two such parallel wires in the presence of a magnetic field perpendicular to the plane of the wires, will be greatly enhanced for electrons with a very specific momentum, dictated by the magnetic field and the voltage difference imposed on the wires. Thus we are able to perform tunneling spectroscopy on such a set of wires. The reason for using three wires is that we may both inject and subtract an electron at two known (and different) positions.

First of all we looked at how we imagine the system could be fabricated. Using Cleaved Edge Overgrowth and a smart choice of gating we could see no fundamental reason why our desired system could not be fabricated and be utilized as we desired. In connection with this we also discussed a conceptually very simple model for the current, which made it possible to imagine the connection between the tunneling current in the system, which is what is measured, and the electron or hole relaxation in the second of three one-dimensional wires.

We generally distinguish between two regimes: the incoherent regime and the coherent regime. In the coherent regime electrons may violate energy conservation i a single tunneling event, whereas in the incoherent regime energy must be conserved individually in each tunneling event. Only in the incoherent regime can we speak of wire spectroscopy and so we limit any further considerations to this regime.

Using this model we concluded, that in some situations, the presence of a measurable current would rely on the ability of holes to relax. But there is a clear breaking in the symmetry between electron and holes. Whereas an excited electron above the Fermi Sea has no problem relaxing by creating multiple electron-hole pairs, in a single mode wire a single hole situated in the Fermi Sea cannot relax by similar means at zero temperature. We have proven this remarkable property. This lack of relaxation rested on a dispersion which had a positive curvature, and so for the Luttinger Liquid, which requires linearization of the dispersion, we would not encounter it.

Excited electrons generally don't mind relaxing, and so a current will run in the system, when it depends on electron relaxation. Using the semi-classical Boltzmann Equation we tried to set up a way of calculating the tunneling current. We made several approximations along the way, mostly by assuming that several in reality extended regions were point-sized. The approximations would be justified, as taking into account the finite size of these regions

would correspond to higher order corrections to the current and we only wanted it to the lowest possible order. In the end we ended with a rather messy expression for the current (Eq.s (4.82)-(4.87)) valid even at a finite temperature (and thus also encompassing the hole-relaxation regions, since after all holes are allowed to relax at a finite temperature).

We were however not able to get much further with these expressions, so after some small initial calculations (mostly eliminating integrations with delta-functions) we integrated them numerically at zero temperature to get a current. We were thus able to compute how the current changed when we changed the two system parameters, the magnetic field and the voltage applied between two of the wires. We were never able to get absolute numbers out of the calculations, we only worked in proportionalities. As it turned out, the current was completely featureless in one of the regions, where it just fell off monotonously. In another region it sported a ridge along which the current was at a maximum.

We also briefly examined what effect the range of the interaction would have on the current. No conclusion was reached apart from the calculation itself.

We could remark, that what we succeeded in doing is to calculate the tunneling current (albeit with a lot of approximations and only to lowest order in the three-particle scattering rate) from the interaction, what the experimentalist has, is the inverse problem. The current is measured and from this needs to be deducted some information about the interaction. But this is the same as in all of physics.

Bibliography

[1] David J. Griffiths. *Introduction to Quantum Mechanics*. Pearson Prentice Hall, second edition, 2005.

[2] A. Yacoby, H. L. Stormer, K. W. Baldwin, L. N. Pfeiffer, and K. W. West. Magneto-transport spectroscopy on a quantum wire. *Solid State Communications*, 101(1):77–81, January 1997.

[3] Marc Bockrath, David H. Cobden, Jia Lu, Andrew G. Rinzler, Richard E. Smalley, Leon Balents, and Paul L. McEuen. Luttinger-liquid behaviour in carbon nanotubes. *Nature*, 397(6720):598–601, February 1999.

[4] Loren Pfeiffer, K. W. West, H. L. Stormer, J. P. Eisenstein, K. W. Baldwin, D. Gershoni, and J. Spector. Formation of a high quality two-dimensional electron gas on cleaved gaas. *Applied Physics Letters*, 56(17):1697–1699, 1990.

[5] O. M. Auslaender, A. Yacoby, R. de Picciotto, K. W. Baldwin, L. N. Pfeiffer, and K. W. West. Tunneling spectroscopy of the elementary excitations in a one-dimensional wire. *Science*, 295(5556):825–828, 2002.

[6] A. Yacoby, H. L. Stormer, Ned S. Wingreen, L. N. Pfeiffer, K. W. Baldwin, and K. W. West. Nonuniversal conductance quantization in quantum wires. *Phys. Rev. Lett.*, 77(22):4612–4615, Nov 1996.

[7] Loren Pfeiffer, H. L. Störmer, K. West, and K. W. Baldwin. Quantum wire structures by mbe overgrowth on a cleaved edge. *Journal of Crystal Growth*, 111(1-4):333–338, May 1991.

[8] Loren Pfeiffer, H. L. Störmer, K. W. Baldwin, K. W. West, A. R. Goñi, A. Pinczuk, R. C. Ashoori, M. M. Dignam, and W. Wegscheider. Cleaved edge overgrowth for quantum wire fabrication. *Journal of Crystal Growth*, 127(1-4):849–857, February 1993.

[9] M. Grayson, C. Kurdak, D. C. Tsui, S. Parihar, S. Lyon, and M. Shayegan. Novel cleaved edge overgrowth structures for tunneling into one- and two-dimensional electron systems. *Solid-State Electronics*, 40(1-8):233–236, 1996.

[10] A. R. Goni, L. N. Pfeiffer, K. W. West, A. Pinczuk, H. U. Baranger, and H. L. Stormer. Observation of quantum wire formation at intersecting quantum wells. *Applied Physics Letters*, 61(16):1956–1958, 1992.

[11] L. Pfeiffer, A. Yacoby, H. L. Stormer, K. L. Baldwin, J. Hasen, A. Pinczuk, W. Wegscheider, and K. W. West. Transport and optics in quantum wires fabricated by mbe overgrowth on the (110) cleaved edge. *Microelectronics Journal*, 28(8-10):817–823, 1997.

[12] Henrik Bruus and Karsten Flensberg. *Many-Body Quantum Theory in Condensed Matter Physics: An Introduction*. Oxford University Press, 2004.

[13] Johannes Voit. A brief introduction to luttinger liquids. In Hans Kuzmany, Jorg Fink, Michael Mehring, and Siegmar Roth, editors, *AIP Conf. Proc.*, volume 544, pages 309–318. AIP, 2000.

[14] Yaroslav Tserkovnyak, Bertrand I. Halperin, Ophir M. Auslaender, and Amir Yacoby. Interference and zero-bias anomaly in tunneling between luttinger-liquid wires. *Phys. Rev. B*, 68(12):125312, Sep 2003.

[15] R. de Picciotto, H. L. Stormer, L. N. Pfeiffer, K. W. Baldwin, and K. W. West. Four-terminal resistance of a ballistic quantum wire. *Nature*, 411(6833):51–54, May 2001.

[16] R. de Picciotto, H. L. Stormer, A. Yacoby, L. N. Pfeiffer, K. W. Baldwin, and K. W. West. 2d-1d coupling in cleaved edge overgrowth. *Phys. Rev. Lett.*, 85(8):1730–1733, Aug 2000.

[17] G. Barak, H. Steinberg, A. Yacoby, L. N. Pfeiffer, and K. W. West. Fractionization and energy relaxation in 1d quantum wires. Unpublished, 2008.

[18] N. W. Ashcroft and N. D. Mermin. *Solid State Physics*. Holt-Saunders, 1976.

[19] Anders Mathias Lunde, Karsten Flensberg, and Leonid I. Glazman. Three-particle collisions in quantum wires: Corrections to thermopower and conductance. *Physical Review B (Condensed Matter and Materials Physics)*, 75(24):245418, 2007.

Appendix A

The energy eigenfunctions and tunneling between them

Here we will find the energy eigenstates of a single wire by solving the time-independent Schrödinger equation with a potential, which mimics the physical situation, while still being (more or less) exactly solvable. This resulting energy eigenvalues are quadratic in the (kinematic) momentum along the wires and contains several modes corresponding to excitations in the transversal directions. Next we consider a system consisting of two such wires running parallel to each other. From the wavefunctions of the energy eigenstates we can calculate the tunneling matrix element between the different modes of the wires, and we observe the momentum boost in tunnelling between the wires, which is due to the perpendicular magnetic field.

We orient our x-axis along the wire, our z-axis perpendicular to the cleaved edge (along the B-field) and our y-axis in the cleaved edge, perpendicular to the wire direction. We assume the potential to be separable in these three directions, enabling us to write the total potential $V(\mathbf{r})$ as

$$V(\mathbf{r}) = V_x(x) + V_y(y) + V_z(z). \tag{A.1}$$

On this scale we consider the wire to be of infinite extent, so that is is translational invariant in the x-direction. V_x should therefore be a constant, and we may as well choose $V_x(x) = 0$. Along the y-direction the electrons see the potential that would normally confine them to a plane perpendicular to the first growth direction, thus forming the usual 2DEG. On each side this plane is confined by a atomically smooth layers. We could model it by a finite square well, but for ease of calculation we instead model it by a harmonic potential, with a harmonic frequency ω_0 and a minimum value of 0 situated at $y = y_0$. Thus $V_y(y) = \frac{1}{2}m\omega_0^2(y - y_0)^2$. Along the z-direction we model the potential with a triangular well, which approaches infinity very fast to the right of the well because electrons are not allowed to leave the material altogether. The well itself is what binds the electrons to the cleaved edge thus forming our 1DEG. This potential also supports non-localized states corresponding to the extended 2DEG states of the full system. All three potentials are shown in Fig. A.1.

In the presence of a magnetic field the kinetic energy for an electron changes from the usual $T = \frac{\mathbf{p}^2}{2m}$ to

$$T = \frac{(\mathbf{p} - q\mathbf{A})^2}{2m}, \tag{A.2}$$

with $\mathbf{p} = -\mathrm{i}\hbar\nabla$ being the canonical momentum, q the electron charge ($q = -e$, $e > 0$) and

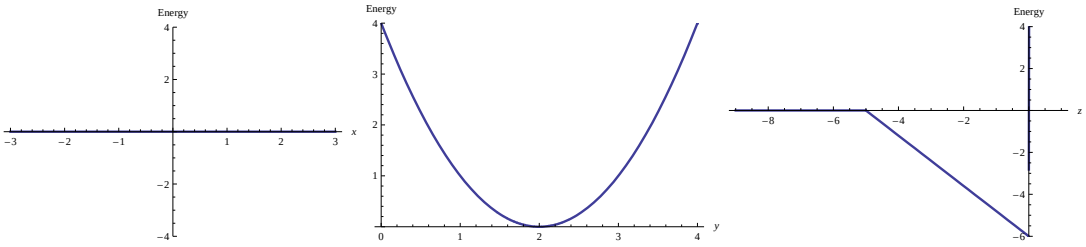

(a) V_x (b) V_y (c) V_z

Figure A.1: Examples of the potential in the three different directions. Units are arbitrary (but on the order of nm and eV).)

$\mathbf{A}$ the magnetic vector potential with the property that $\mathbf{B} = \nabla \times \mathbf{A}$. The magnetic field is $\mathbf{B} = B\hat{\mathbf{z}}$, so we choose $\mathbf{A} = -By\hat{\mathbf{x}}$.[1] The Hamiltonian can now be written

$$H = T + V = \frac{(\mathbf{p} - eBy\hat{\mathbf{x}})^2}{2m} + V(\mathbf{r}) = \frac{((p_x - eBy)^2 + p_y^2 + p_z^2}{2m} + V_y(y) + V_z(z), \tag{A.3}$$

and is separable in z, since it can be written $H = H(x, p_x, y, p_y) + H(z, p_z)$. We also observe that $[H, p_x] = 0$ allowing us to find common eigenfunctions of H and p_x. The eigenfunctions of p_x goes as $\exp(-\mathrm{i}kx)$ and thus we conclude, that we can choose the eigenfunctions of H such that they can be factorized completely as

$$\Psi(x, y, z) = \mathrm{e}^{\mathrm{i}kx} Y(y) Z(z), \tag{A.4}$$

where $Y(y)$ and $Z(z)$ are solutions to the one-dimensional Schrödinger equations

$$\Big(\frac{p_z^2}{2m} + V_z(z)\Big) Z(z) = E^{(z)} Z(z) \tag{A.5}$$

$$\Big(\frac{(\hbar k - eBy)^2 + p_y^2}{2m} + V_y(y)\Big) Y(y) = E_k^{(y)} Y(y), \tag{A.6}$$

and the eigenenergy of Ψ is $E^{(z)} + E_k^{(y)}$.

A.1 The z-equation

The z-equation (Eq. (A.5)) can only be solved numerically[2], but we shall see how it becomes much easier to solve by changing the potential slightly. Assuming that the ground state and the first couple of excited states lies far below the energy of the first extended state, their wavefunctions are vanishingly small outside the triangular well. We can thus change the potential outside of the well and still retain these states as eigenstates. Changing the potential into an infinitely deep triangular well, the Schrödinger equation Eq. (A.5) changes into

$$\Big(-\frac{\hbar^2}{2m}\frac{\mathrm{d}^2}{\mathrm{d}z^2} - (z + z_0)\frac{V_0}{z_0}\Big) Z(z) = E^{(z)} Z(z), \tag{A.7}$$

[1] There is a large degree of freedom (the choice of gauge) associated with selecting the vector potential, and any one choice which fulfills $\mathbf{B} = \nabla \times \mathbf{A}$ will in principle do the job. However some choices could be easier to work with than others, and this specific choice seems to do the job pretty well.

[2] Numerically in the sense that a solution can be found in each of the three regions, but the matching of the wavefunction and its first derivative at the boundaries yields equations which can only be solved numerically.

with the boundary condition $Z(0) = 0$.[3] Introducing a dimensionless position p as

$$\frac{2m}{\hbar^2}\Big(V_0\frac{z}{z_0} + E^{(z)} + V_0\Big) \equiv -\Big(\frac{2mV_0}{\hbar^2 z_0}\Big)^{2/3} p, \tag{A.8}$$

the equation now reads in terms of $Q(p(z)) = Z(z)$, $0 = \Big(\frac{\mathrm{d}^2}{\mathrm{d}p^2} - p\Big)Q(p)$, with the boundary condition $Q(p_0) = 0$, p_0 being the value of p when $z = 0$. Now the solutions to this equation is the well known Airy function of the first kind, $Ai(p)$[4],

$$Q(p) = Ai(p) = \frac{1}{\pi}\int_0^\infty \mathrm{d}t \cos\big(\frac{t^3}{3} + pt\big). \tag{A.9}$$

Quantization of the energy is achieved by imposing the boundary condition; this gives us the eigenenergies in terms of the zero points p_n of the Airy function as,

$$E_n^{(z)} = (-p_n)\Big(\frac{V_0^2\hbar^2}{2mz_0^2}\Big)^{1/3} - V_0. \tag{A.10}$$

The first few zero points are given in Table A.1. We will use the same n to label the corresponding eigenfunction, $Z_n(z)$, the first few of which are shown in Fig. A.2.

n	0	1	2	3	4	5	6
p_n	-2.33811	-4.08795	-5.52056	-6.78671	-7.94413	-9.02265	-10.0402

Table A.1: The first seven zero points of the Airy function $Ai(p)$.

The infinitely deep well obviously only has bound state solutions, but the original potential also supported unbound states. These would be relevant if we were to look at tunneling between a 1DEG wire-mode in the lower wire and the 2DEG of the upper wire. But since the 2DEG modes are extended whereas the 1D modes are limited, the overlap (and thereby tunneling) would be small compared to tunneling between the 1DEG modes of the two wires.

A.2 The y-equation

Now let us consider the y-equation (Eq. (A.6)). The Hamiltonian of this problem is rewritten

$$H_y = \frac{(\hbar k - eBy)^2 + p_y^2}{2m} + V_y(y) = \frac{(\hbar k - eBy)^2 + p_y^2}{2m} + \frac{1}{2}m\omega_0^2(y - y_0)^2 \tag{A.11}$$

$$= \frac{p_y^2}{2m} + \frac{1}{2}m\omega^2(y - y_0')^2 + \frac{(\hbar k - eBy_0)^2}{2m}\frac{\omega_0^2}{\omega^2}. \tag{A.12}$$

Here we have introduced the cyclotron frequency $\omega_c \equiv eB/m$ and an effective frequency $\omega^2 \equiv \omega_c^2 + \omega_0^2$. We observe, that the total potential is still a parabola in y, but with ω as the

[3] Since the potential is infinite for $z > 0$ the electron is prohibited from being here. Now, a general solution to Eq. (A.7) does not fulfill this. So if we construct our eigenfunctions as solutions $Z(z)$ to Eq. (A.7) for $z < 0$ and as zero for $z > 0$ we must require that $Z(0) = 0$, so that the eigenfunctions are continuous. The derivative of the wave function is on the other hand not required to be continuous at this point, as the potential changes by an infinite amount.

[4] The Airy function of the second kind $Bi(p)$ also solves the equation, but its behavior is unphysical as it is exponentially growing in the classically forbidden region that lays below some z.

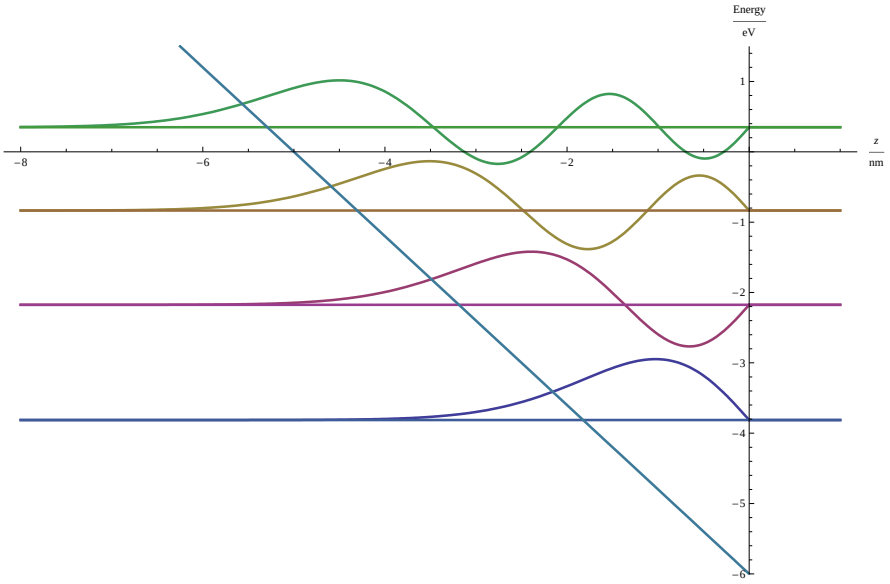

Figure A.2: The first four normalized eigenfunctions of the infinite, triangular potential well. In this case we have used $V_0 = 6eV$ and $z_0 = 5nm$. (Of course, what really matters is only the slope of the potential, so it is really a redundancy to use two variables to describe the potential.)

frequency and no longer centered around y_0 but around

$$y_0' \equiv \frac{eB\hbar k/m^2 + \omega_0^2 y_0}{\omega^2}. \tag{A.13}$$

So we just have a harmonic oscillator Hamiltonian, the solving of which is very well known. The eigenfunctions are labeled by an integer m ($m = 0, 1, 2, 3, \ldots$) and we can immediately write down the corresponding eigenenergy

$$E_{k,m}^{(y)} = \hbar\omega(m + 1/2) + \frac{(\hbar k - eBy_0)^2}{2m}\frac{\omega_0^2}{\omega^2}. \tag{A.14}$$

Here the second term is carried directly over from the Hamiltonian, since it only involves c-numbers. Thus the eigenfunctions and -energies of the original problem are

$$\Psi_{kmn}(x, y, z) = \frac{1}{\sqrt{2\pi}} \mathrm{e}^{\mathrm{i}(k + eBy_0/\hbar)x} Y_m(y - y_0') Z_n(z) \tag{A.15}$$

$$E_{kmn} = \frac{\hbar^2 k^2}{2m}\frac{\omega_0^2}{\omega^2} + \hbar\omega(m + 1/2) + (-p_n)\Big(\frac{V_0^2\hbar^2}{2mz_0^2}\Big)^{1/3} - V_0, \tag{A.16}$$

where m and n are any non-negative integer and k is any real number (with dimensionality of $length^{-1}$). Note that we redefined k, so that $\hbar k$ is now the kinematic momentum and no longer the canonical momentum. $Y_m(y)$ is the m'th excited state of a harmonic oscillator with frequency ω, mass m and centered at $y = 0$, whereas $Z_n(z)$ is the n+1'th eigenfunction of the infinite triangular potential well. What we observe from the first term in the energy expression is, that in the absence of a magnetic field, the energy would depend quadratically on the momentum along the wire direction, the constant of proportionality being just $1/2m$, as

we would have expected. Now, in a finite magnetic field, the energy still depends quadratically on the kinematic momentum in the middle of the wire with a renormalized mass. Also the energy due to excitations along the y-direction are modified, whereas the last term in the energy is unchanged, this is because this term is due to motion along the z-direction which is parallel to the magnetic field and therefore ignorant of its existence.

We also observe that since no constrains are imposed on k, the energies associated with the longitudinal direction are a continuum. The confinedness in the transversal directions lead to quantization of the energy associated with these directions corresponding to different modes of the wire.

A.3 Origin of momentum boost

In the previous subsection we looked at a single wire, now let us imagine, that we have two such wires running in parallel. One is centered around $y_0 = 0$ and the other around $y_0 = d$.[5] We will assume that the frequency ω_0 describing the binding potential is the same for both wires.[6]

For the simple 1D system known as the double well, since the barrier between the two wells in not of infinite height, a single eigenstate is not confined to a single well, but will unavoidably leak into the other. The same problem occurs in our situation. We will assume the barrier between the wells to be sufficiently large, that we may talk about two separate wires, and yet also sufficiently low, that tunneling between the wires is possible. Thus the single wire modes we found previously are also eigenstates of the two-wire system. A wire mode is labeled by the wire (U or L for respectively upper or lower) and the three quantum numbers k, m and n.

The tunneling matrix element between a mode $k_u m_u n_u$ of the upper wire and a mode $k_l m_l n_l$ of the lower wire is

$$\begin{aligned}
T_{k_u m_u n_u, k_l m_l n_l} &= \int \mathrm{d}\mathbf{r}\Psi^*_{Uk_u m_u n_u}(\mathbf{r}) H(\mathbf{r}) \Psi_{Lk_l m_l n_l}(\mathbf{r}) && \text{(A.17)}\\
&= E\int \mathrm{d}\mathbf{r}\Psi^*_{Uk_u m_u n_u}(\mathbf{r}) \Psi_{Lk_l m_l n_l}(\mathbf{r}) && \text{(A.18)}\\
&= \frac{E}{2\pi}\int \mathrm{d}\mathbf{r} \mathrm{e}^{-\mathrm{i}(k_u + eBd/\hbar)x} Y^*_{m_u}(y - y_0'^U) Z^*_{n_u}(z) \mathrm{e}^{\mathrm{i}k_l} Y_{m_l}(y - y_0'^L) Z_{n_l}(z) && \text{(A.19)}\\
&= \frac{E}{2\pi}\int \mathrm{d}x \mathrm{e}^{\mathrm{i}(k_l - k_u - eBd/\hbar)x} \int \mathrm{d}y Y^*_{m_u}(y - y_0'^U) Y_{m_l}(y - y_0'^L) \int \mathrm{d}z Z^*_{n_u}(z) Z_{n_l}(z)\\
&= E\delta(k_l - k_u - eBd/\hbar)\delta_{n_u,n_l} \int \mathrm{d}y Y^*_{m_u}(y - y_0'^U) Y_{m_l}(y - y_0'^L). && \text{(A.20)}
\end{aligned}$$

Several comments are in order. In the second equality we used that the Ψ's by construction are eigenfunctions of the total Hamiltonian H. Since we may apply $H(\mathbf{r})$ equally well to the right and left, the energy E which is pulled out, must be the common eigenenergy of the two states $\Psi_{Uk_u m_u n_u}$ and $\Psi_{Lk_l m_l n_l}$; if they do not have the same eigenenergy, the integral - and thereby the tunneling matrix element - is zero. In the last step we used that $\int_{-\infty}^{\infty} \mathrm{d}x \exp(-\mathrm{i}kx) = 2\pi\delta(k)$. We also used the ortogonality $\int \mathrm{d}z Z^*_{n_u}(z) Z_{n_l}(z) = \delta_{n_u,n_l}$, since Z_{n_u} and Z_{n_l} are eigenfunctions of the same Hamiltonian.

[5] So the orthogonal distance between the wires is d.

[6] In reality the lower well is 30 nm wide wile the upper is only 20-25 nm wide.

The last integral $\int \mathrm{d}y Y^*_{m_u}(y - y_0'^U) Y_{m_l}(y - y_0'^L)$ is nothing but the overlap of two harmonic oscillator states displaced relative to each other. Atomic physicists may recognize it as the Franck-Condon factor, which is used in calculating transition probabilities between electronic states in atoms.[7]

What is most important to observe, is the momentum boost an electrons experiences when it tunnels between the wires. An electron starting in an upper wire mode with momentum $\hbar k_u$ can only end up in lower wire modes with momentum $\hbar k_l = \hbar k_u + eBd$, so by tunneling from the upper wire to the lower wire an electron gains a momentum eBd. And vice versa; an electron tunneling from the lower to the upper wire looses a momentum eBd. Since we prefer to work with wavenumbers instead, we shall write this momentum boost as $k_l = k_u + q_B$, where $q_B \equiv \frac{eBd}{\hbar}$.

A.3.1 Direct calculation from the Lorentz force

We consider a classical particle of charge $(-e)$ moving in a homogenous magnetic field $\mathbf{B} = B\hat{\mathbf{z}}$. The only force acting on the particle is the Lorentz force, so the equation of motion for the particle is

$$\frac{\mathrm{d}\mathbf{p}}{\mathrm{d}t} = \mathbf{F} = -e\mathbf{v} \times \mathbf{B} = -eB(v_y\hat{\mathbf{x}} - v_x\hat{\mathbf{y}}), \tag{A.21}$$

which when integrated from some initial time to some final time yields

$$\Delta\mathbf{p} = -eB(\Delta y\hat{\mathbf{x}} - \Delta x\hat{\mathbf{y}}). \tag{A.22}$$

Now consider the two-wire system; an electron in the middle of the upper wire which (somehow) tunnels to the middle of the lower wire will move a vertical distance $\Delta y = -d$ and thus gain a momentum along the wire direction of eBd. If the tunneling is in the opposite direction, the elctron suffers a momentum loss of eBd. So the Lorentz force is directly responsible for the momentum boost we have derived.

An interesting observation: Here we assumed that the electrons moves along in the middle of the wires, however as the full calculation shows, the distance between the wire modes is not the same as the lithographic (replace with better word; growth?) distance d between the wells but is in fact $y_0'^U - y_0'^L = \frac{\omega_0^2}{\omega^2} d$, because of the presence of the magnetic field. But still the momentum boost acts as if the distance between the modes was just d.

[7] The Franck-Condon factor generally does not require the same oscillation frequency in both subsystems.

Appendix B

Proof of H-theorem

We look at an expression of the form

$$\begin{aligned} A &= n_F(\varepsilon_1)\cdot\ldots\cdot n_F(\varepsilon_m)\cdot(1-n_F(\varepsilon_{m+1}))\cdot\ldots\cdot(1-n_F(\varepsilon_{2m})) && \text{(B.1)}\\ &\quad -n_F(\varepsilon_{m+1})\cdot\ldots\cdot n_F(\varepsilon_{2m})\cdot(1-n_F(\varepsilon_1))\cdot\ldots\cdot(1-n_F(\varepsilon_m)), && \text{(B.2)}\end{aligned}$$

which typically appears in composite rates for processes where m particles scatter on each other. Using a reexpression of the Fermi distribution,

$$\begin{aligned} n_F(\varepsilon) &\equiv \frac{1}{1+\mathrm{e}^{\varepsilon/T}} = \frac{\mathrm{e}^{-\varepsilon/2T}}{\mathrm{e}^{-\varepsilon/2T}+\mathrm{e}^{\varepsilon/2T}} = \frac{\mathrm{e}^{-\varepsilon/2T}}{2\cosh(\varepsilon/2T)} && \text{(B.3)}\\ 1-n_F(\varepsilon) &= 1-\frac{1}{1+\mathrm{e}^{\varepsilon/T}} = n_F(-\varepsilon) = \frac{\mathrm{e}^{\varepsilon/2T}}{2\cosh(\varepsilon/2T)}, && \text{(B.4)}\end{aligned}$$

A is rewritten

$$\begin{aligned} A &= \frac{\mathrm{e}^{\frac{1}{2T}(\varepsilon_{m+1}+\ldots+\varepsilon_{2m}-\varepsilon_1-\ldots-\varepsilon_m)}-\mathrm{e}^{-\frac{1}{2T}(\varepsilon_{m+1}+\ldots+\varepsilon_{2m}-\varepsilon_1-\ldots-\varepsilon_m)}}{2^{m+n}\cosh(\varepsilon_1/2T)\cdot\ldots\cdot\cosh(\varepsilon_{2m}/2T)} && \text{(B.5)}\\ &= \frac{2\sinh(\frac{1}{2T}(\varepsilon_{m+1}+\ldots+\varepsilon_{2m}-\varepsilon_1-\ldots-\varepsilon_m))}{2^{m+n}\cosh(\varepsilon_1/2T)\cdot\ldots\cdot\cosh(\varepsilon_{2m}/2T)}. && \text{(B.6)}\end{aligned}$$

Now, the rate that is considered might also contain the requirement of energy conservation in the scattering, $\varepsilon_1+\ldots+\varepsilon_m=\varepsilon_{m+1}+\ldots+\varepsilon_{2m}$. But if this energy conservation is imposed on A, we get

$$A\cdot\delta(\varepsilon_1+\ldots+\varepsilon_m-\varepsilon_{m+1}-\ldots-\varepsilon_{2m})=0, \qquad \text{(B.7)}$$

since sinh is an odd function. This result is a property of the Fermi function, and does not extend to a general distribution function.

Appendix C

Mathematica Source Code

For completeness we include the source code for the Mathematica program used to perform the numerical integrals.

In[1]:=
```
hbar = 1.05457148 * 10^-34 (*hbar in J*s*);
e = 1.60217646 * 10^-19 (*Electron charge in C*);
kb = 1.3806503 * 10^-23 (*Boltzmann constant in J/K*);
m = 0.067 * 9.10938188 * 10^-31 (*Effective electron mass in kg*);
d = 6 + 15 + 10 (*Distance between wires in nm*);
qb[B_] = e * B * d * 10^-9 / hbar (*Wavevector boost when tunnelering in 1/m*);
kf3 = 0.8 * 10^8 (*Fermi wavevektor for wire 3 in 1/m*);
kf2 = 0.9 * 10^8 (*Fermi wavevektor for wire 2 in 1/m*);
kf1 = 0.7 * 10^8 (*Fermi wavevektor for wire 1 in 1/m*);
disp[k_] = hbar^2 k^2 / (2 m) (*Dispersion in J*);
k2A[VA_, qb_] = 1 / (2 qb) * (kf2^2 - kf1^2 + qb^2 - (2 e m VA) / (hbar^2))
 (*Valid for quadratic dispersion*);
k2B[VB_, qb_] = 1 / (2 qb) * (kf2^2 - kf3^2 + qb^2 + (2 e m VB) / (hbar^2))
 (*Valid for quadratic dispersion*);
V[q_] := 4 π e^2 * 1 / (q^2 + qt^2);(*Interaction in J*)
qt = 0.2 * kf2; (*Range of interaction in q-space*)
nf[ξ_] := UnitStep[-ξ]; (*Zero temperature Fermi Distrribution*)
```

In[16]:=
```
Vtilde[q_] := V[q] + V[-q];
eta = 0;
VV[ka_, kb_, kc_, kd_, ke_, kf_, sa_, sb_, sc_, sd_, se_, sf_] :=
  KroneckerDelta[sa, sd] * KroneckerDelta[sb, se] * KroneckerDelta[sc, sf] *
   ( Vtilde[kb - ke] * Vtilde[kc - kf] / (disp[ka] + disp[kb] - disp[ke] -
         disp[ka + kb - ke] + i * eta) + Vtilde[kb - ke] * Vtilde[kc - kf] /
       (disp[ka] + disp[kc] - disp[kf] - disp[ka + kc - kf] + i * eta) + Vtilde[ka - kd] *
      Vtilde[kb - ke] / (disp[ka] + disp[kc] - disp[kd] - disp[ka + kc - kd] + i * eta) +
     Vtilde[ka - kd] * Vtilde[kb - ke] / (disp[kb] + disp[kc] - disp[ke] -
         disp[kb + kc - ke] + i * eta) + Vtilde[ka - kd] * Vtilde[kc - kf] /
       (disp[ka] + disp[kb] - disp[kd] - disp[ka + kb - kd] + i * eta) + Vtilde[ka - kd] *
      Vtilde[kc - kf] / (disp[kb] + disp[kc] - disp[kf] - disp[kb + kc - kf] + i * eta));
VGV[ka_, kb_, kc_, kd_, ke_, kf_, sa_, sb_, sc_, sd_, se_, sf_] :=
  (VV[ka, kb, kc, kd, ke, kf, sa, sb, sc, sd, se, sf] + VV[ka, kb, kc, ke, kf, kd,
      sa, sb, sc, se, sf, sd] + VV[ka, kb, kc, kf, kd, ke, sa, sb, sc, sf, sd, se] -
     VV[ka, kb, kc, kd, kf, ke, sa, sb, sc, sd, sf, se] - VV[ka, kb, kc, ke, kd, kf,
      sa, sb, sc, se, sd, sf] - VV[ka, kb, kc, kf, ke, kd, sa, sb, sc, sf, se, sd]) * 1 / 4;
W[ka_, kb_, kc_, kd_, ke_, kf_, sa_, sb_, sc_, sd_, se_, sf_] :=
  (2 π / hbar) * Abs[VGV[ka, kb, kc, kd, ke, kf, sa, sb, sc, sd, se, sf]]^2;
```

In[21]:=
```
(*Z1*)
s0 = 1 / 2;
kplus1[k2A_, k2B_, k1m_, k2m_] = 1/2 (k1m + k2A - k2B + k2m +
    Sqrt[k1m^2 + k2A^2 - 3 k2B^2 + 2 k2A (k2B - k2m) + 2 k2B k2m + k2m^2 - 2 k1m (k2A - k2B + k2m)]);
kminus1[k2A_, k2B_, k1m_, k2m_] = 1/2 (k1m + k2A - k2B + k2m -
    Sqrt[k1m^2 + k2A^2 - 3 k2B^2 + 2 k2A (k2B - k2m) + 2 k2B k2m + k2m^2 - 2 k1m (k2A - k2B + k2m)]);
Integrand1[k2A_, k2B_, k1m_, k2m_] := Sum[W[kminus1[k2A, k2B, k1m, k2m], k2B,
     kplus1[k2A, k2B, k1m, k2m], k1m, k2m, k2A, s0, s1, s2, s3, s4, s5], {s1, -1 / 2, 1 / 2},
    {s2, -1 / 2, 1 / 2}, {s3, -1 / 2, 1 / 2}, {s4, -1 / 2, 1 / 2}, {s5, -1 / 2, 1 / 2}] *
   nf[kf2 - Abs[kminus1[k2A, k2B, k1m, k2m]]] nf[kf2 - Abs[kplus1[k2A, k2B, k1m, k2m]]] *
   UnitStep[k1m^2 + k2A^2 - 3 k2B^2 + 2 k2A (k2B - k2m) + 2 k2B k2m + k2m^2 - 2 k1m (k2A - k2B + k2m)] *
   1 / (Sqrt[k1m^2 + k2A^2 - 3 k2B^2 + 2 k2A (k2B - k2m) + 2 k2B k2m + k2m^2 - 2 k1m (k2A - k2B + k2m)]) *
   1 / (2 π)^3;
Z1[k2A_, k2B_] := NIntegrate[2 * 2 * 2 * m / hbar^2 * 3 *
    (1 - nf[disp[k2B] - disp[kf2]]) * Integrand1[k2A, k2B, k1m, k2m],
   {k1m, -kf2, kf2}, {k2m, -kf2, k1m}, WorkingPrecision → 40];
```

In[26]:=
```
(*Z2*)
s0 = 1 / 2;
k1star[k2A_, k2B_, k2m_, k3m_] := (k2A - k2m) (-k2B + k2m) / (k2A + k2B - k2m - k3m) + k3m;
k1mstar[k2A_, k2B_, k2m_, k3m_] := k2A + k2B - k2m + (k2A - k2m) (-k2B + k2m) / (k2A + k2B - k2m - k3m);
Integrand4[k2A_, k2B_, k2m_, k3m_] :=
  Sum[W[k1star[k2A, k2B, k2m, k3m], k2A, k2B, k1mstar[k2A, k2B, k2m, k3m], k2m, k3m,
     s0, s1, s2, s3, s4, s5], {s1, -1 / 2, 1 / 2}, {s2, -1 / 2, 1 / 2}, {s3, -1 / 2, 1 / 2},
    {s4, -1 / 2, 1 / 2}, {s5, -1 / 2, 1 / 2}] * nf[Abs[k1star[k2A, k2B, k2m, k3m]] - kf2] *
   nf[kf2 - Abs[k1mstar[k2A, k2B, k2m, k3m]]] * nf[kf2 - Abs[k2m]] *
   nf[kf2 - Abs[k3m]] * 1 / Abs[k2m + k3m - k2A - k2B] * 1 / (2 π)^3;
Integrand4a[k2A_, k2B_, k2m_] := NIntegrate[Integrand4[k2A, k2B, k2m, k3m],
   {k3m, If[((Min[Re[1/2 (k2A + k2B - k2m + kf2 +
              Sqrt[k2A^2 + k2B^2 - 3 k2m^2 + 2 k2B (k2m - kf2) + 2 k2m kf2 + kf2^2 - 2 k2A (k2B - k2m + kf2)])],
          (k2A^2 + (k2B - k2m) (k2B + kf2) + k2A (k2B - k2m + kf2)) / (k2A + k2B - k2m + kf2)] ≤
        Max[k2A + k2B - k2m, kf2]) || (Re[1/2 (k2A + k2B - k2m - kf2 +
            Sqrt[k2A^2 + k2B^2 - 3 k2m^2 - 2 k2m kf2 + kf2^2 + 2 k2B (k2m + kf2) + 2 k2A (-k2B + k2m + kf2)])]
        ≥ k2m), kf2, Max[Max[k2A + k2B - k2m, kf2], Re[1/2 (k2A + k2B - k2m - kf2 +
           Sqrt[k2A^2 + k2B^2 - 3 k2m^2 - 2 k2m kf2 + kf2^2 + 2 k2B (k2m + kf2) + 2 k2A (-k2B + k2m + kf2)])]]],
    If[((Min[Re[1/2 (k2A + k2B - k2m + kf2 +
              Sqrt[k2A^2 + k2B^2 - 3 k2m^2 + 2 k2B (k2m - kf2) + 2 k2m kf2 + kf2^2 - 2 k2A (k2B - k2m + kf2)])],
          (k2A^2 + (k2B - k2m) (k2B + kf2) + k2A (k2B - k2m + kf2)) / (k2A + k2B - k2m + kf2)] ≤
        Max[k2A + k2B - k2m, kf2]) || (Re[1/2 (k2A + k2B - k2m - kf2 +
            Sqrt[k2A^2 + k2B^2 - 3 k2m^2 - 2 k2m kf2 + kf2^2 + 2 k2B (k2m + kf2) + 2 k2A (-k2B + k2m + kf2)])]
        ≥ k2m), kf2, Min[Min[Re[1/2 (k2A + k2B - k2m + kf2 +
           Sqrt[k2A^2 + k2B^2 - 3 k2m^2 + 2 k2B (k2m - kf2) + 2 k2m kf2 + kf2^2 - 2 k2A (k2B - k2m + kf2)])],
       (k2A^2 + (k2B - k2m) (k2B + kf2) + k2A (k2B - k2m + kf2)) / (k2A + k2B - k2m + kf2)], k2m]]}, WorkingPrecision → 15];
Z2[k2A_, k2B_] := 2 * 3 * 2 * m / hbar^2 * 2 * nf[disp[k2B] - disp[kf2]] *
   NIntegrate[Integrand4a[k2A, k2B, k2m], {k2m, kf2, k2A}, WorkingPrecision → 15];

(*calculation*)
```

In[32]:=
```
convolution[VA_, B_] :=
 (nf[Abs[k2A[VA, qb[B]]] - kf2] - nf[Abs[k2A[VA, qb[B]] - qb[B]] - kf1]) *
  1 / k2A[VA, qb[B]] * 1 / k2B[0, qb[B]] * (m / hbar)^2
```

In[33]:=
```
IBZ2[VA_, B_] := -convolution[VA, B] * Z2[k2A[VA, qb[B]], k2B[0, qb[B]]] * 10^-85 * 10^11;
IBZ1[VA_, B_] := -convolution[VA, B] * Z1[k2A[VA, qb[B]], k2B[0, qb[B]]] * 10^-85 * 10^11;
```

In[35]:=
```
IBZ2[-0.0125, 3.6]
```

NIntegrate::nlim : k3m = If[≪1≫] is not a valid limit of integration. ≫

NIntegrate::slwcon :
Numerical integration converging too slowly; suspect one of the following: singularity, value of the integration is 0, highly oscillatory integrand, or WorkingPrecision too small. ≫

NIntegrate::ncvb :
NIntegrate failed to converge to prescribed accuracy after 9 recursive bisections in k2m near {k2m} = $\{1.588713616512919003170407043796967781827597292701987469211114145 3\times 10^{8}\}$. NIntegrate obtained 2.122494637337057351227138031579153276122864924921922293770186395 5`65.*^−126 and 8.425743277841460670947134764705892039331114528387621131512026113 5`65.*^−131 for the integral and error estimates. ≫

Out[35]= 6.55738×10^{-173}

In[36]:=
```
IBZ2[-0.0125, 3.5]
```

NIntegrate::nlim : k3m = If[≪1≫] is not a valid limit of integration. ≫

NIntegrate::slwcon :
Numerical integration converging too slowly; suspect one of the following: singularity, value of the integration is 0, highly oscillatory integrand, or WorkingPrecision too small. ≫

NIntegrate::ncvb :
NIntegrate failed to converge to prescribed accuracy after 9 recursive bisections in k2m near {k2m} = $\{1.261470583740359734450430977381923224836216191436894442297275473 7\times 10^{8}\}$. NIntegrate obtained 2.301585781671851500827169920119099352217058661999122748448282456 6`65.*^−126 and 8.740400618488725053600118752860292677098345508717389414482176761 4`65.*^−131 for the integral and error estimates. ≫

Out[36]= 7.30095×10^{-173}